Differential aspects of spatial vision in subjects presenting with either macular degeneration or visual snow

Ruba Alissa

Doctor of Philosophy

City, University of London

School of Health Science

Division of Optometry and Visual Science

April 2018

Contents

Table of figures

Table of tables

Acknowledgements

I would like to express my sincere gratitude to my supervisor, Professor John Barbur, for giving me this opportunity to carry out this research work. His valuable support, unceasing patience and his guidance all have been greatly appreciated.

Further, I would also like to thank Dr Franziska G. Rauscher and Professor Gordon Plant for their interest in this research and participation in the project. In addition, I would also like to thank my colleagues, Dr Wei Bi for his support in programming, also wish to thank Mr Alister Harlow for his help and technical support.

To all the subjects who gave up their time to volunteer for these studies I would like to express my gratitude to them all.

Finally, I owe a big thank you to my wonderful family to whom I dedicate this work. Without the love, support and encouragement of my parents, sisters and brothers I would not have been able to complete these studies.

Declaration

I grant powers of discretion to the University librarian to allow this thesis to be copied in whole or in part without further reference to me. This permission covers only single copies made for study purposes, subject to normal conditions of acknowledgement.

Abstract

The aim of this study was to investigate differential aspects of spatial vision in subjects presenting with macular degeneration and visual snow. Emphasis was placed on the effects of aging and/or ocular disease on binocular summation and the measurement of differences between the two eyes in a number of visual tasks. Accommodation performance was measured for both pre-presbyopic and presbyopic observers. The results showed no binocular advantage for either group for far or intermediate stimulus vergences.

The effects of visual crowding upon visual acuity were tested using a Landolt C optotype with surrounding distractors. Binocular advantage was found to be higher along the line of sight and to decrease in the near periphery. The presence of distractors reduced visual resolution significantly at every eccentricity, with the effect becoming more pronounced in the periphery. The latter was observed for both monocular and binocular viewing conditions leading to the suggestion that the involvement of binocularly driven neurons may not be essential for visual crowding.

The effects of healthy aging and ocular disease on spatial and chromatic vision were also investigated. It was found that stimulus presentation time in a gap acuity task affects visual acuity differently in patients with Age-related Macular Degeneration (AMD) when compared to normal subjects. The processing of briefly presented optotypes appears to be severely reduced in AMD patients. Visual performance was also investigated in patients who experience ‘visual snow’. While gap acuity at any stimulus duration and the strength of chromatic afterimages were found to be unaffected, involuntary pupil recovery following brief exposure to chromatic stimuli was found to be delayed in 3 of the 6 visual snow (VS) patients examined. The absence of a normal pupil recovery is consistent with abnormally slow signals that may also play a part in VS.

The novel findings reported in this thesis suggest that advanced vision tests can be used to quantify the effects of normal aging and to detect and monitor the earliest changes in diseases of the eye.

List of abbreviations

AMD	Age-related Macular Degeneration
AO	adaptive optics
CAA	Contrast Acuity Assessment test
CAD	Colour Assessment and Diagnosis test
CD	Chromatic Displacement
CFF	Critical Flicker Frequency
CSF	Contrast Sensitivity Function
DoF	Depth of Focus
DR	Diabetic Retinopathy
ECCE	Extracapsular cataract extraction
EW	The Edinger-Westphal
FCS	Functional Contrast Sensitivity
ICCE	Intracapsular cataract extraction
L	Long- wavelength sensitive cone
LGN	The Lateral Geniculate Nucleus
LGS	Lateral GeniculoStriate
M	Middle-wavelength sensitive cone
MAR	Minimum Angle of Resolution
OPN	Olivary Pretectal Nuclei
PCO	Posterior Capsule Opacification
PLR	Pupil Light Reflex
PSF	Point Spread Function
QAA	Quantitative Afterimage Assessment
RG	Red-Green
RGCs	Retinal Ganglion Cells
RPE	Retinal Pigment Epithelium
S	Short- wavelength sensitive cones
SEM	Standard Error of the Mean
SNU	Standard Normal Units
VS	Visual Snow
YB	Yellow-Blue

Chapter 1. Introduction

The primary sensory organ of the visual system is the eye. The process of vision begins with the formation of the image of the external world onto the retinal mosaic by the optics of the eye. The rod and cone photoreceptors encode variations in light intensity and spectral content into electrical signals which are conveyed via the second order bipolar neurons, which serve as signal amplifiers, on to the retinal ganglion cells (RGCs) which then encode visual information in the form of action potentials for processing by the higher visual centres of the brain.

Because image formation is the initial step in the visual process, any imperfections in the eye's optical apparatus may therefore adversely affect visual perception and specific vision attributes such as acuity and contrast sensitivity. To better understand the limits of visual perception, one must logically begin with the anatomical properties of the eye to discern the optical factors which limit the resolution of the visual system. From an optometric standpoint, an understanding of the retina and its associated visual pathways is essential in understanding how the light is first converted into electrical signals and how these signals are then transmitted to the brain for higher processing (Dowling, 1987).

1.1 The structure of the human eye

The eye is the peripheral organ of vision and one of the most functionally complex organ of the human anatomy (Willoughby, 2010; Kaufman, et al., 1950). It is situated at the front of the skull and embedded within the orbit. The average emmetropic human eye has a diameter of approximately 24 mm and the ocular structure occupies approximately a quarter of the orbit. The remainder of the orbit comprises extraocular muscles, nerves, blood vessels and connective tissue, which all provide some degree of structural support and therefore play a significant role in the visual process.

The human eye can be functionally divided into three layers (Willoughby, 2010) as illustrated in Figure 1.1:

- The outer region, which is composed of the sclera and cornea.

- The middle layer, which consists of the choroid, the ciliary body and the iris.
- The inner layer, which consists of the photosensitive retina and retinal pigmental epithelium.

These three ocular layers enclose three translucent structures, namely the vitreous humour, the aqueous humour, and the crystalline lens. Further, the eye can be functionally divided into the anterior segment (cornea, aqueous humour, pupil and lens), which constitutes the optical system of the eye, and the posterior segment (vitreous humour, retina, choroid), which will be discussed in turn.

1.1.1 The anterior segment of the eye

The anterior segment is the visible part of the eye. Light enters the eye through the pupil and is refracted by both by the cornea and the lens to produce a focused image on the retina. In its resting state, two thirds of the optical power of the eye is provided through refraction of light by the cornea (~ 42 to 45 D), and the remaining third (~ 15 to 18 D), is provided by the internal crystalline lens of the eye (De Valois *et al,* 2000). However, the crystalline lens also confers the capacity of accommodation, in that it is able to change shape to provide additional focusing power when viewing nearby objects, thereby extending the optimal operating range for focused vision which extends from ‘infinity’ to less than 10 cm from the eye in a young person. An eye is said to be ‘emmetropic’ if it produces a clearly focused retinal image of distant targets when the lens has minimal power.

The iris is often considered to be an extension of the ciliary body and has numerous functions within the visual system, including the hydration of the anterior segment and the regulation of the shape (and hence focusing power) of the lens.

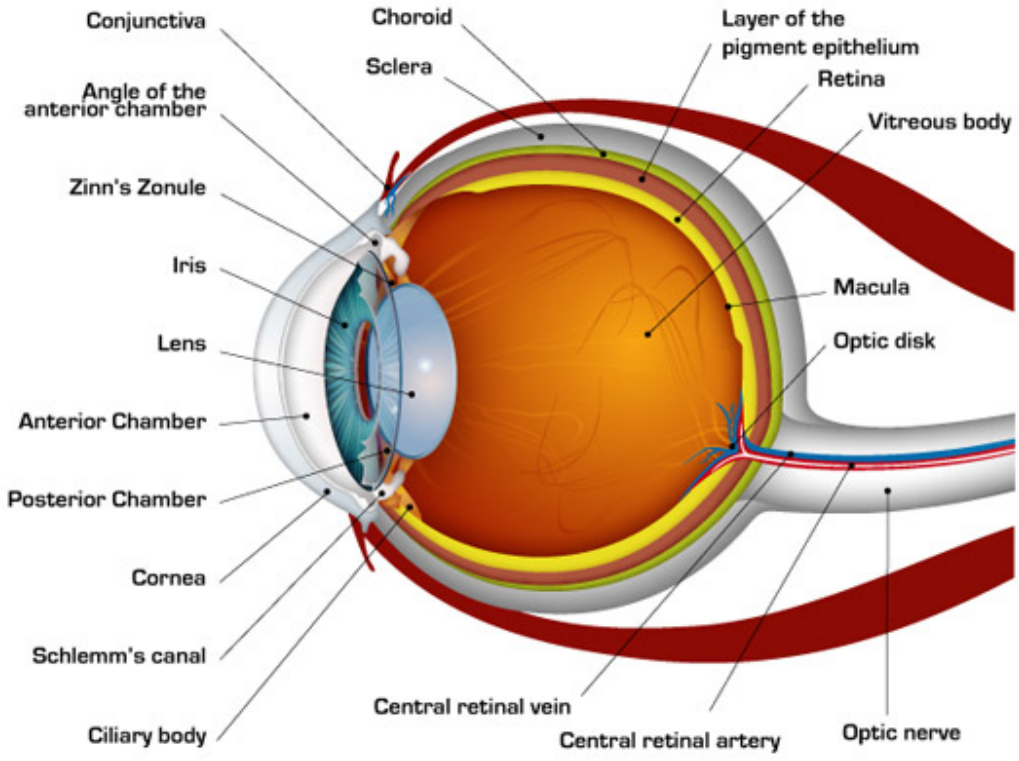

Figure 1.1. Schematic image of the human eye (reproduced from https://scienceeasylearning.wordpress.com/2015/05/27/structure-of-human-eye-and-its-working-and-defects-in-human-eye/)

1.1.1.1 The cornea

The cornea forms the most anterior part of the eye, located in front of the iris and the pupil (Dowling, 1987). The cornea is connected with the sclera at the limbus (Willoughby, 2010) and is protected by the eyelids which produce a tear film which serves to provide protection to the corneal surface from chemical or toxic damage, including microbial invasion (Willoughby, 2010).

In addition to providing the eye with protection from infection and structural damage, the cornea also has a role in refracting and transmitting light to the lens and ultimately the retina. The cornea thus forms the primary refractive element of the eye and therefore must be transparent to wavelengths of light over the visual spectrum (Fuensanta & Vera-Díaz, 2012). However, as for any transparent medium, the

cornea's transmission of light is not perfect; given that light reflects at all interfaces with different refractive indices and scatters from structures within it.

The adult cornea is not a perfect circle, with a height of approximately 10.5 mm and a width of 11.5mm. Its thickness varies from a minimum near the corneal apex (the geometric centre of the cornea), where it is about 0.5 mm thick, to a maximum at the junction between cornea and limbus, where it is in the order of 0.67 to 0.75 mm thick (Jakobiec,1982). The curvature of the cornea is usually treated as being constant (approximating to a sphere) within a given meridian in the optical zone, which is often referred to as the pre-pupillary cornea, a circular region about 4 mm in diameter centred on the corneal apex. However, given that the cornea begins to flatten within 1 mm of the corneal apex, the curvature is always changing. When the corneal curvature along one meridian varies symmetrically with respect to the corneal apex, it is best described as an ellipse. The slight flattening of the corneal curvature toward the periphery reduces the amount of spherical aberration to about one-tenth of that in spherical lenses of similar power (Charman, 1991).

The mechanical strength of the cornea is achieved through the regular arrangement of collagen fibrils that make up the majority of the stromal extracellular matrix. The transparency of the cornea can be attributed to the regular dimension and organization of the collagen fibrils (Charman, 1991). Within the centre region of the cornea, the collagen fibrils are more closely packed as compared to the peripheral cornea. Proteoglycans surround the collagen fibrils, which have a significant role in regulating the hydration of the tissue (Willoughby, 2010), as well as making a contribution to light scattering.

The cornea is densely packed with sensory nerves which are derived from the ophthalmic division of the trigeminal nerve. The cornea comprises five distinct layers, namely the epithelium, Bowman's membrane, the lamellar stroma, Descemet's membrane and the endothelium (Willoughby, 2010).

1.1.1.2 Tear film-cornea interface

The tear film is regarded as the most anterior surface of eye that possesses refractive properties. Due to the differences between the refractive index of this

surface and the surrounding air, it is often referred to as the most powerfully refractive surface. The tear film-cornea interface has a diameter of 7.8 mm and a refractive index of approximately 1.336. Due to the surface properties of this tissue, any variation in the optical quality of the tear film may significantly affect the quality of the projected retinal image.

1.1.1.3 The sclera

Anatomically, the sclera extends from the front of the eye all the way to the back of the eye as far as the optic nerve. While the cornea is transparent, the sclera is almost entirely opaque, given that they have distinct roles in the functioning of the eye. The sclera is a relatively thick, white, and opaque tissue which covers over 85% of the surface of the eye.

The sclera serves to protect the eye from both internal and external forces as well as maintaining its shape. The sclera is the point of attachment of the eye to external structures (namely the muscles and connective tissue) and thus contains portals for the passage of blood vessels and nerves to and from the eye. The conjunctiva is a separate tissue which lies on top of the episclera, which sits atop the sclera and takes the form of a transparent mucous membrane (Kaufman, et al., 1950). The sclera has a thickness of around 530μm, although the layer becomes thicker as it approaches the optic nerve, where its thickness can reach 1 mm. Within the posterior segment of the eye, the sclera takes the form of a net-like material, known as the *scleria reticularis*, through which the optic nerve can pass.

1.1.1.4 The aqueous humour

Aqueous humour is a transparent fluid (Charman, 1991) which is produced by the ciliary body within both the anterior and the posterior compartments of the human eye. The aqueous fluid is responsible for regulating the metabolism of the avascular transparent media, vitreous content, lens, and cornea, as well as the intraocular pressure. Therefore, any imbalance in production and drainage of the aqueous humour can have a significant effect on the health of the eye and result in the development of conditions such as glaucoma which may impair vision (Goel, 2010).

The limited light scattering properties of the aqueous humour make it an excellent ocular fluid. However, scattering may be high if there is an accumulation of debris, an underlying pathology, or any secondary consequences of surgery. The depth of the anterior chamber is progressively reduced throughout adult life, from about 3.8 to 3.0mm, due to a concomitant increase in the thickness of the lens (Charman, 1991). The refractive indices of both the aqueous and vitreous humours are comparable, although they are significantly different when compared to the refractive index of the cornea.

1.1.1.5 The iris and the pupil

The iris appears to be coloured due to its selective spectral absorption of incident light. The primary function of the iris is to regulate the amount of light that enters the eye and to control the optical quality of the retinal image (Kaufman, et al., 1950). The iris contains two competing muscles; namely the sphincter muscle which serve to constrict the pupil, and the dilator muscle which serve to dilate the pupil (Kaufman, et al., 1950). The pupil serves two main optical functions. The first of these is to control the amount of incident light contributing to the retinal image, and the second is to control the quality of the image through its influence on diffraction, aberration, and ocular depth of focus (DoF) (Charman, 1991). The largest pupil captures the most light although, due to aberrations in the eye, a large pupil does not necessarily provide the best image quality. The optimal pupil size is dependent upon a range of criteria, but for the purposes of imaging, the optimal pupil size is between 2.5 and 3.5 mm in diameter. Pupil diameter is also affected by other factors, including age (so-called aging miosis); accommodation (pupillary miosis); emotion and drugs (Charman, 1991). As the pupil lies between the cornea and lens, it acts as a true aperture stop. Given that there is no field stop in the eye, the size of the pupil does not affect the field of view which can reach 90 degrees in some meridians. Ultimately, the field of view is limited by the positioning of the eyes within the skull and the optical constraints of the orbits.

1.1.1.6 The crystalline lens

The lens of the human eye is positioned immediately behind the iris and is a biconvex structure with an anterior surface that is less curved than its posterior counterpart. This adds a further 20–30 diopters to the refractive power of the optical system in its unaccommodated state. The lens is held in place near its equator by the zonules through which it is attached to the ciliary body. The tension imparted upon the zonules is relaxed via contraction of the ciliary muscle which increases lens curvature, thereby increasing the focusing power of the eye, a process known as ‘‘accommodation’’, enabling the eye to focus on more proximal objects (Charman, 1991). Tension applied to the zonules increases through a relaxation of the ciliary muscle, thereby flattening the lens and allowing the eye to focus on more distant objects. This capacity to accommodate tends to decline with age owing to a hardening of the lens with age. This, in combination with other lenticular and extralenticular factors (for example increasing lens size; changing location of the insertion points of the zonules; and the progressive aging of the ciliary muscle) results in ‘‘presbyopia’’, which is a reduced capacity to accommodate.

The lens is composed of densely packed and extremely fine fibres which lack the presence of organelle structures, thereby giving give rise to the 90% transparency of the lens (Charman, 1991). The human lens comprises two convex surfaces and is thus referred to as being ‘biconvex’. The anterior surface of the lens is less curved than the posterior surface (in the unaccommodated state). The midpoints of the two surfaces are referred to as the anterior and posterior poles, respectively. The ‘line’ that interconnects the two poles is known as the axis of the lens while the marginal circumference is referred to as the equator.

The neonatal lens has an equatorial diameter of approximately 6 mm and a sagittal thickness of 4 mm. Lens growth continues throughout life, albeit at a reduced rate in later years. The average lens has a diameter of approximately 10 mm and a thickness, in the unaccommodated state, of approximately 3.5 to 4 mm. These dimensions can change progressively with age due to the addition of new fibres in the equatorial region of the lens. On average, the diameter and thickness will increase approximately two-fold between birth and the age of seventy.

1.1.1.7 The ciliary body

The ciliary body has a major role in regulating the shape and thereby the focusing power of the lens, as well as in secreting aqueous humour (Kaufman, et al., 1950).

The ciliary muscle is composed of three muscle fibre groups, with longitudinal, radial (oblique), and circular orientations, respectively. The ciliary muscle is the 'engine of accommodation' and, upon contraction, it moves forward either centrally or inwardly, relaxing the tone, or tension, on the anterior zonula and lens capsule. The capsule putatively moulds the lens into an accommodated state in which the lens thickens and its equator moves away from the sclera, thereby increasing its focusing power.

Moreover, the ciliary body plays a crucial role in the production of aqueous humour. In terms of anatomy, the ciliary body is considered as the anterior section of the uveal tract, which is positioned in between the iris and choroid. When viewing a cross-section of the ciliary body, it takes the shape of a triangle, with the apex of the structure adjoining the choroid and the base of the structure being located closely to the iris. The entire structure is approximately 6 mm in length.

The choroid itself is a vascular structure which provides the retinal layers with oxygen and nutrients (Dowling, 1987). Superficially the ciliary body attached to the scleral spur which leads to the creation of cavity between the ciliary body and the sclera, known as the supraciliary space. The external surface of the ciliary body forms the frontal insertion of the uveal tract, while the anterior segment of the ciliary body is referred to as *pars plicata* or *corona ciliaris*. The *pars plicata* is attached to the posterior surface of the iris and is around 2.0 mm in length, 0.5 mm in width, and 0.8-1.0 mm in height. Therefore, ciliary processes, which contain hundreds of ridges, are considered to have large surface areas which are ideally suited for ultrafiltration and active fluid transport.

1.1.2 The posterior segment of the eye

1.1.2.1 The vitreous humour

The vitreous humour is a colourless, gel-like material that fills approximately 80% of the posterior chamber of the eye (Kaufman, et al., 1950). It is hollow at the front,

which presents as a deep concavity, the so-called hyaloid fossa, which is anatomically adapted to the lens. The vitreous humour is comprised of approximately 99% water and fine collagen fibres. Towards its centre, the material becomes more fluid due to the presence of glycosaminoglycan chains which occupy the entirety of the vitreous chamber.

The vitreous humour exerts a pressure upon the retina and helps to keep it in place by pressing it against the choroid, although it does not actually adhere to the retina, except at the optic nerve disc and fovea. It is also connected to the *ora serrata* (where the retina ends anteriorly). The way in which the vitreous humour is connected to the main structure of the eye helps to keep the anterior and posterior chambers as distinct compartments. As the vitreous humour ages, so it may liquefy and decrease in volume. Under these circumstances, cells can migrate across with the vitreous humour which can lead to visual phenomena such as floating bodies.

1.1.2.2 The structure of the retina

The retina lies at the posterior pole of the eye and is the photosensitive layer upon which light is focused and subsequently encoded as a series of electrical signals. The retina is comprised of three distinct areas;

- The *macular lutea* which is an area located at about 5mm (~20 deg of visual angle);
- The *fovea*, which lies at the centre of *macular lutea* which has a diameter of about 1.5mm (~5^{o}) and the foveola which lies at the centre of the fovea (~1^{o}). The *foveola* is the thinnest part of the retina and approximates to the visual axis and accounts for the very high degree of spatial resolution owing to very high density of cones present at this point.
- The optic disc, which is located at about ~15 deg of visual angle, nasally to the foveola.

The retina is a complex organ and is anatomically considered to be a part of the brain. It comprises three layers of transparent neurons which serve to absorb photons using pigments, convert these into changes in second messenger activity (cGMP), and thence into graded electrical potentials, and ultimately into action

potentials which propagate via the optic nerve to the higher visual centres of the brain (Dowling, 1987). Human photoreceptors are sensitive to wavelengths within the range of 380 to 780 nm, which encompasses the visible spectrum of light.

The neural retina is comprised of five different types of neuron, namely the rod and cone photoreceptors; horizontal cells (which play a role in adaptation), bipolar cells (second order neurons which play a role in the inversion of signals and amplification of the light signal); highly specialised amacrine cells; and the ganglion cells (see figure 1.2).

1.1.2.3 Layers of the retina

The layers of the retina extend from the Retinal Pigmented Epithelium (RPE) to the ganglion cells. The layers of the retina which are furthest away from the vitreous humour are referred to as the outer layer, whereas the layer closest to the vitreous humour is referred to as the inner retina (figure 1.2).

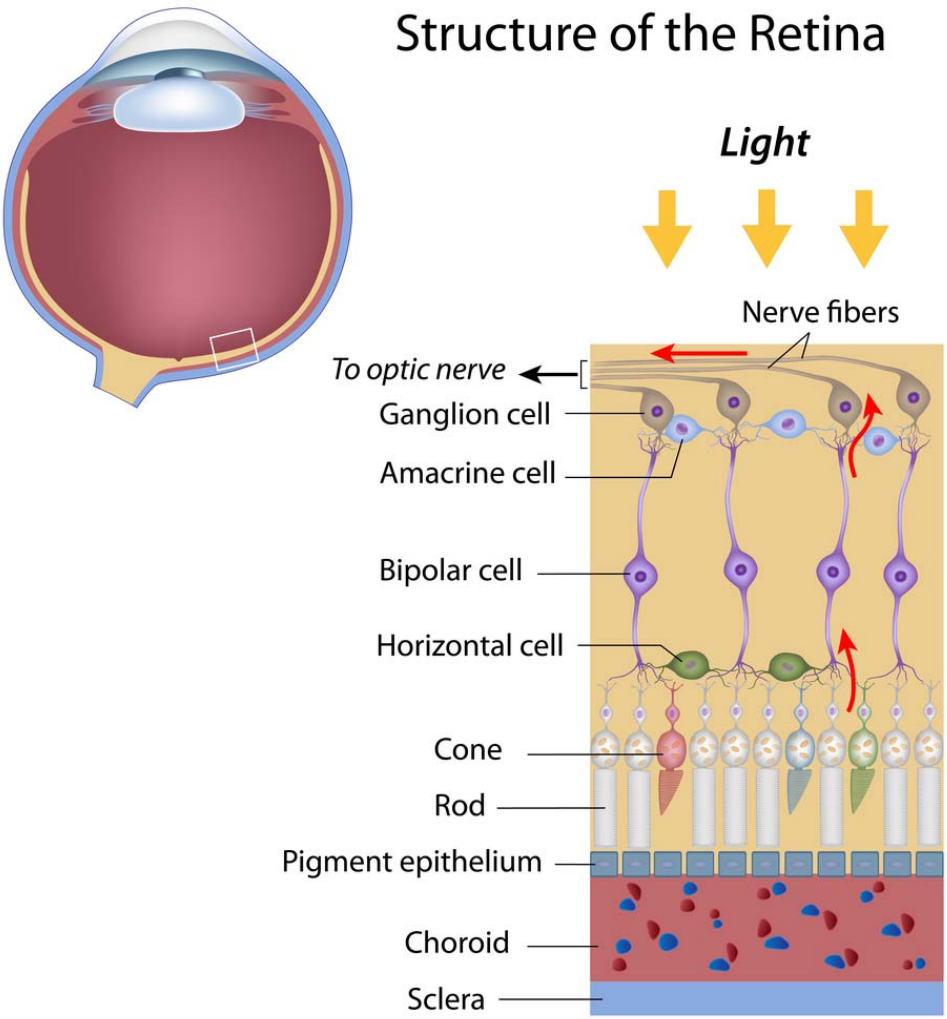

Figure 1.2. The complex structure of the retinal layer (taken from http://discoveryeye.org/layers-of-the-retina).

Retinal pigment epithelium

This is a cuboidal epithelial structure which adjoins Bruch's membrane, the innermost layer of the choroid (also known as the vitreous lamina) which is 2–4 μm thick.

Photoreceptor layer

This layer consists of photoreceptor outer segments and the outer part of the inner segment and comprises both rod and cone photoreceptors.

The external limiting membrane

This layer contains a region of intercellular junctions containing zonula adherens between the structure of radial glial cells and photoreceptor structures. This layer is distinctly visible when viewed under a light microscope.

Outer Nuclear Layer

This is composed of several tiers of rod and cone cells whose nuclei lie on the outer surface. Within the layer, there are a number of outer and inner fibres, which emanate from the same cell bodies and are orientated outwards to the base of the inner segment.

Outer Plexiform Layer

This layer comprises a network of synaptic arrangements between the photoreceptors, bipolar cells, horizontal cells, and interplexiform cells.

Inner Nuclear Layer

This comprises three distinct nuclear strata. The first stratum contains the horizontal cell bodies, followed by bipolar cell bodies, and finally amacrine cell bodies.

Inner Plexiform Layer

This contains the external, or 'OFF' layer, of synapses with 'OFF' bipolar cells, ganglion cells and certain amacrine cells; a central, or 'ON' layer, encompassing synapses with the axons of 'ON' bipolar cells and the dendrites of ganglion cells and displaced amacrine cells; and an innermost 'rod' layer, comprising synapses with rod bipolar cells and displaced amacrine cells (Wässle & Boycott, 1991).

Ganglion Cell Layer

The eighth layer comprises the cell bodies of displaced amacrine cells (at the fovea) and those of the retinal ganglion cells.

Nerve Fibre Layer

The ninth anatomical layer of the retina consists of unmyelinated axons originating from retinal ganglion cells. The thickness of the layer can vary, and it is the only layer in the retina where fibres are free to pass into the optic nerve.

The Internal Limiting Membrane

The final layer of the retina serves as a glial boundary with the vitreous body.

1.1.2.4 The optic disc

The optic disc is both the exit and entry point for the bundled axons of the optic nerve and also for the retinal vasculature. The optic disc is super medial to the posterior pole of the eye, and so lies away from the visual axis. It takes a rounded or oval shape and has a diameter of approximately 1.6 mm in the transverse plane and 1.8 mm in the vertical plane. Because there are no photoreceptors (rods or cones) overlying the optic disc, it corresponds to what is known as the ‘blind spot’ of each eye. The appearance of the disc can vary from one individual to another, and this variation can be attributed to differences in the degree of vascularization between the retina and the optic disc (Kaufman, et al., 1950).

1.1.2.5 The photoreceptors

The photoreceptors form a thin layer, approximately 0.1 to 0.5 mm in thickness on the inner surface of the choroid. The photoreceptors lie in the outer portion of the retina, at the very back of the eye and, consequently, light must pass through almost the entire thickness of the retina in order to reach the photopigments of the photoreceptor.

There are two types of photoreceptors present in the human eye, namely rods and cones. Cones are sensitive to light under photopic conditions in bright light, whereas rods operate most efficiently under scotopic conditions in which a low ambient light intensity prevails. Under mesopic (dusk or early dawn) conditions, both rods and cones are highly active.

The outer segments of both rods and cones contain a photosensitive pigment which are synthesised within the inner segment of the photoreceptor and subsequently transported to the outer segment, where they are incorporated into extensively folded membranes. Thus, the outer segments of the photoreceptors contain all of the components necessary for the conversion of light into an electrical signal, whereas the inner segments contain most of the components necessary for the metabolism and homeostasis of the cell.

The spatial distribution of the rods is very different from that of the cones (see figure 1.3). Rods are entirely absent from the foveal centre of the human retina. The average diameter of the rod-free zone is approximately 0.35mm, or 1.25°. The highest rod densities (175,000 rods/mm^2) are to be found along an elliptical ring at the eccentricity of the optic disc, extending into the nasal retina with the point of highest density typically occurring within the superior retina. The human retina contains between 80 and 110 million rods, whereas the number of cones is about 4 to 6 million (Curcio, 1990).

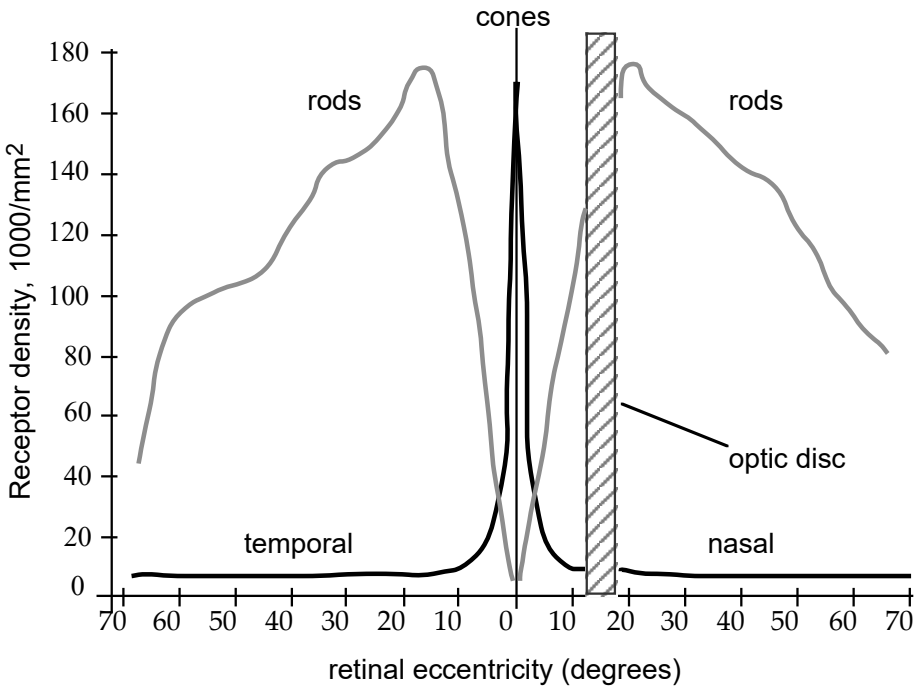

Figure 1.3. Distribution of rods and cones across the human retina (replotted from Østerberg (1935)).

Humans and primates possess a single type of rod photoreceptor which contains a single photopigment, known as rhodopsin. Rhodopsin has a peak absorption of visible light at around 507 nm. Unlike rods, human cones do not all contain the same photopigment, enabling sensitivity to different wavelengths within the visual spectrum. In a typical human subject, there are three different cone photopigments, with each cone containing only one type of photopigment. The three cone photopigments are called erythrolabe, chlorolabe, and cyanolabe. These three photopigments show peak absorbance at 565 nm, 535 nm, and 430 nm, respectively (Figure 1.4), correlating to red, green and blue within the visual spectrum. As such, the cones can be classified into three categories; namely the erythrolabe-containing cones, which are referred to as long-wavelength-cones (L cones); the chlorolabe-containing cones, or medium-wavelength-cones (M cones); and the cyanolabe-containing short-wavelength-cones (S cones).

The spectral sensitivities of each of these classes of cones are not equally spaced across the visible spectrum; but rather, the spectral sensitivities of the L and M cones lie relatively close together (Figure 1.4). Moreover, the spatial distribution of S cones across the retina differs from that of L and M class cones, with S cones constituting only around 10% of the cone population, being absent from the central 1.25° of the retina (Curcio, 1990).

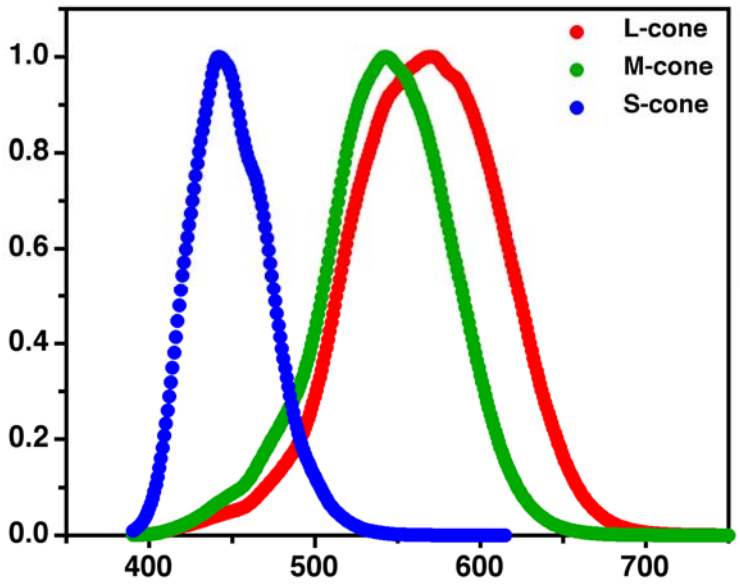

Figure 1.4. Schematic drawing of absorption spectra of the three human cone pigments: cyanolabe (S), chlorolabe (M), erythrolabe (L). *The functions represent relative sensitivities. The y axis displays relative absorbance and the x axis wavelength in nm.*

Our ability to resolve detail, or visual resolution, is substantially superior under phototopic, or daylight conditions. Although rods are able to detect light sources that are much dimmer than cones, cones serve to provide greater resolution and rods superior sensitivity. This may be attributable to several biophysical parameters, including the photochemical gain, or amplification, of the light signal which is greater in rods; the greater density of cones within the fovea; and the degree of convergence of the light signal to bipolar and ganglion cells. As there are more photoreceptors, around 120 million, than ganglion cells (around one million), each ganglion cells receives and summates light signals from an average of 120 photoreceptors (its photoreceptive field). Both rods and cones contribute to this convergence although, owing to their greater number, there is a greater degree of convergence for rods (Sharpe LT, 1993). This phenomenon is known as spatial summation. The cones, on the other hand, summate less, because relatively fewer few cones impinge upon a given ganglion cell. The greater degree of spatial summation by rods affords high scotopic sensitivity but decreased spatial resolution as their signal is diffused across a greater number of ganglion cells (Dowling, 1987).

1.1.2.6 The retinal pigment epithelium (RPE)

The retinal pigment epithelium (RPE) is a monolayer of cells positioned between the retina and choroid. The RPE layer has a neuroectodermal origin and is considered anatomically to be a part of the retina. The RPE layer is darkly pigmented and encompasses the outer segments of the rod and cone cells to capture stray photons, while the basolateral membrane faces the Bruch's membrane. The RPE also serves an important role as part of the blood-retinal interface, or blood-retinal barrier and adjoins the endothelial cells with which it forms very tight junctions. This is essential in regulating the diffusion of molecules and solutes across the barrier, including preventing the entry of toxins, and is this essential for the integrity of the retina (Strauss, 2005). Damage to the blood-retinal barrier or RPE can lead to conditions such as macular degeneration, in which vision is gradually lost or impaired (Bonilha, 2008).

The RPE has a number of important functions (Dowling, 1987), including the:

- Transportation of nutrients, ions and water
- Protection against photo-oxidation and absorption of light
- Responsible for reisomerization of *trans* retinal to 11-*cis* retinal
- Phagocytosis of shed rod and cone membranes
- Secretion of essential factors in order to maintain retina integrity

1.1.3 Post-retinal (photoreceptor) processing

The final stage in the encoding of light information is performed by the retinal ganglion cell layer. The ganglion cells receive signals from specific clusters of photoreceptors within the retina, known as its 'receptive field' which it encodes into action potentials for higher processing within the brain. The receptive field of the ganglion cells may change in response to a number of factors, including light intensity (Dowling, 1987). The receptive fields of the ganglion cells dendritic tree are thus circular, and have two regions, known as the centre and periphery, which are differentially innervated by ON- and OFF-bipolar cells (Dowling, 1987). For instance, the centre ON-receptive field may respond when the photoreceptors corresponding to the central area are illuminated and the periphery is not, and the centre OFF-

receptive fields will respond optimally when the centre is not strongly illuminated while the periphery is.

There are three different types of ganglion cells, namely the parvo, the magno- and the small bistratified ganglion cells, and this classification is based upon the region of the Lateral Geniculate Nucleus (LGN) to which they project (Remington, 2011). The parvo (P) cells represent the largest population of the ganglion cells and have relatively small receptive fields which lie within the fovea. These are ganglion cells which mediate the channels for colour vision, which is a construct of the visual cortex (Sacks, 2012), and receive afferent information from the L and M cones (the 'green-red' pathway) and project to the P laminae of the LGN. The magno ganglion cells are fewer in number than the parvo, have larger receptive fields, and receive afferent inputs primarily from the periphery of the retina and subsequently project to the M laminae of the LGN. In contrast, the small bistratified ganglion cells are responsible for the blue-yellow pathway, receiving inputs from the S cone pathway and project to the koniocellular laminae of the LGN (Brodal, 2010).

The axonal projections of the ganglion cells travel in the direction of the fibre layer at the vitreal surface and then converge in the direction of the optic disc and, ultimately aggregate via the optic nerve. The next synapses within the visual pathway occur within the LGN and, although they are presented with information from both eyes, they receive half of the visual field. The axons from neurons located within the LGN project to the ipsilateral primary visual cortex. Generally, the left primary visual cortex will receive information from the right visual field whereas the right primary visual cortex receives inputs from the left visual field (Remington, 2011).

The higher centres of the visual system which will be considered in more detail are the:

- LGN
- Visual Cortex
- Optic Nerves and Optic Tracts

1.1.3.1 The lateral geniculate nucleus

The optic nerve is comprised of the aggregated ganglion cell axons which exit the eye via the optic disc and terminate within the LGN. There are two nuclei within the LGN, one on each side of the brain and are these are, anatomically speaking, located within the thalamus. Each nucleus of the LGN comprises six distinct cellular layers (Kaas, 1978) which can be differentiated into two layers (see Figure 1.5). The two ventral layers are the magnocellular nuclei and receive inputs from the magno M. These cells originate within the perifoveal region and are responsible for processing movement and motion. The dorsal layers are the parvocellular nuclei and receive information from the P ganglion cells. These cells are particularly sensitive to colour and fine detail. Each layer receives independent impulses from each eye, and so layers 1, 4 and 6 receive information from the contralateral eye and layers 2, 3 and 5 from the ipsilateral eye. Between each layer, the koniocellular layers were later discovered and these are believed to receive inputs from the smaller bistratified ganglion cells (Casagrande, 1994).

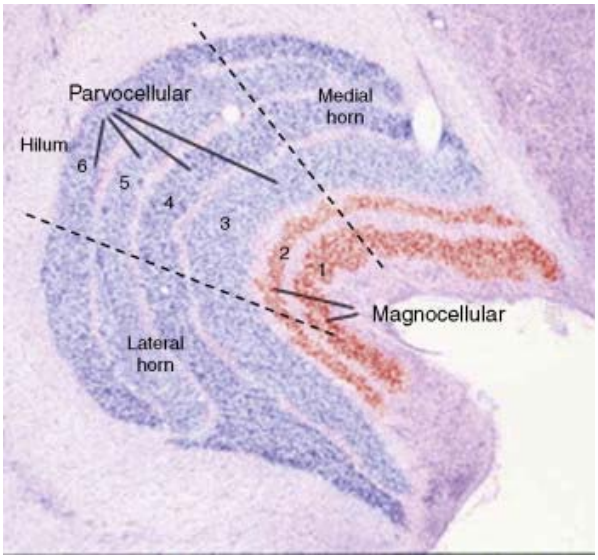

Figure 1.5. Layers of the LGN. The two lowest layers of the LGN are the magnocellular nuclei; layers 3 to 6 are the parvocellular nuclei, and between the parvo layers may be found the koniocellular layers (from https://psyc.ucalgary.ca/PACE/VA-Lab/Brian/neuralbases.htm.)

1.1.3.2 The visual cortex

The majority of the afferents from the LGN project to the Primary Visual Cortex. The Primary Visual Cortex, which is also called the Striate Visual Cortex or V1, lies in the occipital lobe at the rear part of the brain (Brodal, 2010). V1 comprises six layers of cells and is approximately 1.5mm thick and has a striated appearance. The axons from the parvo cells of the LGN terminate within laminae 4Cβ and 4A; while those of the magno cells terminate within 4Cα. This information is duly processed and projected to other layers of V1 from 4Cα to 4B, from 4Cβ to layers 2, 3, and, ultimately, to other areas of the visual cortex for higher processing.

As the primary visual cortex (V1) is the first cortical structure to receive afferent neurons from the lateral geniculate nuclei, it is responsible for primary processing of the information from the retina, including visual space, orientation, wavelength (as a substrate of colour) and form (Tovée, 1996). The major outputs of V1 project to V2, which processes stereopsis and object direction. V2 projects its outputs to V3 and V4, where both colour and form are thought to be analysed and constructed (Zeki, 1993), and MT/V5 (medial temporal lobe), where depth and motion are analysed (Zeki, 1974). These regions in turn project to the superior colliculus, the higher visual areas (V7, V8), and the posterior parietal core (which is responsible for spatial perception), as well as various subdivisions of the thalamus. In addition, each of these regions projects back to the area or areas from which it receives input.

Chapter 2. Spatial vision and visual performance

2.1 What limits spatial vision in visual performance?

Over the years, various optical tests have been developed and refined to assess the resolution and quality of the retinal image as well as the efficacy of post-retinal processing.

We can divide these into three main categories which relate to:

- The study of the anatomic characteristics of the neurons and other structures of the eye that are essential for the understanding of the flow of visual information.
- Neurophysiological tests, such as single cell electrophysiology or whole brain or retinal electrophysiology, study the processing of the optical information within the visual pathway.
- Psychophysical experiments which study the functional characteristics of the optical system by testing the relationship between variations in the physical pattern of stimuli and perceptual responses (*i.e.* what an observer sees and reports).

2.1.1 Spatial vision

Visual perception is mediated by variations in physical parameters, such as size (subtense), colour, motion, differences in luminance (contrast), depth and texture. Visual science thus places great emphasis on measuring sensitivity across a wide range of parameters under a broad range of conditions. However, most of measurements in ophthalmology are focused upon evaluating sensitivity to “spatial detail”. This is not surprising, as advanced visual processing takes place at the post-retinal stage, whereas pre-retinal factors (optics) principally affect spatial visual performance (i.e. by attenuating image resolution and/or contrast). Spatial vision refers to our ability to resolve or discriminate detail within the spatial domain (Varadharajan, 2012). Spatial visual performance is usually studied using a range of techniques, such as measures of visual resolution (acuity), contrast sensitivity, hyper-acuity, peripheral vision, and binocular depth perception.

2.1.2 Visual resolution – visual acuity

Visual resolution defines the “sharpness” of vision; that is the capability to recognize the details of objects (Tovée, 1996). For the purposes of tests, spatial resolution is defined as the ability of the best corrected eye to distinguish two points in space as being distinct and separate. Visual acuity is thus a psychophysical method for assessing the quality of the optical image and has certainly become the preferred test for estimating the spatial resolution of the visual system in both clinical and preclinical research. It refers to an “angular measurement relating testing distance to the minimal object size resolvable at that distance” (Eperjesi, 2004), known as the visual angle. Today, the measurement of visual acuity (VA) has become the universal standard procedure for assessing the integrity of the visual function.

2.1.2.1 Methods for assessing visual acuity

Testing for VA is an essential component of the routine ophthalmological examination and is also employed as part of the basic set of diagnostic examinations in the detection of underlying ocular pathology. It also comprises one of the principal criteria that establish visual “fitness” for driving a vehicle or visual “readiness” for many occupations, including professional pilots.

The medical assessment of VA usually involves letter recognition. However, although the ETDRS (Early Treatment Diabetic Retinopathy Study) charts (Sloan, 1959) have been widely adopted by the ophthalmologic and optometric communities as the international standard for basic and clinical vision research (see Figure 2.1), there are a variety of charts available which may differ in terms of the optotypes used (*e.g.* Landolt C, illiterate E) and the testing procedure (*e.g.* Snellen charts, (Sloan, 1959)).

Figure 2.1. A logMAR chart used in the evaluation of ETDRS acuity.

While the test may appear simple, letter recognition is a complex process, one which requires several different dimensions of retinal (Tovée, 1996). For instance, it involves the optical ability to identify the image, the cognitive ability to recognize the character, as well as the motor capacity to respond to the item as required. In young children or the elderly, there may be a cognitive incapacity to react to or else identify the item, and thus a lack of the expected reaction to a visual cue may not be due to underlying optical or even visual deficits. Therefore, there is a need to understand the limits of resolution of the technique and to minimise the number of cognitive and motor requirements involved in the testing.

2.1.2.2 Effect of contrast and luminance on visual acuity

The degree of contrast and level of luminance both affect the measurement of VA. For instance, VA tends to be adversely affected as the stimulus luminance or contrast is reduced. Fortunately, in terms of the scope of those parameters that are widely used with the clinic, this effect is negligible. If the degree of contrast between the letters and the luminance of the background is reduced to a level where it does affect VA, we speak of a contrast sensitivity test. If the level of illumination is lowered

to threshold values, we may speak in terms of a dark adaptation test (Colenbrander, 2001).

2.1.2.3 High contrast VA

The most common form of VA test is based upon an individual's ability to identify letters of ever decreasing size on a standard eye chart. This type of test is routinely carried out during eye examinations (Heiting, 2014).

2.1.2.4 Variation of VA with degree of eccentricity

VA decreases very rapidly as the position of the image moves further away from the fovea. When a stimulus is fixated upon the fovea, as the human eye tracks and focuses upon it, the equivalent retinal image of that stimulus falls directly upon the fovea. However, when a stimulus mark is presented at a location other than the fixation point, its corresponding retinal image falls outside of the foveal region. As the fovea contains that highest number and density of cones, in addition to being served by a greater number of neuronal connections, this is the retinal region which achieves the greatest level of VA. Thus, the intricate tracking movements of the eye are intended to ensure that objects or images of greatest interest at any given point in time are projected and focused directly upon the fovea (Lane, 2005).

2.1.3 Contrast sensitivity

In addition to considerations of VA, contrast sensitivity is another important parameter within visual perception, and any optical system that provides less-than-perfect focus will reduce edge contrast. One important feature encountered within natural scenes is contrast, i.e. the relative change in luminance across the field of view. Studies have shown that the visibility of any object can be directly related to its degree of contrast which differentiates it from its surroundings and, consequently, the measurement of contrast sensitivity is a key parameter in the testing of vision and visual input. Contrast visibility is however also dependant upon the spatial frequency components of any given object or stimulus.

Therefore, an important measure of visual behaviour is the evaluation of contrast sensitivity (which forms the reciprocal of contrast threshold) for a range of spatial

frequencies, using stimuli known as gratings. This procedure, which can be assessed using various psychophysical methods, results to a function known as the contrast sensitivity function (CSF) (see Figure 2.2).

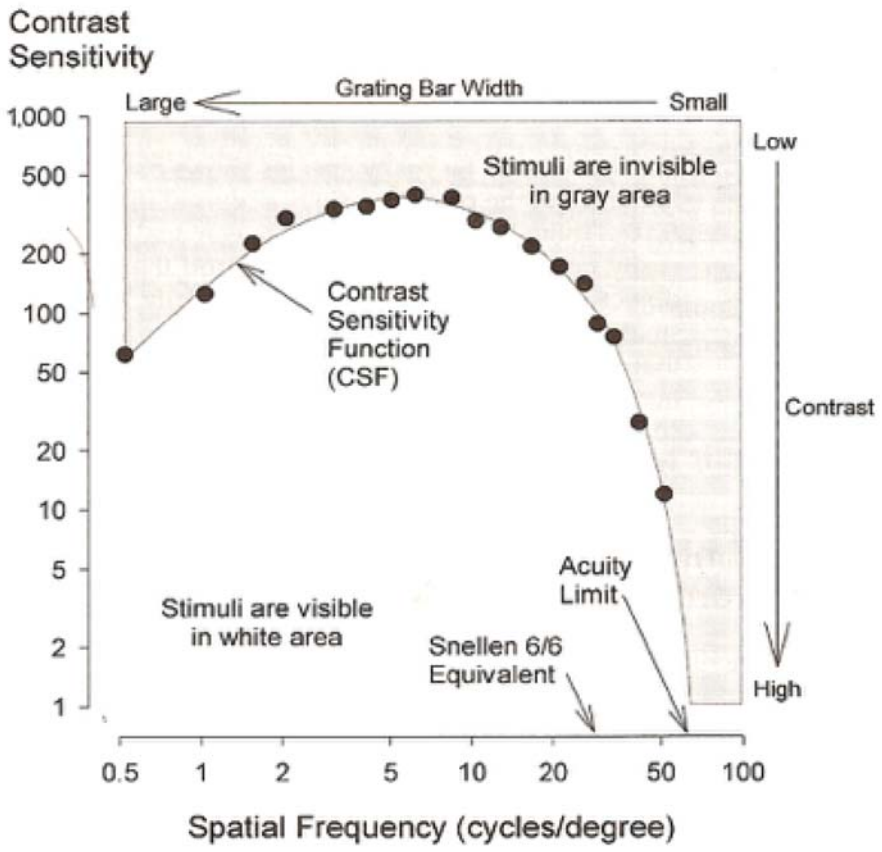

Figure 2.2. A typical contrast sensitivity function (Norton, Corliss et al. 2002)

The CSF has a characteristically inverted U-shape, and the areas below and above the line represent the areas where the individual gratings are visible (below) and invisible (above). From this function the peak contrast sensitivity can be determined. For humans, peak contrast sensitivity normally lies between 3 and 10 cycles per degree, depending on the luminance and degree of light adaptation, with a limit of resolution in the healthy eye of around 60 cycles per degree (Barten, 1999). From this we may infer that, as only a selective range of spatial frequencies are detected, this means that the visual system in effect works as a band pass filter.

Fortunately, the visual system is quite 'forgiving' for moderate reductions in contrast for large objects (*i.e.* at low spatial frequencies). For smaller objects, such as letters, which occur at higher spatial frequencies, the effect is more noticeable.

A loss of contrast may occur as a result of optical factors, such as the refractive error, presbyopia, higher-order aberrations, or scatter, and may arise from cataracts or other opacities. Contrast perception also depends upon the sensitivity of the retinal photoreceptors and on the ability of the retina to adapt to changes in background illumination (Reuter, 2011).

However, the phenomenon of low contrast sensitivity may occur even with good VA. Due to interaction of many factors in contrast perception, establishing a differential diagnosis in a case of contrast loss is not always easy. Detecting a contrast deficit may however be helpful in explaining the patient's symptoms, especially in such instances where VA is otherwise unaffected. This is certainly the case in specific eye conditions, such as cataracts, glaucoma, or diabetic maculopathy. Changes in contrast sensitivity may also arise as a consequence of refractive surgery.

2.1.4 Binocular summation

The acuity, sensitivity and depth perception of the visual system with two eyes is substantially enhanced relative to that which would be expected for just one eye alone, or even the average of the output of two eyes taken individually (Stidwell & FLETCHER, 2011). Greater sensitivity makes objects which are small, dim or fast-moving appear more visible. This phenomenon is called *binocular summation*. Binocular summation is dependent upon the phenomena of binocular overlap and fusion which will be discussed in further details below.

Assuming that the visual system integrates both signal and uncorrelated noise from the two eyes, a physiological model has been proposed which gives a linear binocular summation ratio (the ratio of binocular to monocular sensitivities) equivalent to a factor of $\sqrt{2}$ (Campbell and Green, 1965). This could simply be explained by the greater probability, due to the use of two independent detectors, of detail being accurately presented to and detected by the photoreceptor mosaic. Early experiments proved that the increase in binocular sensitivity is in actual fact greater

than the classical theoretical value of √2, a phenomenon which is explained by probability summation (Matin, 1962). It was later found that some cells in the visual cortex, when they receive input from both eyes simultaneously, display the phenomenon of binocular facilitation (Hubel & Wiesel, 1982). This led to the widely accepted idea that binocular summation may arise through both probability summation, noise averaging, and some other physiological mechanism that further enhances binocular vision (i.e. neural summation). It should be noted, however, that the improvement in VA with binocular viewing at high contrast is less evident, ranging from 5% to 13%, although this does not correlate to the theoretical gain in VA of √2 (41%).

2.2 Effects of normal aging

Aging affects all aspects of the human optical system as a consequence of structural and physiological changes, affecting many aspects of visual performance and spatial vision (Gordon, 2000).

2.2.1 Changes in the optical media

2.2.1.1 Cornea

Unlike the lens itself, the corneal form and structure do not tend to alter markedly with age. Nonetheless, some optically relevant changes do take place. Although, corneal curvature, thickness, and refractive index remain essentially constant, there is usually a slow drift from predominantly with-the-rule (direct) to against-the-rule (inverse) corneal astigmatism, largely as the result of steepening in the horizontal meridian and some change in the asphericity of both the anterior and posterior surfaces.

Light scattering within the cornea increases only modestly with age. The observed age-dependent decline in corneal sensitivity are however of interest. For instance, the decline in endothelial cell density may be accelerated by cataract surgery as the loss of endothelial cell function may cause an increase in corneal thickness which will induce corneal decompensation and a resulting loss of vision (Böhnke, 2001).

2.2.1.2 Iris and pupil

The iris, through dilation and constriction, adjusts the pupil to maximize DoF according to the ambient light level (Kaufman, et al., 1950). The pupil diameter under constant lighting conditions reduces progressively with age, a phenomenon referred to as senile miosis (Sioan, 1988). The smaller pupil of the older eye may actually be beneficial in reducing the impact of ocular aberrations and light scatter, by increasing depth-of-focus, thereby protecting the already vulnerable older retina from phototoxic damage (Sioan, 1988). On the other hand, senile miosis results in a reduction in retinal luminance, which may adversely affect visual performance under photopic light levels, the resulting reduction in useful light flux reaching the retina having a modest impact upon vision under mesopic and scotopic levels of illumination (Owsley, 2011).

2.2.1.3 Lens

The lens undergoes a gradual change in its dimensions, the curvature of its surfaces, and refractive index distribution owing to the progressive addition of new fibres as it ages. In the unaccommodated state, the surface radii decrease with age, although there is little change in lens diameter. These changes, together with the changes in the refractive index gradient, are likely to affect the optical power and lead to aberrations of the optical performance of the eye.

The non-cataractous lens also suffers from a gradual loss in transmittance (*i.e.*, an increase in optical density), particularly at the blue end of the spectrum, which is caused by increases in light absorption and scattering.

The most significant effect of the aging lens is the loss in accommodation, caused by its changing shape, which limits the ability of the eye to focus on objects at close distances (Koretz, et al., 2002). This condition is known as presbyopia and is the most common ocular affliction. Accommodative ability progressively declines in an almost linear manner with age, from the early teens onwards, with presbyopic symptoms generally arising in the age range of 40 to 45 years (Sher, 1997). This is in stark contrast to other aspects of visual performance, which typically only start to decline at the age of 50.

2.2.1.4 Aqueous and vitreous humour

Due to its constant replenishment, the aqueous humour normally retains its clarity and refractive index throughout life, although its translucency can be reduced by conditions such as uveitis. As the eye ages, the outflow of aqueous humour may decrease, increasing intraocular pressure, which can lead to the development of glaucoma.

2.2.1.5 Axial length

Although there have been numerous transverse and longitudinal studies on the changes in axial length from infancy and childhood to young adulthood, the possibility of further changes in later life has received little attention. One exception to this is the work of Grosvenor (Grosvenor, 1988), who hypothesized, based on the transverse studies of Sorsby et al. (1958, and other related works), that axial length decreased by approximately 0.6 mm (equivalent to a hyperopic shift of roughly 2.00 D) through adulthood, and that this played a role in compensating for changes in the refractive power of the eye and maintaining approximate emmetropia. However, no longitudinal studies appear to have been conducted to follow up this hypothesis.

2.2.1.6 Changes in refraction with age

Although refraction in individual eyes may follow divergent courses, with myopic shifts in childhood being notably common, it appears that slow drifts in mean spherical refraction typically occur in all eyes. The broad trends are illustrated in Figure 2.3. As can be seen, there is general agreement that a progressive reduction in levels of hyperopia in childhood and early adulthood is followed (Myrowitz, 2012), at the approximate age of 40, by a gradual drift back toward low hyperopia, with the strong suggestion of a reversal of this trend around the age of 70. Data of this type can be criticized on the basis of possible patient selection effects, but the observed trend of a hyperopic refractive shift of approximately 1.00 D between the ages of 40 and 70 years appears real (Elliott, 2003) and poses problems for the long-term effectiveness of some forms of surgical presbyopic correction.

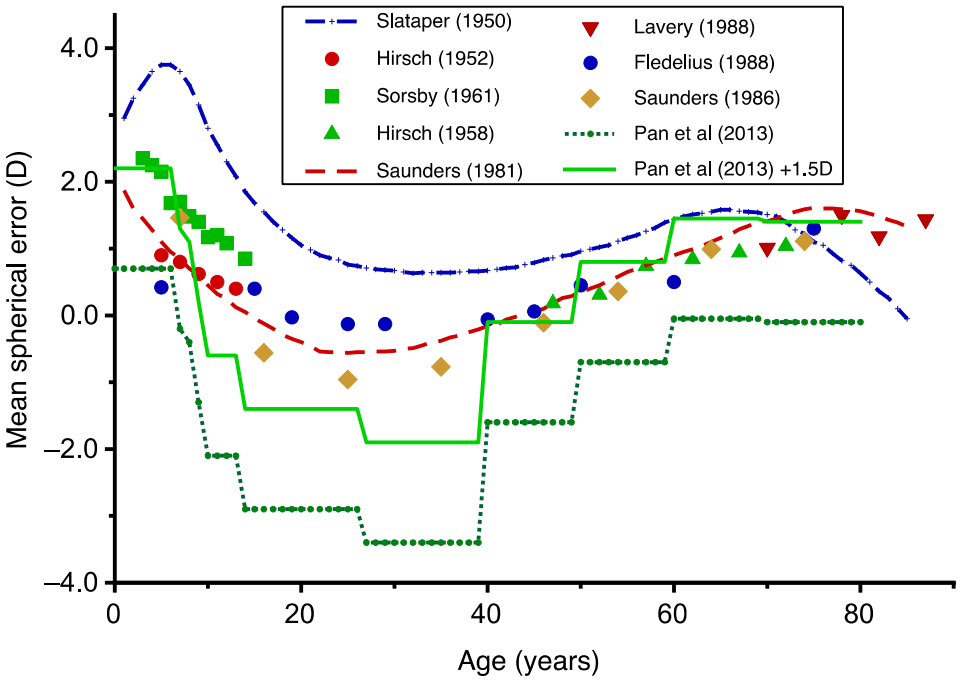

Figure 2.3. Changes in mean ocular refraction with age as observed in different cross-sectional studies. The continuous curves are studies based on self-selected clinical patients, and the isolated symbols are based on randomly selected, non-clinical groups. Absolute levels of refraction differ between studies as a result of factors such as patient selection criteria and the use of either overall means or modes (redrawn from Plainis and Charman, 2015).

2.2.1.7 Overall retinal image quality

Overall retinal image quality is affected by both wavefront aberration and scattered light. Because both increase with age, it would reasonably be expected that image quality at a constant pupil diameter would be reduced in the older eye.

Optimal vision necessitates the transparency of all elements of the visual axis of the eye and proper refractive shape of the lens and cornea. Any loss of transparency or surface aberrations may cause associated wavefront aberrations and light scattering errors which are commensurate with a reduction of visual quality. As both the cornea and lens must be almost perfectly transparent and maintain a smooth and stable curvature to focus the image precisely upon the retina without any distortions, a simple test for VA is not necessarily indicative of secondary light scattering, as this requires the measurement of back and forward light scattering (Spadea, 2016).

Image quality can be directly measured using double-pass techniques. The double-pass technique has been widely employed for sixty years (Flamant, 1955), and is based upon the recording of images of a single point source which is projected onto the retina after retinal reflection and a double passage through the ocular media (Artal, 2000). This serves to demonstrate the marked reduction in monochromatic modulation transfer at all spatial frequencies that occur within the normal older eye in comparison with a younger eye of the same pupil diameter.

2.2.2 Neural changes in the aging eye

2.2.2.1 Photoreceptors

The transduction of light into electrical energy is differentially affected by the following aging processes (Jakobczyk-Zmija, 1995):

- There is a decline in the number of rods.
- Cone density remains relatively constant in the foveal region.
- Cone density is reduced somewhat within the peripheral retina.

2.2.2.2 Ganglion cells

- Number of retinal ganglion cells that serve the macular region tends to decrease with age, thereby reducing the number of axons in the optic nerve (Calkins, 2013).
- The neural layer of the retina thins with age.

2.2.2.3 Retinal pigment epithelium

As the RPE provides essential metabolic support for the photoreceptor layers, participates in recycling of the outer segments and also absorbs stray light, any loss in terms of the integrity of the RPE may have profound effects upon VA and the processing of light information (Bonilha, 2008).

- During the aging process there may be a tendency for the accumulation of the yellow pigment lipofuscin within the RPE and a loss of the brown pigment

granules containing melanin, leading to damage and degeneration of the RPE (Constable, 1995).

- Deposits, called drusen, can also accumulate within the RPE. The degeneration of the RPE that is a key characteristic of AMD has been attributed to the accumulation of intracellular lysosomal lipofuscin and extracellular drusens, which may be further exacerbated by a deterioration in the vascular supply to the RPE. The intracellular accumulation of lysosomal lipofuscin and extracellular drusens may lead to a decline in the cellular housekeeping in aging RPE cells and an associated degeneration of the retinal photoreceptor layer (Kaarniranta, 2011). These deposits decrease the efficiency of the metabolic exchange between the RPE and the photoreceptors, and thereby contribute to the age-related loss of photoreceptors.

2.2.2.4 Visual pathways

Although the numbers of both "Parvo" and "Magno" cells within the LGN appear to decline with age, the loss appears to be slightly greater for Parvo cells (Yoonessi, 2011).

The primary visual cortex (V1) where most of the LGN axons synapse, also shows some changes with age (Brewer& Barton, 2012) which can be summarized as follows:

- There is evidence of decreased synaptic density and dendritic degeneration with advancing age.
- Signal transmission from axon to axon is decreased.
- Cortical cells become more broadly tuned in their response to orientation.
- Neural density in the cortex is however relatively stable as we age.

2.2.3 Age changes in visual performance

One of the major tasks of neural mechanisms in the human visual system is to overcome or otherwise circumvent problems which are created by the imperfect optics of the eye which increase with age.

2.2.3.1 Changes in spectral sensitivity

The limits of sensitivity across the visual spectrum depend upon the absorption characteristics of the eye's optics at shorter wavelengths and the photopigment absorption spectrum at longer wavelengths. As the ocular media, primarily the lens, increase in density with age, so sensitivity to shorter wavelengths progressively declines, becoming apparent in middle age.

Psychophysical studies have quantified the age-related losses in visual sensitivity under both scotopic (dark adapted) and photopic (light adapted) conditions (Steven, 1946). While early studies documented changes in dark adaptation (thresholds measured as a function of time) which affected both branches of recovery in light sensitivity (Steven, 1946); the first branch being mediated by cone photoreceptors and the second by rods. Not only are the asymptotes of each of these branches elevated, but the rate of photopic and scotopic dark adaptation also decreases with age (Gunkel & Gouras, 1963; Jackson et al., 1999).

More recent studies have sought to separate the effects of the reduced pupil area and increased optical density of the elderly eye from neural losses in sensitivity. It is clear from these studies that age-related losses in visual sensitivity arise partly due to pre-retinal changes in the optical pathway and partly due to neural losses that occur within the photoreceptors and neural pathways.

2.2.3.2 Changes in colour discrimination

Losses in visual sensitivity which occur with age arise due to a reduction in the level of light reaching the retina and a reduced sensitivity of the photoreceptors. These changes could be viewed as consistent with the notion that an older person is similar to a younger person, although effectively operating at a reduced light level. Because visual performance often depends on luminance, some changes in the elderly eye can be simulated by a reduction in light level, as is the case for colour discrimination (Barbur & Rodriguez-Carmona, 2015).

As with cone sensitivity losses, hue discrimination as measured with standardized arrangement tests, declines with age, beginning in adolescence or early adulthood.

When chromatic discrimination is tested under conditions that equate stimuli for individual subjects at the retina (i.e., corrected for pupil size and ocular media density), losses are observed throughout the colour space for both spectral and non-spectral stimuli (Werner, 2016). These studies demonstrate that age-related losses in chromatic discrimination are due, in part, to changes in neural pathways.

It is reasonable to expect that the effects of lens *brunescence* (a yellowing of the lens) would cause a shift colour perception in the elderly, owing to the effects of band pass filtering. In fact, although the colour appearance of short-wave stimuli is initially modified by yellow filters, such short-term effects of spectral filtering are not the same as the long-term adaptation to the slowly changing lens colouration that is associated with aging. Studies have however demonstrated that colour perception is surprisingly stable across the lifespan when tested with colour-naming methods using spectral lights, reflective surfaces, and simulated Munsell samples (Shinomori, 2005; Kinnear and Sahraie, 2002).

2.2.3.3 Changes in spatial vision

In clinical settings, spatial vision is usually defined by visual acuity, which is the minimum angle of resolution as measured with high contrast symbols and moderate illumination. A wide range of results have been reported, with some older studies reporting that visual acuity is stable until approximately the age of 50 years before progressively declining (Figure 2.4).

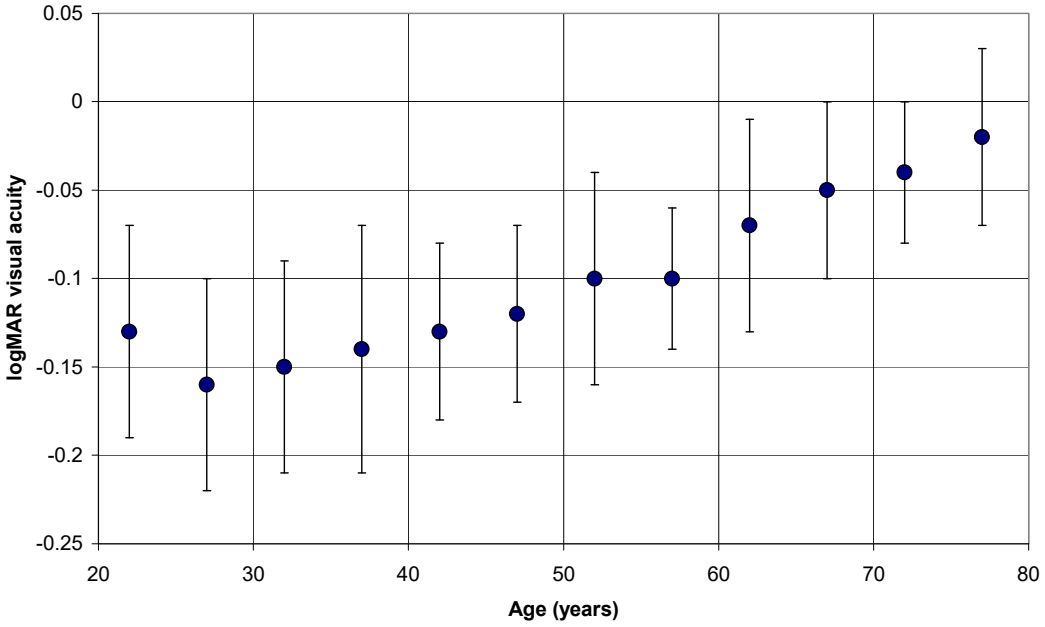

Figure 2.4. Mean and standard deviation of the high-contrast logMAR visual acuity of normal eyes. Each point refers to the mean of eyes within a 5-year interval (from Elliott *et al.* 1995). As the large error bars indicate, there is large intersubject variability at every age.

A more complete characterization of spatial vision is provided by the CSF as measured with sinusoidal gratings of varying spatial frequency. Under photopic conditions, a greater age-related sensitivity loss is reported for high as compared with low spatial frequencies (Gillespie-Gallery et al., 2013). As with most other performance characteristics, careful studies that refract subjects for the test distance and screen for ocular and retinal disease tend to reveal nearly linear changes in VA as a function of age after adolescence or early adulthood. These losses have been attributed to both optical (e.g., smaller pupils, greater ocular media scatter and absorption) and neural factors (Madden, 1987).

This study clearly demonstrates that neural factors may set upper limit on how much vision can be improved with compensation of higher-order aberrations in the elderly (Elliott et al., 2009).

2.2.3.4 Changes in temporal vision

The classical method for assessing temporal resolution in vision is the Critical Flicker Frequency (CFF), which is defined the lowest frequency at which an image is experienced as a fused entity and therefore not discriminable from a steady stimulus. Because the CFF declines with retinal illuminance, studies that do not control for age-related changes in ocular media transmission invariably find losses in temporal resolution in the elderly. For example, it has been reported that the CFF falls from around 40 Hz in the twenties to about 32 Hz in the sixties (Schraffa, 1964).

As with acuity in the spatial domain, CFF characterizes only the high temporal resolution of an individual. A more complete characterization of the visual system is provided by the temporal CSF. Direct measurements of the temporal CSF reveal small age-related losses that are greater for higher temporal frequencies (see Figure 2.5). These results are generally consistent with those quantifying temporal vision using a psychophysical measure of the temporal impulse response function, which is the theoretical response to a stimulus of infinitely short duration (Shinomori&Werner, 2003).

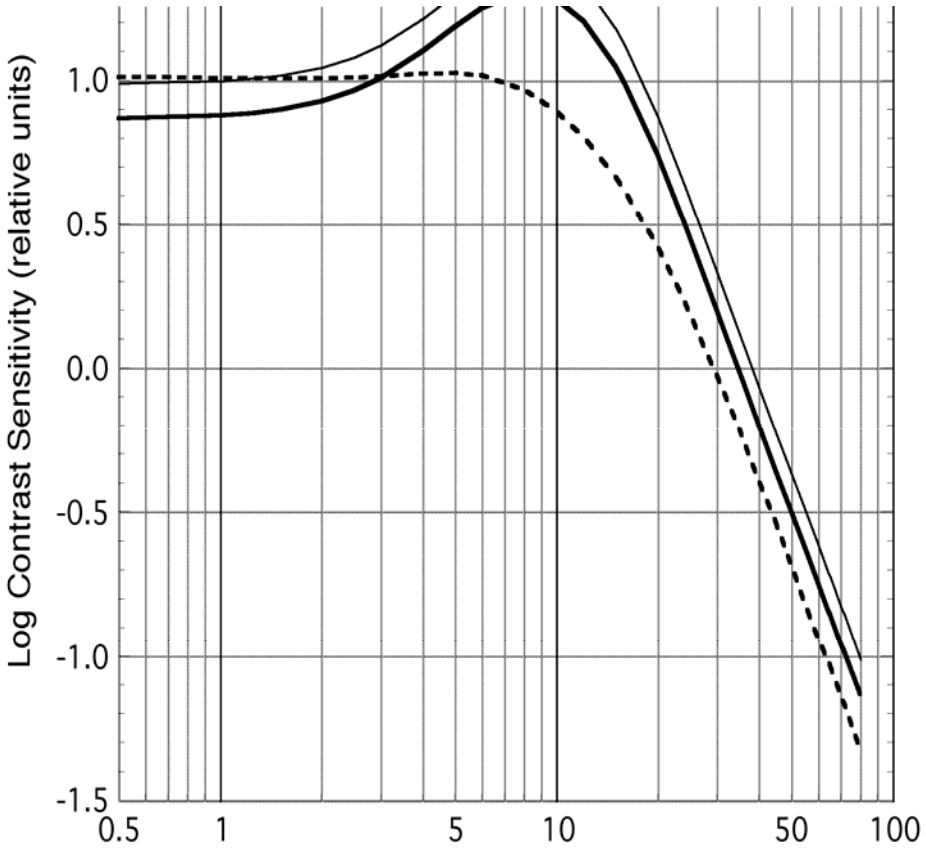

Figure 2.5. Temporal contrast sensitivity functions. Log contrast sensitivity plotted as a function of temporal frequency for a theoretical 20-year-old subject (grey solid curve) and 80-year-old subjects with either normal (black solid curve) or no inhibition (dashed curve). The peak sensitivities for the young and older subjects correspond to 1.3 and 1.4 log units **(Shinomori&Werner, 2003)**.

2.2.3.5 Changes in binocular vision and stereopsis

Tests for binocular vision provide a valuable probe for evaluating age-related changes in cortical mechanisms. Clinically, it is important to understand binocular vision in relation to refractive corrections that affect the two eyes differently (*e.g.*, monovision), especially if aging has selective effects on binocular integration.

One index of binocular integration is based on the summation of signals to the two eyes, such as the improvement in contrast sensitivity measured binocularly versus monocularly. Theoretically, binocular viewing is expected to improve contrast sensitivity by a factor of approximately $\sqrt{2}$ over monocular viewing. This value is in agreement with data obtained for young individuals. However, for elderly individuals,

binocular summation is significantly reduced (Pardhan, 1996), which likely represents a degradation in cortical binocular neurons at some level.

A more specialized function of cortical binocular mechanisms is to mediate stereopsis based on retinal disparity for objects at different distances from the point of fixation. Stereopsis refers to the depth information that the visual brain is able to extract from the differences in perspective arising between retinal images owing to the lateral separation of the two eyes. With standardized tests, stereo resolution - the minimum retinal disparity that can be detected - decreases with age. This could, in part, be due to changes in spatial vision at a monocular level. To control for this, Laframboise et al. (2006) measured the binocular correlation required for different thresholds, where binocular correlation is the first step in achieving global stereopsis (Lankheet & Lennie, 1996) which declines with decreasing distance from the plane of fixation (Faubert, 2006). They found that the binocular correlation required to perceive stereo depth was significantly higher in older than in younger observers.

2.2.3.6 Changes in peripheral vision

Age differences in spatial vision tend to be more pronounced within the visual periphery than in central vision (Sekuler R, 1980). The mean binocular visual field, as measured by the ability to detect small light targets in the visual periphery, drops from 180 degrees in young adulthood to around 140 degrees by the age of 70 (Nelson-Quigg, 2000). Factors that are known to contribute to this loss include:

- The age-related reduction in retinal illuminance.
- A reduced density of photoreceptors in the periphery of the retina.
- Greater deficits for short wavelength targets implicating a loss of peripheral short-wavelength (S) cone photopigment.
- Deficits in neural mechanisms.

2.3 Ocular disease in the elderly

2.3.1 Common diseases of vision in the elderly

There are a range of visual impairments that are associated with disease in the elderly. These include cataract, glaucoma, diabetes, vascular disease and AMD (Gordon, 2000). As this thesis will address visual impairments in patients presenting with AMD in more detail, other common impairments of vision among the elderly will be discussed only briefly.

2.3.2 Cataract

Cataracts related to the process of aging can lead to partial or full vision loss and are characterized by a slow but progressive thickening and yellowing of the crystalline lens (Ocampo, 2015). Cataracts are the most common cause of vision loss in individuals over the age of forty and the main cause of blindness across the world. There are also some suggestions that the formation of cataracts are triggered by oxidative alterations in the human lens (Baily, 2014).

Although cataract can cause a decrease in VA, disability glare, a myopic shift in refraction, and monocular diplopia (Ocampo, 2015), not to mention an increase in intraocular light scatter, which can lead to a decrease in retinal image contrast, affecting mainly contrast sensitivity (Shadi, 2010).

2.3.3 Glaucoma

Glaucoma refers to eye diseases which are associated with damage to the optic nerve and vision loss, if left untreated (Trope, 2011). Despite a variability in its aetiology, the major risk factor for most glaucomas is an increase in intraocular pressure arising via the failure of drainage of the aqueous humour via the trabecular meshwork (Alguire, 1990), and is associated with the displacement of the optic nerve head owing to a loss of retinal ganglion cells (Albert, 1996). The two common tests for glaucoma are tonometry, which measures intraocular eye pressure caused by ocular hypertension, a major risk factor for chronic open-angle glaucoma, and a visual field test, known as perimetry, which assesses missing areas of vision (ROSENRTHAL&WERNER, 1969).

2.3.4 Diabetes

Diabetic retinopathy (DR) is a common feature of diabetes, affecting up to 80% of sufferers, and is associated with damage to the retina leading to a dysfunction of the neurons of the inner retina (Cunha-Vaz, 2011). As the formative stages of the disease, known as non-proliferative diabetic retinopathy (NPDR) are usually without overt symptoms, the disease can rapidly progress to macular oedema which is characterised by a blurring and subsequent rapid loss of vision. DR is readily detected by standard tests for VA, pupil dilation, an examination of the retina using an ophthalmoscope, fluorescein angiography, and optical coherence tomography (Taylor& Batey, 2012).

2.3.5 Age-related macular degeneration

AMD is by far the leading cause of blindness among the older population within industrialised countries, affecting between 20% and 25% of those aged over 70 and giving rise to approximately 50% of those registered as blind in England and Australia (Boretsky et al., 2012).

AMD is a progressive degenerative condition of the central retina (the macula), which is characterised by a steady reduction in central vision. The early clinical signs of AMD are large, soft drusen and pigmentary changes within the central retina. At this stage, visual acuity is usually only slightly affected. However, as the condition advances, yellow debris from photoreceptors, known as drusen, accumulate within the extracellular matrix below the RPE layer, leading to damage of the photoreceptor cells owing to a failure of metabolic supply by the RPE (Kinnunen, et al., 2012) by mechanisms which are thought to be similar to those induced by light damage (Organisciak&Vaughan, 2011). The changes in the photoreceptor layer are progressive, eventually leading to decreased macular vision. Early AMD frequently progresses to late AMD in which central vision is severely damaged by atrophic changes (in dry AMD) or choroidal neovascularisation and subsequent scarring (in wet AMD). The dry form of the disease is most common, yet may lead to the development of the wet form (DeAngelis, 2016). However only 10% of the population who have dry AMD clinically progress to develop the wet form. As a result dry AMD

is the most prevalent form of the condition, corresponding to approximately 85-90% of known cases (Klein *et al.*, 2011).

The dry form of AMD is characterized by deposition of drusen (Figure 2.6), which is one of the earliest biomarkers associated with AMD. As the drusen increase in size, vision is impaired and, as the disease progresses, there is a gradual loss of RPE cells which leads to the degradation of central vision (Holz et al., 2001, Curcio et al., 2000, Curcio et al., 1996) which can frequently be identified with the Amsler grid, which detects perceived distortions of the grid stimulus, in combination with optical coherence tomography and angiography (Jackson, 2008).

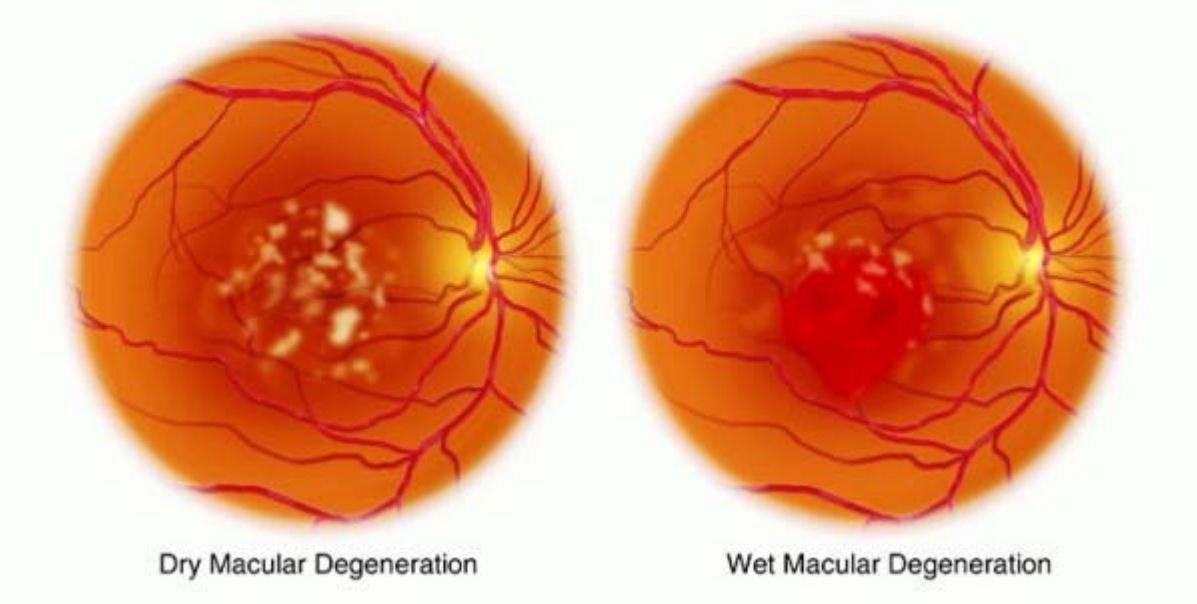

Figure 2.6. Comparison of dry and wet forms of AMD (from http://wilsoneyecentre.com.au/conditions-treatment/macular-degeneration/macular-degeneration-treatment/).

The wet form of AMD is characterized by the abnormal growth of blood vessels originating from the choroid beneath the macula, which eventually break through Bruch's membrane and sometimes even the outer blood retinal barrier itself (Lim, 2012). Although its causation remains largely unknown, this process is referred to as choroidal neovascularization, and leads to the leaking of blood and other fluids

into the retina. This extravasation leads to a distortion of vision as well as the development of blind spots and changes in foveal and parafoveal vision which significantly impair VA. The presence of the abnormal blood vessels eventually leads to scarring of the retina which consequently leads to the permanent loss of central vision.

There are however many gaps in our understanding of AMD, and the early aetiology of the disease is particularly puzzling. Although there may be an inherited component, common risk factors include smoking, high blood pressure, elevated cholesterol, and diabetes (McKendrick, et al., 2007).

Those presenting with macular degeneration in its early form may not display any overt symptoms although, as the disease progresses, patients may experience a distortion affecting foveal vision (i.e. dark and blurry regions), one which can impair all aspects of macular vision; including acuity, reading, colour perception, and so forth.

Patients presenting with AMD may be severely visually handicapped and unable either to drive or to read. The rapid onset of blindness at such an advanced age means that AMD patients frequently have problems adapting to their condition and require care. Although AMD is a common condition, there are relatively few treatments available for this condition, although injections of anti-VEGF antibodies have been shown to be successful in reducing inflammation .and slowing down the progression of AMD (Mitchell, 2011).

2.4 The phenomenon of visual snow

Another major aspect of this thesis is a study of the loss of VA and light scattering in patients presenting with visual snow (VS, Figure 2.9), a rare condition in which ‘intrinsic’ noise is present in the visual image under all light conditions (Raghavan, et al., 2010). Owing to its association with a number of other symptoms, including palinopsia (visual trailing and afterimages), photopsia, blue field entoptic phenomenon, photophobia, tinnitus, and impaired night vision, it is now widely believed to be a neurological condition, although few studies have been conducted to date (Ghannam & Pelak, 2017; Schankin, et al., 2013).

This thesis will address specific aspects of vision in VS patients, including VA.

Figure 2.7. Subject presenting with visual snow accessed from http://behdad.org/mirror/www.braindecoder.com/what-its-like-to-have-visual-snow-syndrome-1582715658.htm.

Chapter 3. Does normal binocular vision improve the accommodation response?

3.1 Introduction

Binocular vision results from the interaction of two normal monocular visual systems by integrating and cross-referencing their inputs within the higher processing centres of the brain. Binocular single vision is achieved by fusional eye movements, mediated by the extraocular muscles of the eye, which serve to keep objects at various distances from the eye focused upon the corresponding regions of the retina which yield the of greatest acuity. The two monocular representations of the external world are then combined into a single image within the visual cortex to provide additional contextual information through the process of binocular fusion, a mechanism which results in the integrated perception of these two different images with the benefit of stereopsis and enhanced acuity (Rogers, 1995).

A crucial question is whether there are fundamental differences in visual performance between monocular and binocular viewing conditions in functions that do not involve stereopsis. Many studies have shown that binocular vision confers significant advantages through an enlargement of the field of vision, owing to the overlap of the two “smaller” monocular fields (see Figure 3.1).

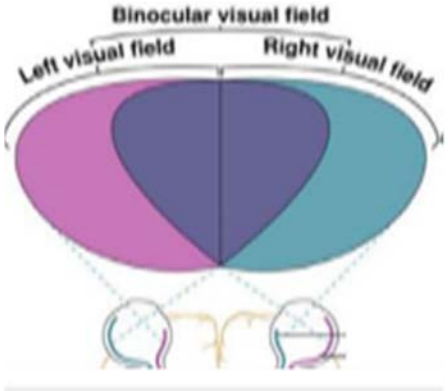

Figure 3.1. The enlarged binocular field of view compared to the two “smaller” monocular fields (from http://www.d.umn.edu/~jfitzake/Lectures/DMED/Perception/VisualCortex/TopographicMaps.html).

As the eyes converge when fixating upon a near object, so the vergence angle becomes larger. When fixating upon a far object, the eyes diverge and so the vergence angle becomes smaller (see Figure 3.2). This angle serves as a binocular

cue for depth perception (Mather, 2006). However, it should also be noted that depth perception can also be achieved monocularly through monocular cues such as motion parallax (Mather, 2006), which is the relative motion of an object against the background, or the perspective of an object, although in every case, binocular cues have proven more efficient for depth perception (McKee & Taylor, 2010). In terms of binocular summation, a series of classical psychophysical investigations into the predicted versus actual advantages of binocular vision was conducted by examining several threshold visual tasks, including increment detection, flicker fusion, brightness magnitude, and contour resolution (Fox & Blake, 1973). The landmark study concluded that, 'the two eyes are better than one for many visual tasks, but not by very much' (Fox & Blake, 1973). The binocular summation observed was, more or less, the 1.4-fold enhancement predicted by the probability summation model (Townsend, 1968).

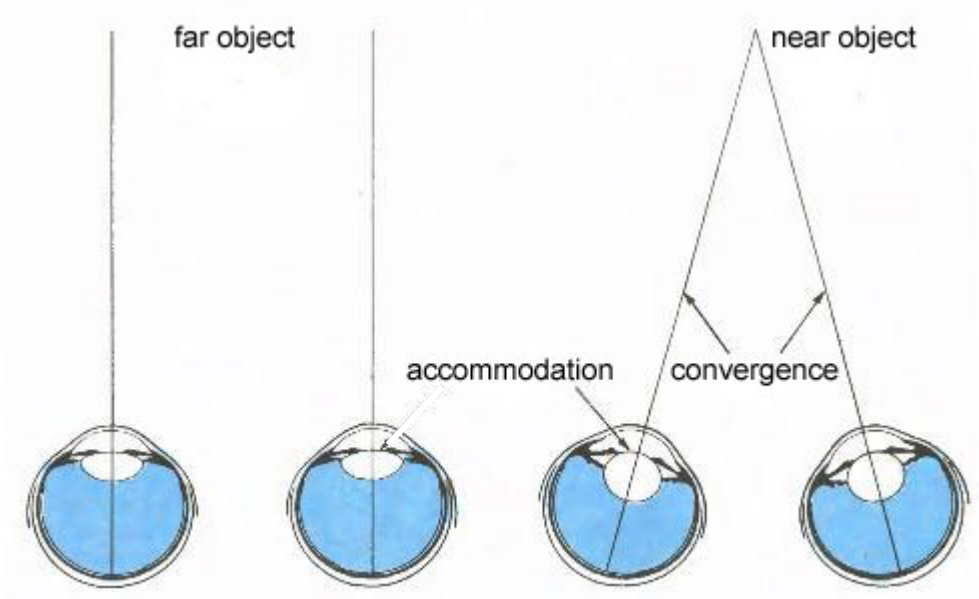

Figure 3.2. Near viewing is achieved through convergence of the two eyes (right), while distant vision is achieved through divergence of the eyes (left), thereby affecting the angle of vergence (α) (from http://www.forbestvision.com/accommodation-and-convergence/).

Visual performance is also enhanced when using both eyes in other tasks such as detecting camouflaged objects, reading, or tasks that involve hand eye coordination and depth perception (Sheedy, 1986). The benefits of binocular summation are also

indisputable in terms of VA, with an improvement of around 5 to 10% *(Cagenello, et al*., 1993), although this was found to depend strongly on luminance (Home, 1978). Binocular summation also predicts improved fixation stability under binocular viewing conditions as compared to monocular viewing. Intriguingly, greater fixation instability has been observed during monocular as compared to binocular viewing (Gonzalez, 2012), especially for the occluded eye. This study also showed, in agreement with previous studies, that both microsaccades and drifts are fewer in number and reduced in their amplitude during binocular viewing.

Binocular enhancement also occurs at the 'brightness level', as the interaction between visual channels in the binocular processing of brightness information strongly infers a partial summation of monocular brightness, especially when they approach equality (Curtis & Rule, 1978). Further evidence in terms of the advantage of binocular over monocular vision arises in the enhancement of visually evoked responses, an electrophysiological measurement that demonstrates significant levels of binocular cooperation at the cortical level (Heravian, 1990).

3.2 Accommodation

In general, the VA one can achieve is influenced by many stages of visual processing, including the involvement of binocularly driven neurons. When the subject views near or distant objects, changes in accommodation and the positioning of the two eyes follow in order to produce sharp images on the retina that map accurately the corresponding points in the visual field to ensure accurate focusing of the twin images. This binocular process of accommodation is strongly associated with changes in the shape of the crystalline lens, a mechanism which is important in keeping visual information focused on the fovea over a range of object distances. Accommodation is driven mainly by image defocus as related to object proximity, while vergence is primarily driven by retinal disparity (Walton, 1957).

3.2.1 Basic mechanism of accommodation

Some 150 years ago, von Helmholtz (1924) remarked that,

> "there is no other subject in physiological optics about which so many antagonistic opinions have been entertained as concerning the accommodation system of the eye" (Helmholtz, 1924).

Since that time, much progress has been made, and there is now broad agreement on how mechanisms of accommodation operate in human vision. If we consider the available optical components of the eye it is clear that, in principle, various mechanisms could actively serve to change ocular focus to produce sharply focused retinal images of objects across a range of distances. These may include a change in corneal curvature, axial movement of the crystalline lens, a change in the power of the lens, or a change in axial length.

As pupillary miosis is usually observed in near vision. It was therefore suggested that the associated increase in DoF may be sufficient to render an active change of focus unnecessary and that the same effect could be achieved via multifocality in the lens. However, classical experiments (Young, 1801) successfully eliminated most of these possibilities and confirmed that a change in lenticular power was a crucial factor, as had long been postulated (Descartes, 1677). Subsequent experimental findings have fully supported Young's basic conclusion (Charman, 2008), although there is still some disagreement as to whether very minor changes in corneal curvature, axial length, and lens position occur during accommodation.

How is the required change in the shape and power of the crystalline lens achieved? The classical view is that both the lens and its capsule are elastic, and that the shape of the isolated lens is determined by the balance between these elastic forces. This balance results in the isolated lens and capsule taking up their most accommodated form, with steeply curved surfaces. However, within the eye, the lens is supported by the meridionally oriented zonule fibres that are attached in the region of the lens equator (see Figure 3.3).

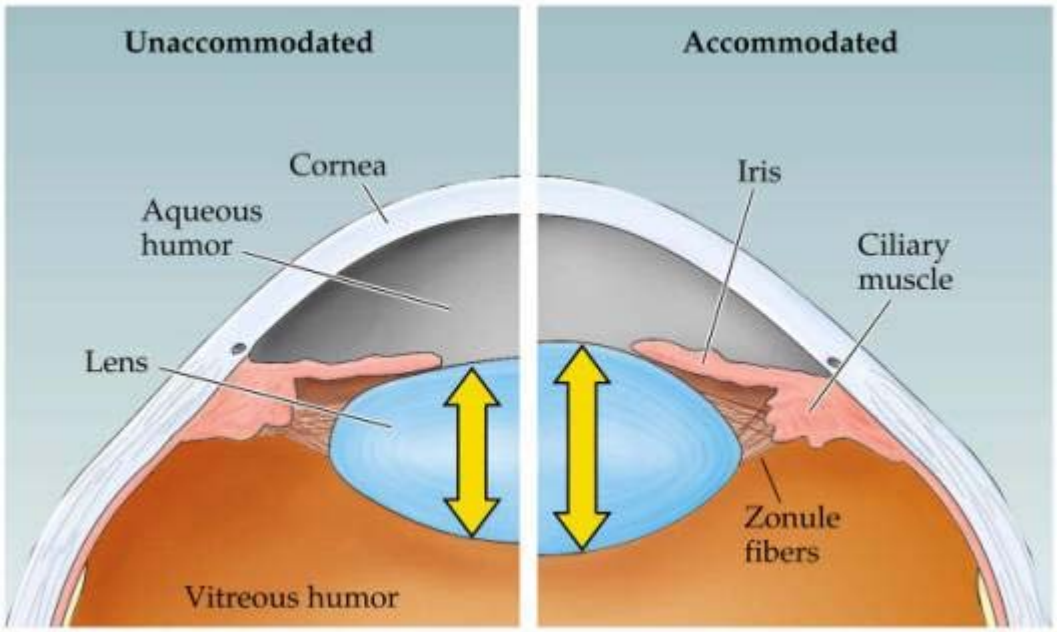

Figure 3.3. Mechanism of accommodation of the human lens through changes in the tension of the zonule fibres radiating from the ciliary muscle (from http://www.rci.rutgers.edu/~uzwiak/AnatPhys/NPSpringLect4_files/image006.jpg).

Depending on their tension, these fibres apply additional forces to the capsule, which are then distributed by the capsule across the lens to alter its three-dimensional shape. Rohen (1979) suggested that three distinct sets of anterior zonular fibres are attached near the lens equator (Rohen, 1979). Two of these sets are attached approximately 1.5 mm anterior and posterior to the lens equator respectively, and the third, finer set is attached along the equator itself. In direct contradiction, Glasser and Campbell (1999) asserted that the attachment of these anterior fibres is essentially continuous across the equatorial region of the lens, with many fibres cross-crossing other fibres (Campbell, 1999). Additional long posterior (or peripheral) holding fibres extend forward from the *pars plana* to pass through the valleys between the ciliary processes, while shorter tension fibres insert into the ciliary epithelium. The ciliary muscle thereby acts as a unit, although it contains a mixture of meridional, radial, and circular muscle fibres. The circular fibres run around the free edge of the ciliary body, just behind the root of the iris (Delamere, 2005).

When the accommodation of the lens is “relaxed” for distance vision, the apex of the ciliary muscle is of a relatively large diameter and the anterior zonular fibres are

stretched by tension from the posterior pars plana fibres. The resultant tension in the anterior zonule exerts strong radial forces on the capsule, thereby tending to stretch it. Consequently, the balance of forces on the substance of the lens causes it to be flattened and its ‘power’ to decrease to a value appropriate for distance vision. In parallel with these changes, the lens diameter tends to increase while its thickness is reduced.

In contrast, the accommodation required for near vision results from the contraction of the ciliary muscle. This causes the bulk of the muscle mass to move forward and toward the axis, thus reducing the diameter of the ciliary ring. This in turn reduces the tension in the anterior zonular fibres and the force they exert upon the lens capsule. Thus, the combined lens-capsule system can change toward the more powerful form that it assumes when isolated *in vitro*. The surface curvature and lens thickness both increase, and the lens diameter is thereby reduced, with a consequent increase in the power of the lens.

3.2.2 Changes in lens parameters

The changes in lens radius which occur with accommodation are greater for the anterior surface of the lens (Yap, 1997; Rosales, 2006), possibly because the tensional changes are greater in the more anterior zonule and the anterior capsule is thicker and hence capable of exerting a greater elastic force on the lens body (see Figure 3.4). As the lens thickens during accommodation, its anterior pole undergoes marked forward movement, with a consequent reduction in the depth of the anterior chamber, and there is only a minor posterior movement of the rear lens surface (Drexler, 1997). Some typical data for these changes are shown in Figure 3.4, although these values vary with other factors such as age.

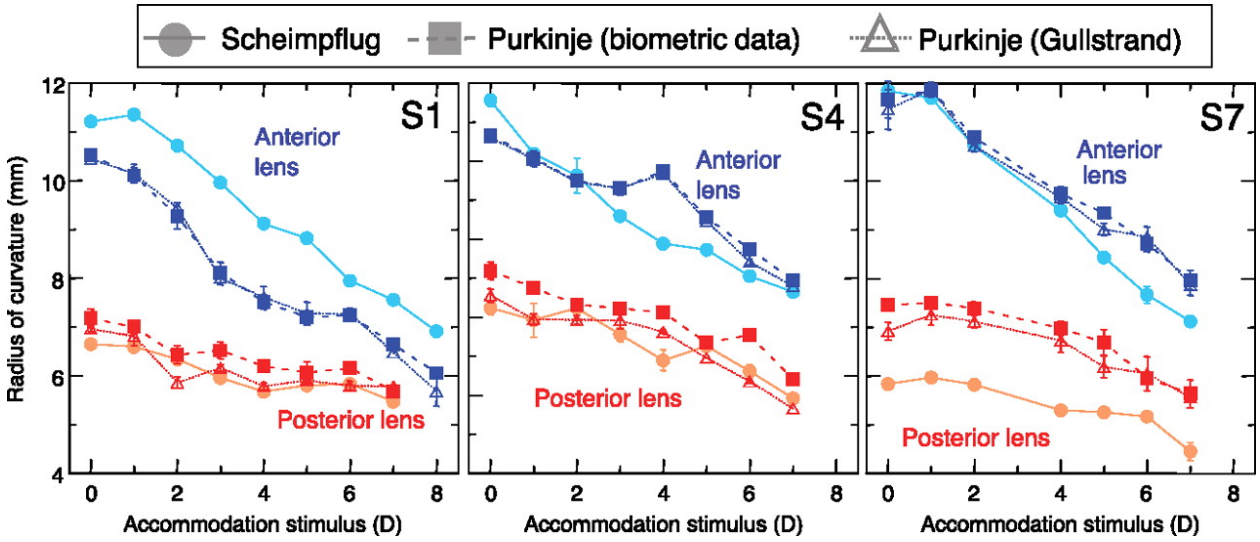

Figure 3.4. Change of anterior and posterior lens radii of curvature as a function of accommodation in three individual eyes (Rosales, 2006).

3.2.3 Components of accommodation

A variety of factors influence the final accommodation response achieved when the eye is presented with a near object of interest. Heath (1956) suggested that the response has several components:

1. Reflex accommodation is a quasi-automatic adjustment of refractive state over, perhaps, a 2.00-D range to maintain a sharp retinal focus of the object of regard. There are, however, some doubts as to whether a true involuntary reflex is present because many normal individuals fail to accommodate when presented with modest amounts of defocus, particularly under monocular conditions.

2. Proximal accommodation triggered by knowledge (or a belief of knowledge) of the distance of the object.

3. Convergence accommodation, driven by fusion disparity vergence.

4. Tonic accommodation, the slightly myopic refractive state to which the system reverts in the absence of an adequate accommodative stimulus.

3.2.4 Accuracy of the steady-state accommodation response

Because the accommodative control system generates a signal to minimize image blur on the retina, it would be expected that optimal accommodative performance, resulting in an in-focus retinal image, would automatically be achieved for the full range of distances within the objective amplitude of accommodation. However, it is now well accepted that steady state errors in focus are an idiosyncratic feature of the accommodation system as noted by Charman (2010). The system is characterized by over-accommodation for far targets, known as “lead” of accommodation, and under-accommodation for near targets, known as “lag” of accommodation. When the mean steady-state response is plotted as a function of stimulus vergence (accommodative demand), then a quasi-linear response/stimulus curve of the form shown in Figure 3.5 is found.

As shown in Figure 3.5, the response/stimulus slope varies substantially between individuals. It is also age dependent and is affected by inherent ocular characteristics such as spherical aberration, pupil size, and the nature of the stimulus (its contrast, form: letter versus grating, spatial size and colour (Plainis et al, 2005)). All of these factors are known to influence ocular DoF. It is also well known that the slope becomes flatter (i.e., errors in focus are more pronounced) with increasing age (Heron, 2004). The observed increase in accommodative errors is mainly due to the decreased accommodation ability with age. Figure 3.6 shows that the subjective amplitude of accommodation undergoes a steady reduction with age. Note that the difference between binocular and monocular subjective amplitude of accommodation may range up to 1.50 D or more (Otake, 1993), the average difference being approximately 0.60 to 0.70 D for ages up to 18 years, 0.50 D for ages between 19 and 30 years, and 0.40 D for ages between 31 and 50 years. Binocular viewing has also been shown to increase the accuracy of the accommodative response (Ibi, 1997)

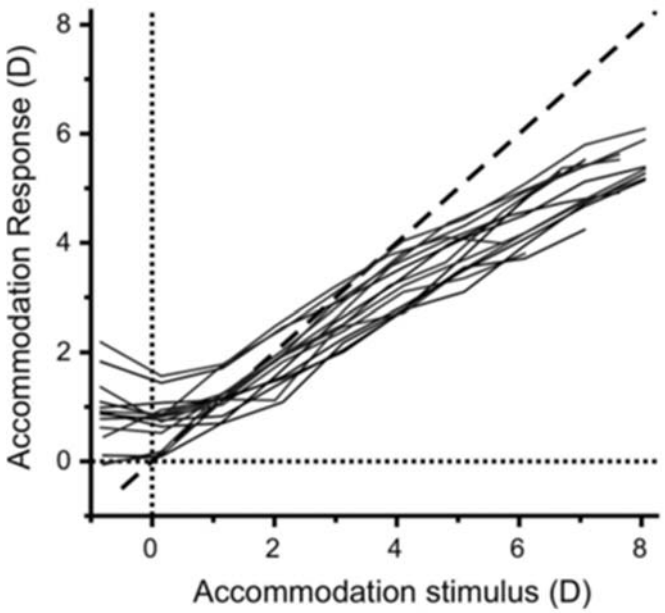

Figure 3.5. Accommodation response/stimulus curve under constant photopic conditions. The dashed line represents the ideal one-to-one relationship required for "perfect" focus Accommodation was measured using a wavefront analyser (COAS, AMO Wavefront Sciences Ltd, Albuquerque, NM) in conjunction with a purpose-built Badal optometer (from Plainis et al., 2005.)

Accommodation is driven by signals generated in cone photoreceptors. Thus, it is expected to be less effective under low lighting conditions. It has been shown that the errors in focus within the accommodative response become progressively higher as luminance is decreased (i.e., the response/stimulus curve becomes flatter), thus pivoting about the point for which stimulus and response are equal (Johnson, 1976). At scotopic levels of illumination, when only rods are active, the accommodative system ceases to function, and the response remains constant at its myopic dark focus or tonic level, which is one of the components of accommodation as classified by Heath (1956). Several studies have investigated the accommodation response in the absence of a stimulus or in complete darkness, suggesting that the tonic level has a mean value of approximately 1.00 D (Owens, 1978), although it varies dramatically amongst individuals.

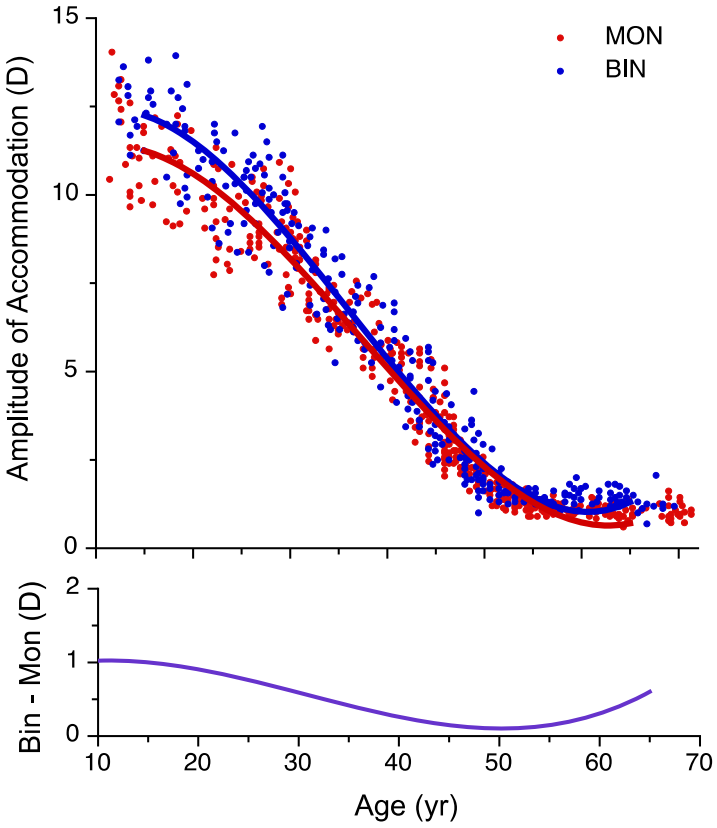

Figure 3.6. Comparison of binocular (blue dots) and monocular (red dots) amplitudes of accommodation (upper) and their difference (lower) as a function of age. (Based on data compiled and replotted from (Duane, 1912).

3.2.5 Stability of the accommodative response

Under all conditions, the accommodative response is not steady but rather changes rapidly and continuously. These small oscillations in the dioptric power of the eye, called microfluctuations, typically have values of between 0.20 and 0.50 D (*for review see Charman, 1988)*). Their main frequency spectrum, which mainly extends up to a few hertz, shows two distinct peaks, corresponding to a low- and a high-frequency component. The low-frequency component is thought to be at least partly under neural control, and the higher-frequency fluctuations are associated with factors such as heartbeat and breathing. The magnitude of the fluctuations, although varying considerably among individuals, tends to increase in conditions in which perceived contrast is decreased for small pupils and as the target approaches the eye (Gray, 1993). The increased level of fluctuation for very near stimuli may result from increased instability of the lens, as the lens zonules relax during accommodation. Under the same stimulus conditions, microfluctuations are slightly reduced in older as compared with younger eyes, perhaps because of reduced elasticity in the lens zonules and/or capsule (Gray, 1993).

3.2.6 Dynamics of accommodative response

Changes in focus when accommodating (far to near, or FN), or when relaxing accommodation (near to far, or NF) are not achieved instantaneously (Charman, 1988). In the presence of a typical 2.00 D step stimulus, there is a reaction time (latency) of about 300 to 400 ms before the accommodative response begins (Anderson, 2010). In addition, there is a response time of about 400 to 1000 ms, during which the accommodation changes before stabilizing at its new level. Response times relate to the amplitude of accommodation needed, but not when the demand is to relax accommodation. The reaction time is fairly constant for similar levels of accommodation/relaxation, whereas the response time is shorter for relaxation in both young and old patient groups, when the only cue to accommodation is blur. This can be appreciated more readily if one of the relative step responses is inverted for direct comparison (Figure 3.7). However, studies suggest that, within the amplitude of accommodation, the dynamic characteristics decline only modestly with age, wherein the FN is faster in younger individuals (and more sluggish in older individuals), while the NF response is faster in older patients (Heron, 2004).

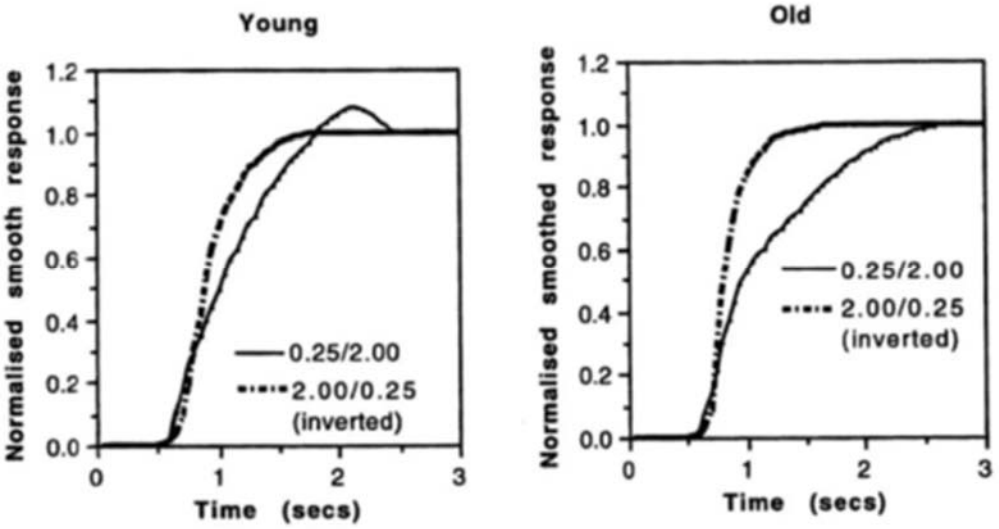

Figure 3.7. Responses of young (left) and old (right) patients to both directions (accommodation, far to near [FN], vs relaxation, near to far [NF]) of stimulus change between 0.25 and 2.00 D. The NF responses are shown inverted to allow direct comparison of their temporal profile with the FN responses (from Heron and Charman, 2004).

3.3 Purpose of study

The purpose of this study was to establish whether binocular vision confers any measurable advantage during the process of accommodation. As for most aspects of visual processing, a binocular advantage is predicted when fusion is achieved, although whether the proposed advantage is significant remains to be established. In theory, a binocular advantage during the process of accommodation would present as a higher accommodative response, whereby the refractive state of each eye would be more myopic (in a myopic shift) or less hyperopic (in hyperopes). In early presbyopes, a binocular advantage would suggest that having two eyes may in fact serve to delay the symptoms of presbyopia, wherein monocular individuals or severely binocularly impaired individuals may experience earlier symptoms of presbyopia. Within this study, monocular and binocular refractive responses at near, intermediate and far distances are evaluated. Differences in binocular and monocular refractive responses are analysed and compared at varying distances and between subject groups, namely non-presbyopes and early presbyopes.

3.4 Materials and methods

3.4.1 Study population

Sixty-two (62) subjects were recruited from the student and staff population at City, University of London. Subject selection was according to the following inclusion criteria following individual optical examination: no binocular anomalies compromising binocular function such as strabismus or amblyopia or a history of such; no ocular diseases; intact fundus and an overall healthy ocular status, with clear ocular media and normal binocular status. Subjects were also required to have a minimum best corrected visual acuity of 6/6 (which corresponds to an acuity of 1 min arc also referred to as 20/20 vision or 0 on the LogMAR scale). VA was measured in each subject using a high contrast Bailey-Lovie LogMAR back-illuminated chart at a distance of six meters.

The age range of subjects tested varied from 18 to 57 years, with the average age being 33.1±11.4 years. Subjects were divided into two categories by age; namely

presbyopes (age 41 to 57 years) and non-presbyopes (18 to 40 years). The likely presbyopes were selected from a population aged 41 and above who presented with reading glasses (to enable the detection of early onset), with a view to comparing differences in the accommodation response between presbyopes and non-presbyopes at each vergence distance. After assessing their compliance with the inclusion criteria, 6 had to be excluded. A total of 56 subjects finally participated in this study.

As expected, the presbyopic group showed reduced accommodation amplitude (as measured subjectively and objectively), but only presbyopes > ~ 52 years are expected to have small or close to zero remaining accommodation. In terms of refractive error, twenty-five subjects were myopic, with myopia defined as a mean spherical equivalent refraction greater than -0.50D; twenty-nine subjects were emmetropic, with emmetropia defined as a mean spherical equivalent between -0.50 and +0.50 D. Two were hyperopic, with hyperopia defined as anything greater than +0.50 D. Refraction was performed at a distance of 3m (vergence = 0.33D). The mean spherical equivalent for the myopic subjects was -3.00 D, with range -0.56 to -5.00 D, whilst the emmetropic subjects had a mean spherical equivalent of -0.03 D, with range -0.50 to +0.50 D.

Subjects participating in this study derived from a wide range of ethnic backgrounds and all experimental procedures were conducted in accordance with the City University of London research and ethical guidelines. The procedures involved and the purpose of the study were explained in detail to every subject before informed consent was obtained (see Appendix B). The flow diagram illustrated in Figure 3.8 presents the breakdown of the subjects.

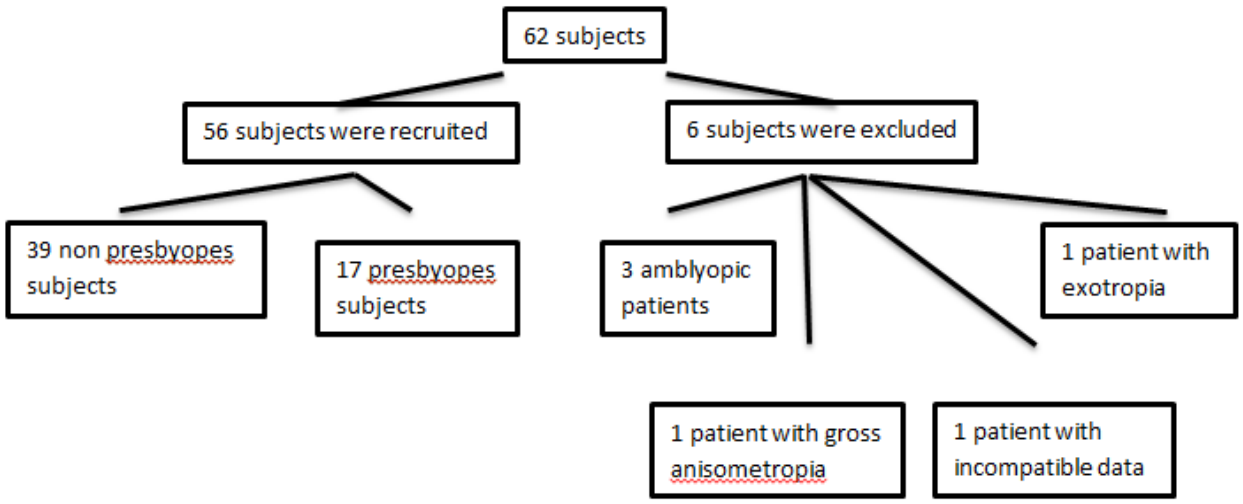

Figure 3.8. Inclusion criteria and breakdown of experimental subjects (*nota bene*. one patient had data that was incompatible with the normal range of accommodative responses).

3.4.2 The autorefractor

The experiment was conducted using the Shin Nippon NVISION-K 5001 infrared, open view refractometer. This instrument measures objectively the overall refraction at different object distances (vergences), both monocularly and binocularly. The binocular open field of view facilitates the binocular refraction to be evaluated when a natural environment (scene) is viewed. This is achieved by measuring monocular refraction when both eyes are open. The experiment was conducted in a darkened room to ensure that pupil size was controlled mostly by the display chart luminance and that the influence of other peripheral stimuli was minimised. The instrument has been shown to provide precise and reliable on-axis refraction as compared with subjective refraction (Gilmartin, 2003). Finally, the absence of an internal fixation target or enclosed viewing reduces the risk of proximal accommodation and enables the observation of real-world targets across a range of environments (Ciuffreda, 1991).

The instrument's LCD monitor allows viewing of the pupil and facilitates alignment of the instrument head with respect to the subject's visual axis. It also displays refractive and keratometric data. A focus detector enables precise focusing of the instrument in modes measuring corneal curvature (see Figure 3.9).

Figure 3.9. Instrument's LCD monitor display of pupil alignment (left), Binocular open view refraction at distance (middle), refraction at near (right). The Figure is reproduced from the operation manual for the Shin Nippon NVISION-K 5001 infrared open view refractometer.

The refractive state and keratometric values are calculated by analysing the image of an infrared light ring target after reflection off the retina. Initially a lens is moved on a motorized track to place the ring in focus. Once it has been refracted by the optics of the eye, the image formed is analysed digitally through multiple meridians to calculate the toroidal refractive prescription derived from the distances from the digital image. Due to the improved optical design and image sensor, the instrument facilitates accurate refraction measurements to be taken in small pupils of up to 2.3 mm and with inter-pupillary distances up to 85 mm (Gilmartin, 2003).

3.4.3 Experimental procedure

All subjects with a refractive error were required to be fully corrected at distance to enable accurate quantification of accommodation changes and thus subjects were encouraged to wear contact lenses to avoid potential errors in autorefractor measurements caused by use of spectacles. This was the ideal correction, as contact lenses eliminate the effect of spectacle magnification and any prismatic effects induced by trial lenses as well as minimising artefacts caused by reflections. Only 15 of 56 subjects wore spectacles, and no high myopes or hyperopes were included in the study. The target was a high contrast contoured letter with a black aperture to reduce the effect of crowding and to maintain fixation. The use of such a target also results in reduced microfluctuations during accommodation which have been shown to increase as the contrast of the accommodative target decreases (Bour, 1981).

All 56 subjects were refracted at far (6m, 0.16D vergence) and near (0.33m, 3.0 D vergence) distances, while 33 were also refracted at an intermediate distance (0.5m, 2.0 D vergence). However, as the more distant correction for all subjects was achieved for 3m (0.33D vergence), the corresponding accommodation demands for the three conditions were: -0.17D (0.16-0.33 D), 1.67 D (2.00 – 0.33 D) and 2.67D (3.00 – 0.33 D), respectively.

To minimise micro fluctuations in accommodation, we employed a back-illuminated tests chart of high luminance with close to 100 percent contrast letters. In order to ensure the contrast remained high, the ambient light level in the room was low mesopic. To ensure consistency in the data, the results for each measurement were taken in triplicate and the average refraction was recorded. The order in which the readings were taken was as follows: right eye binocularly; then left eye binocularly; then right eye monocularly; and finally, left eye monocularly. The refraction was measured first at far, then at intermediate, and finally at near distances.

Two subjects were tested at the same time of day on both days, and the order of presentation was altered (see table 3.1) as follows to determine whether the order of presentation affected the outcome. The outcome was analysed using paired-sample t-test that showed statistically insignificant ($p>0.05$) and was also analysed using Wilcoxon signed-rank test that exhibited insignificant results ($p>.001$).

First day	RE bino	LE bino	RE mono	LE mono
After 15 minutes	LE mono	LE bino	RE bino	RE mono
Second day	RE mono	RE bino	LE bino	LE mono
After 15 minutes	RE bino	RE mono	LE mono	LE bino

Table 3.1. Order of presentation of stimuli in accommodation experiments over two days.

3.5 Results

The correlation between spherical equivalent and sphere for the right eyes of all participants at 'far' distance (under binocular refraction condition) is shown in Figure 3.10. It is evident that spherical equivalent is, on average, about 0.20 D more hyperopic as compared to "sphere", although the slope is parallel to the 1:1 relationship, meaning that either of the two can be used. Similar trends were found for all distances and under all measurement conditions. We decided to use spherical equivalent, since it contains both the spherical and astigmatic components, which are expected to influence the response. Further analysis was thus performed for the spherical equivalent conditions.

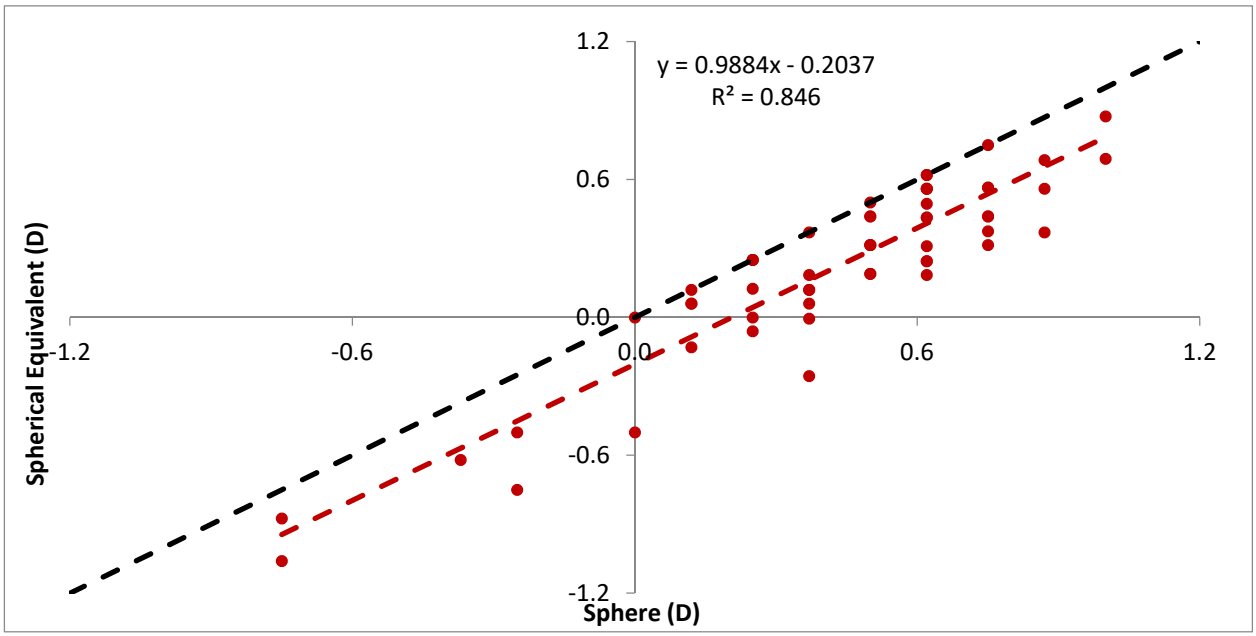

Figure 3.10. Correlation between spherical equivalent and sphere. The dashed black line represents the 1-1 function. Data comes from far, binocular refraction of the right eyes.

3.5.1 Intraocular differences in accommodative response

Figure 3.11 presents accommodative responses at all distances for each condition (*i.e.* Right Eye and Left Eye under binocular viewing and Right Eye and Left Eye under monocular viewing conditions). It is evident that the response is accurate (1:1) at the 'far' distance, while a lag in accommodation comes into play as the target comes nearer. Moreover, the difference in accommodative response between the

left and right eyes is not found to be significant. However, it should be noted that data from 33 subjects were collected for the intermediate distance, as compared to 56 subjects for both far and near distances.

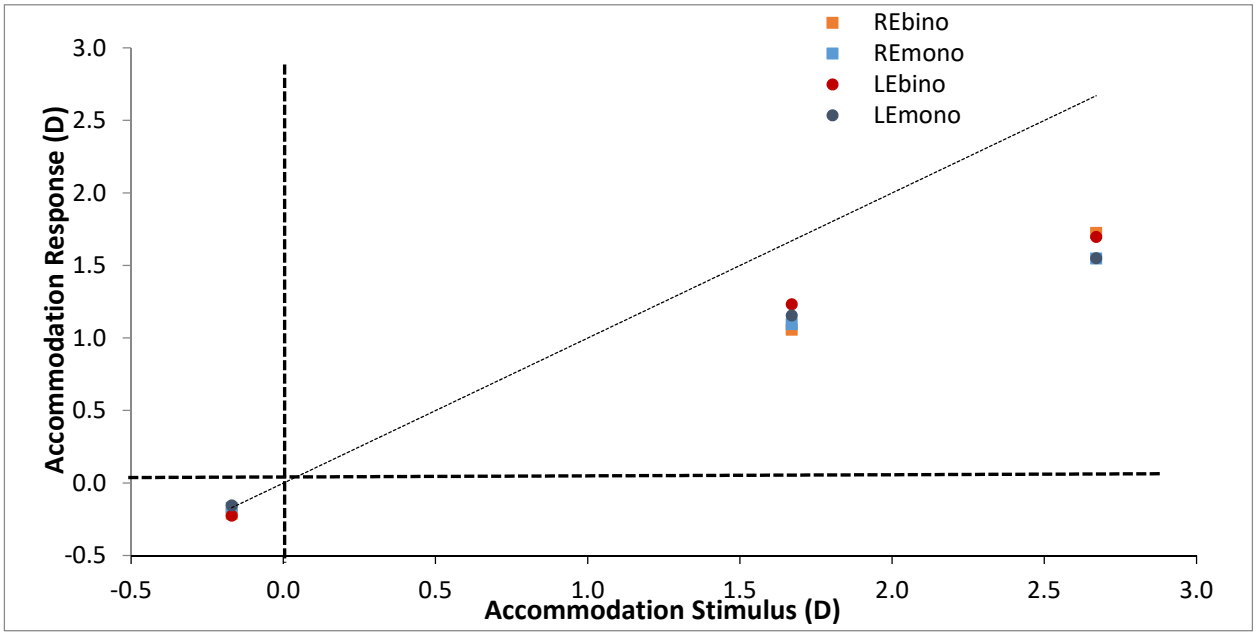

Figure 3.11. Accommodative response of right and left eye for three distances in both monocular and binocular condition. The dashed line represents the ideal 1-1 accommodative response. Data for both NP and P are presented together.

When comparing the values obtained between the two eyes, no statistically significant differences were found (p values > 0.05 in all cases, please see table 3.2). Since no difference was found between the two eyes, further analysis was performed using the average values from the two eyes for each subject.

	Binocular Condition			Monocular Condition		
	RE	LE	P	RE	LE	p
Far (-0.17D)	-0.21±0.16	-0.22±0.17	0.43	-0.17±0.18	-0.15±0.23	0.42
Intermediate (1.67D)	1.06±0.58	1.23±0.49	0.17	1.09±0.63	1.16±0.47	0.37
Near (2.67D)	1.72±1.06	1.69±0.95	0.44	1.54±0.98	1.55±0.95	0.49

Table 3.2. Mean values and p values of right vs. left eyes accommodation response (D) under both binocular and monocular conditions (paired-sample t-test).

3.5.2 Binocular vs. monocular accommodation response

The accommodation response at each vergence (accommodation stimulus under both binocular and monocular conditions) is shown for all participants in Figure 3.12. The difference between binocular and monocular accommodation responses, when all participants were included, was not found to be statistically significant (paired t-test: far, p=0.30; intermediate, p=0.42). An increased binocular advantage was however observed for the near distance (2.67 D vergence), but did not reach the point of statistical significance (p=0.17).

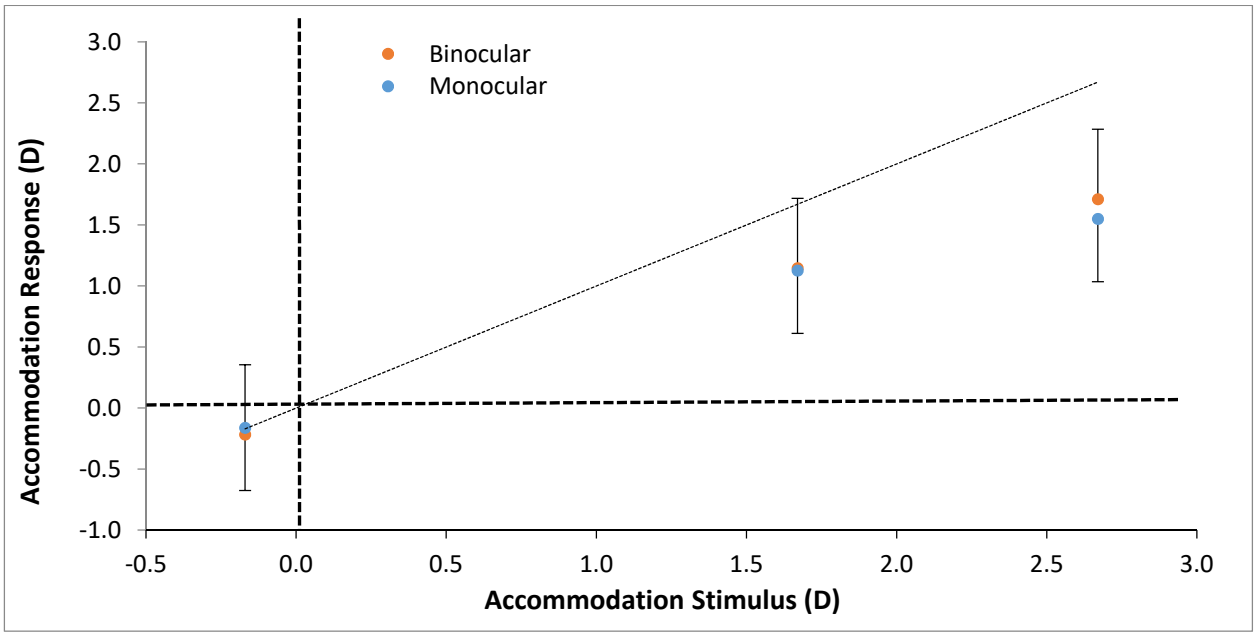

Figure 3.12. Accommodation response under binocular and monocular viewing. The error bars represent the standard error of the mean. Data was taken from 33 subjects at the intermediate distance (1.7D) and from 56 subjects for the far and near distances.

The accommodation error is expressed as the difference between the actual and the ideal response. Figure 3.13 plots the errors in accommodation response as a function of target vergence revealing, as might be expected from the literature, that the error is more pronounced as the stimulus distance is decreased (*i.e.* increased vergence).

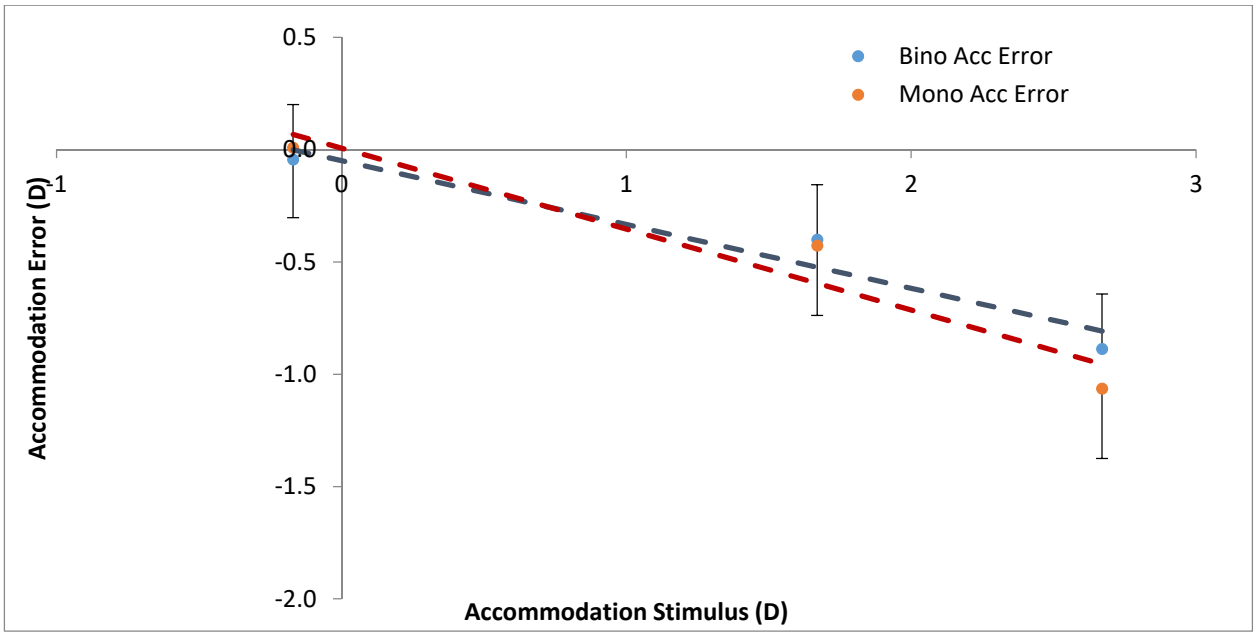

Figure 3.13. Accommodation errors for both binocular and monocular conditions. The accommodation error is expressed as the difference between the actual and the ideal response **(Allen &O'Leary, 2006).**

3.5.3 Binocular vs. monocular accommodation response: presbyopes vs. non-presbyopes

Figure 3.14 depicts a plot of the data for the accommodative response (D) at each vergence (accommodation stimulus) for the two age groups (presbyopes vs. non-presbyopes) tested, under both binocular and monocular conditions. As can be seen, although there are no significant differences arising between the two groups for the 'far' target, the response is significantly reduced, as might reasonably be expected, for presbyopes at both intermediate and near distances.

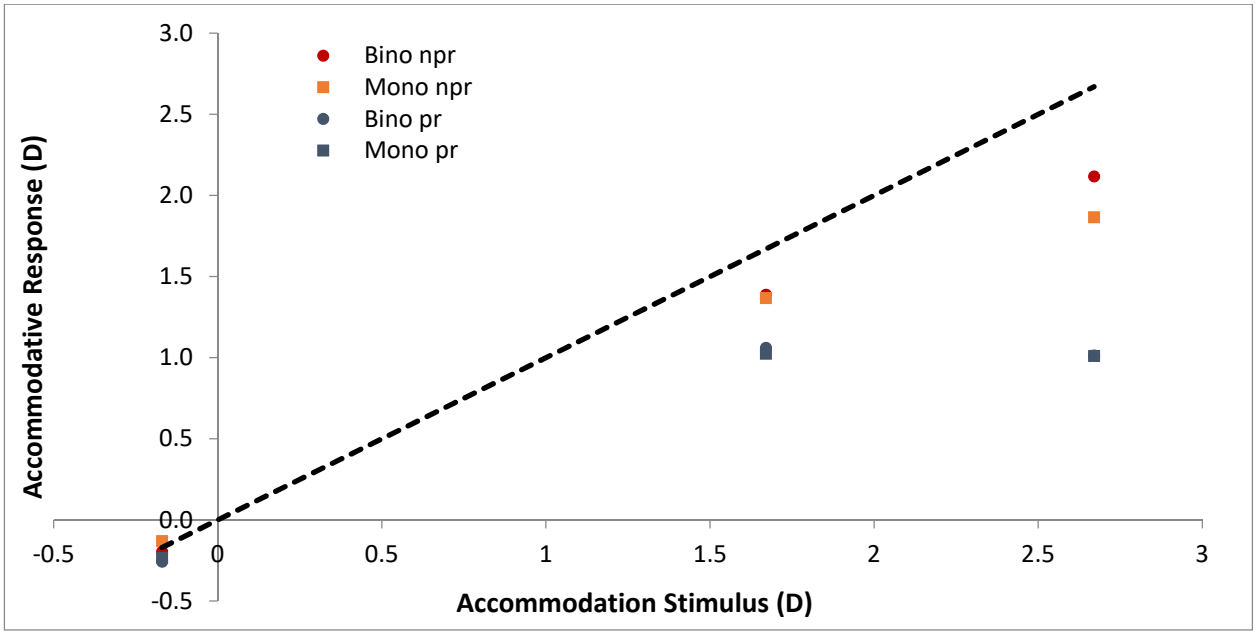

Figure 3.14. Accommodative response at the three stimulus vergences for the two age groups (pr, presbyopes; npr, non-presbyopes) and for the monocular / binocular viewing conditions. The black dashed line represents the ideal (1:1) accommodative response.

Figures 3.15 and 3.16 present the accommodation error under both binocular and monocular viewing conditions for each age group (*i.e.* presbyopes vs. non-presbyopes). It is evident that the accommodation error increases as the target becomes nearer for both groups, although the error is notably more pronounced in presbyopes (Figure 3.16) than non-presbyopes (Figure 3.15). More specifically, the error in accommodation response for the non-presbyopes was -0.02 D for the far stimulus and -0.28 and -0.55 D for the intermediate and near stimulus, respectively, under binocular viewing conditions. The corresponding errors of accommodation under monocular viewing conditions were 0.04 D, -0.30 D and -0.80 D, respectively (see table 3.2). Therefore, an average binocular advantage of 0.25 D is found for the near stimuli, a difference which reached statistical significance (t-test, p=0.01).

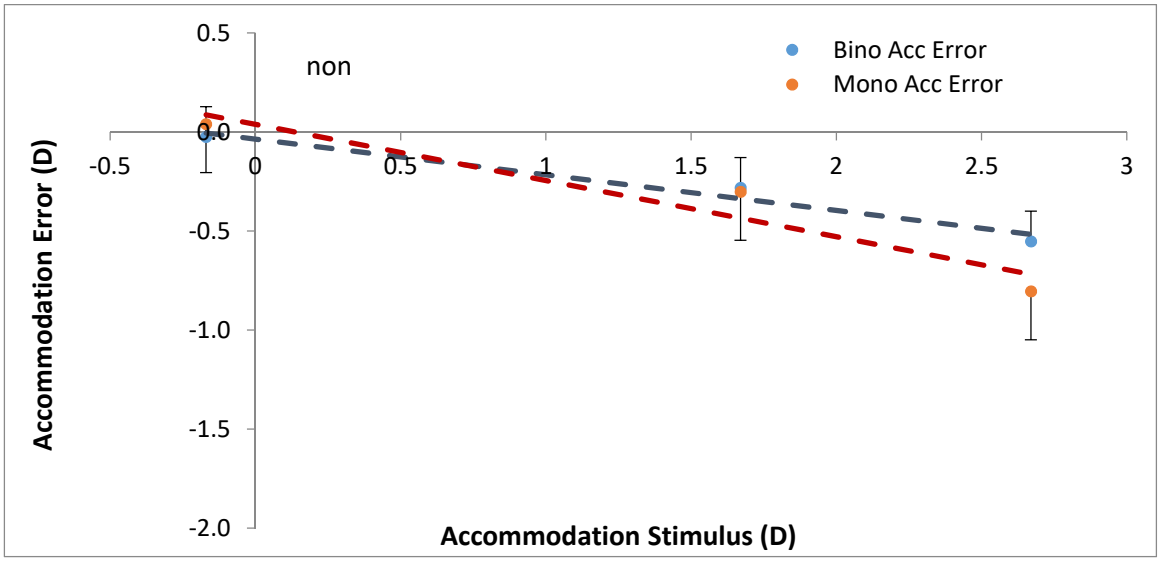

Figure 3.15. Accommodation error under binocular and monocular viewing condition for the group of non presbyopes.

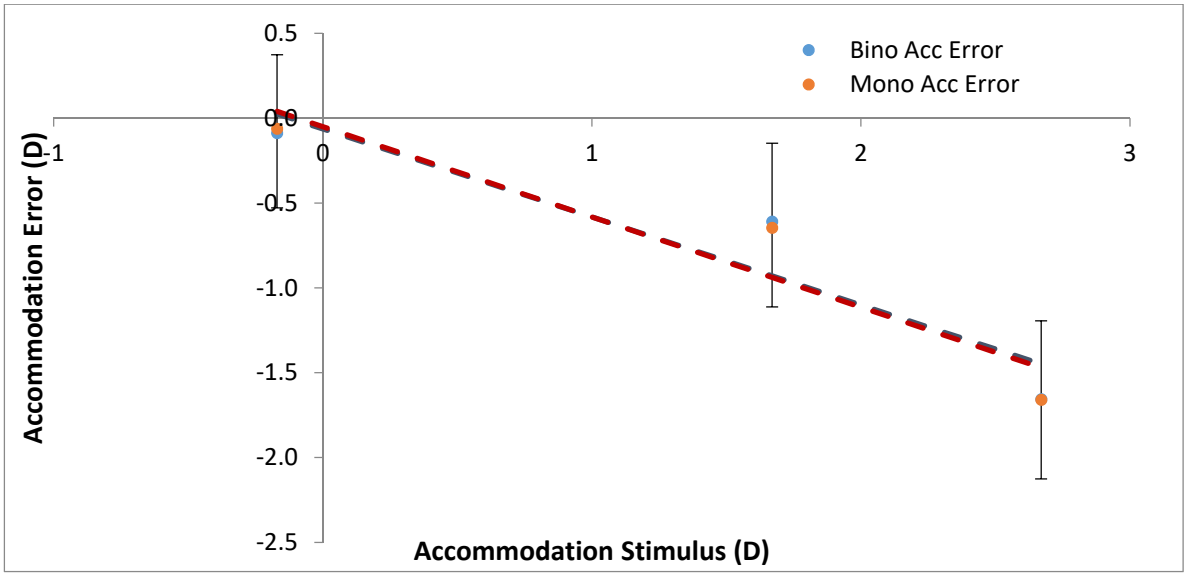

Figure 3.16. Accommodation error under binocular and monocular viewing condition for the group of presbyopes.

For the group of presbyopes the accommodation error was -0.08 D, -0.61 D and -1.66 D under binocular conditions, respectively, and 0.06D, -0.64 D and -1.66 D under monocular conditions for the far, intermediate and near accommodation stimuli which was not statistically significant (Figure 3.16).

	Non Presbyopes			Presbyopes		
	Binocular	**Monocular**	**P**	**Binocular**	**Monocular**	**p**
Far (-0.17D)	-0.02±0.11	0.04±0.17	0.23	-0.08±0.11	-0.06±0.11	0.49
Intermediate (1.67D)	-0.28±0.07	-0.30±0.06	0.40	-0.61±0.47	-0.64±0.50	0.45
Near (2.67D)	-0.55±0.20	-0.80±0.33	0.01	-1.66±1.07	-1.66±1.03	0.49

Table 3.3. Mean values and p values of right vs. left eyes accommodation response (D) under both binocular and monocular conditions.

3.5.4 Binocular advantage: effect of aging.

Figures 3.17 and 3.18 plot the correlation of binocular advantage with age for the two target vergences (far, -0.17 D [Figure 3.17] and near 2.67 D [Figure 3.18]) and for the two age groups (n=56. It is evident that there is no significant effect of age upon binocular advantage when participants were accommodating at the 'far' distance.

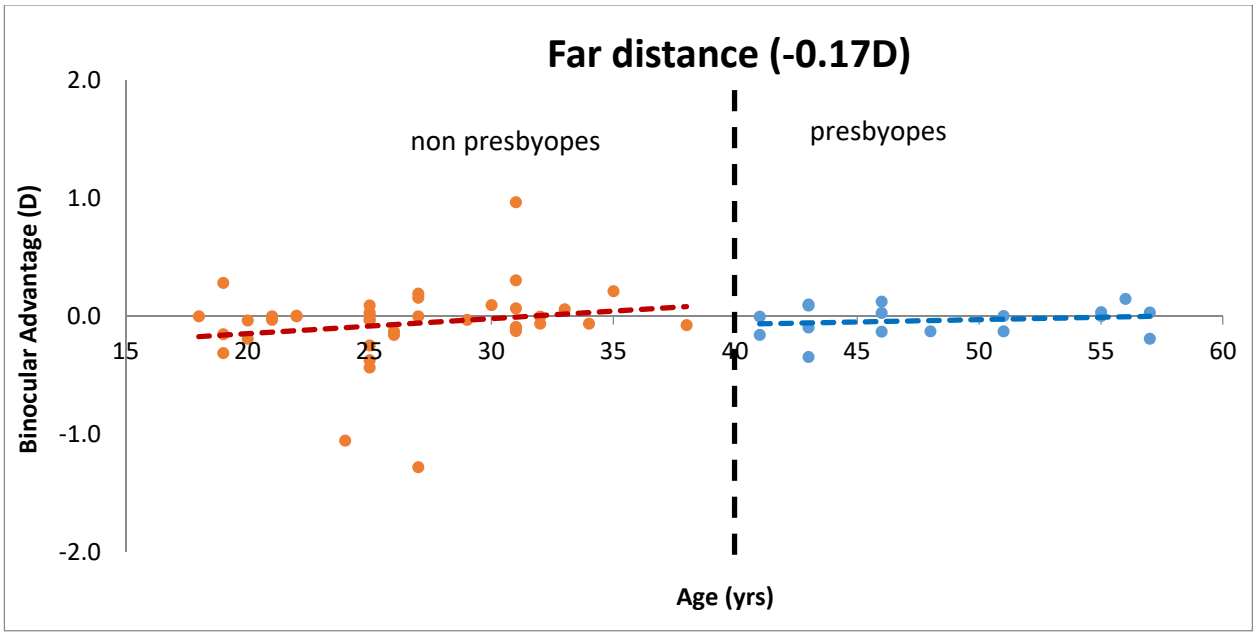

Figure 3.17. Binocular advantage in accommodation response as a function of age for the far target (-0.17 D target vergence).

In contrast, for the 'near' target (Figure 3.18), a correlation between binocular advantage and age was found for the non-presbyopic group, with the binocular advantage being ~ 0.50 D in the younger age group, decreasing to about zero at 30 years of age. For the presbyopic group, no significant binocular advantage was conferred at any age tested.

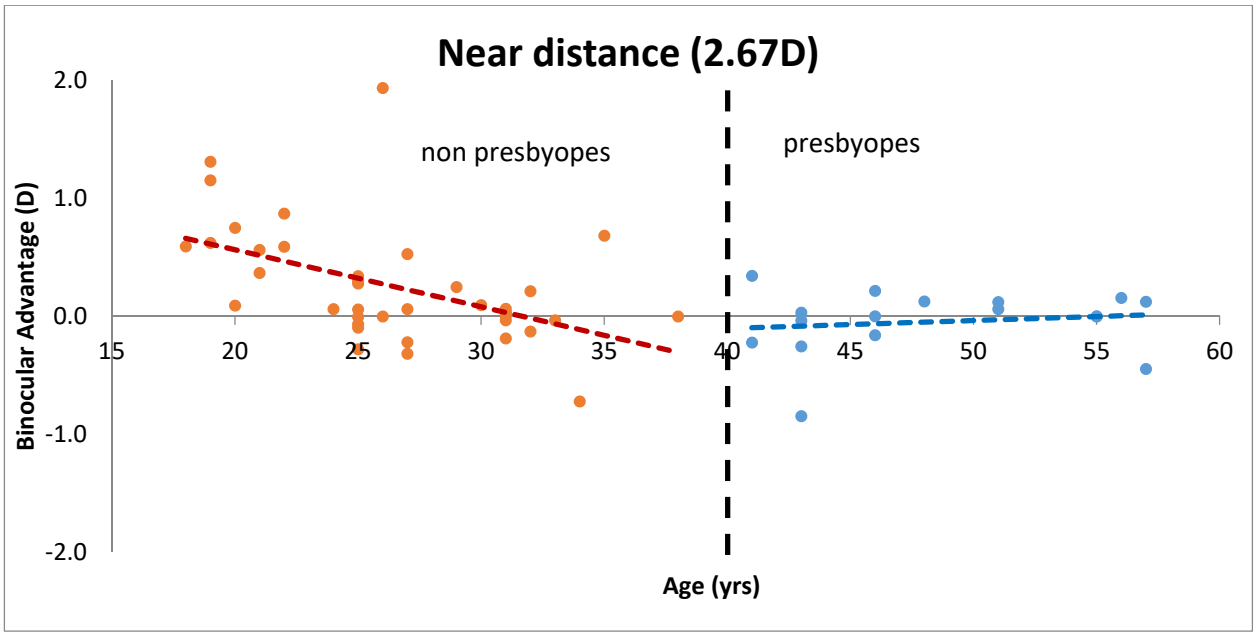

Figure 3.18. Binocular advantage in accommodation response as a function of age for the near target (2.67 D vergence).

Figures 3.19 and 3.20 plot the errors in the accommodation response as a function of age for both binocular and monocular conditions, respectively. Data for both far and near target vergences are presented. Under both conditions, no effect of age on accommodation error for the far target was observed, with the errors being close to zero at all ages. In contrast, a strong correlation was found between accommodation error and age for the near target (see also Table 3.4).

For presbyopes, the error of accommodation was higher for older participants under both viewing conditions (as anticipated). For the younger, non-presbyopic participants, no significant difference was found, under monocular conditions.

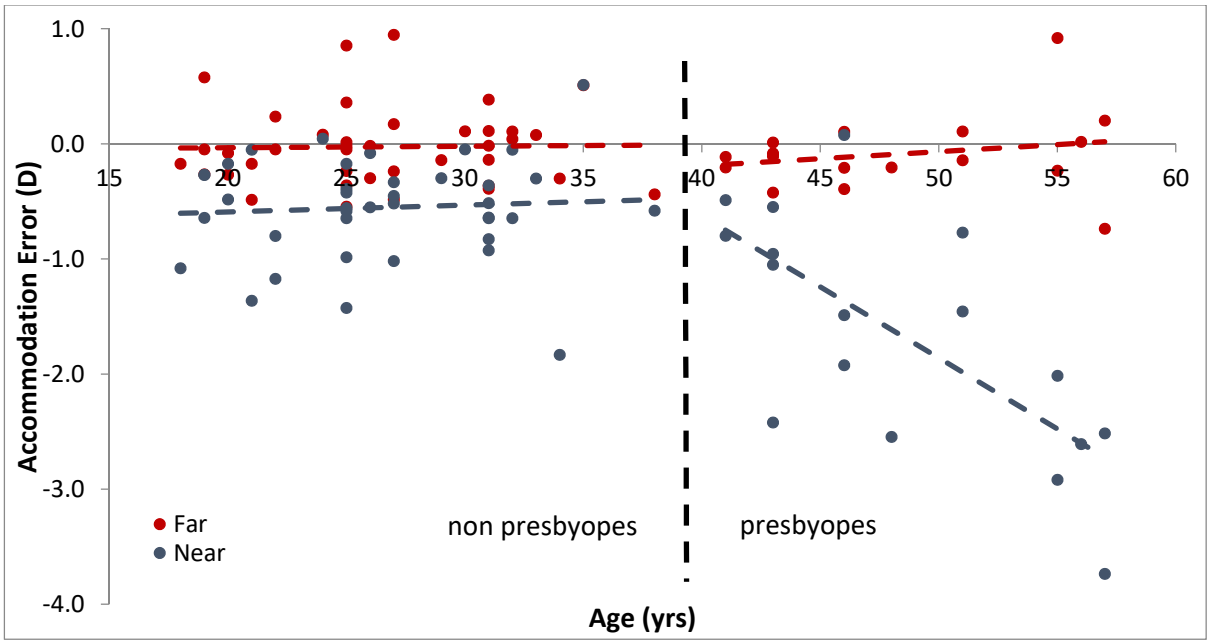

Figure 3.19. Accommodation error, for both far (-0.17 D) and near (2.67 D) targets, as a function of age under binocular viewing conditions.

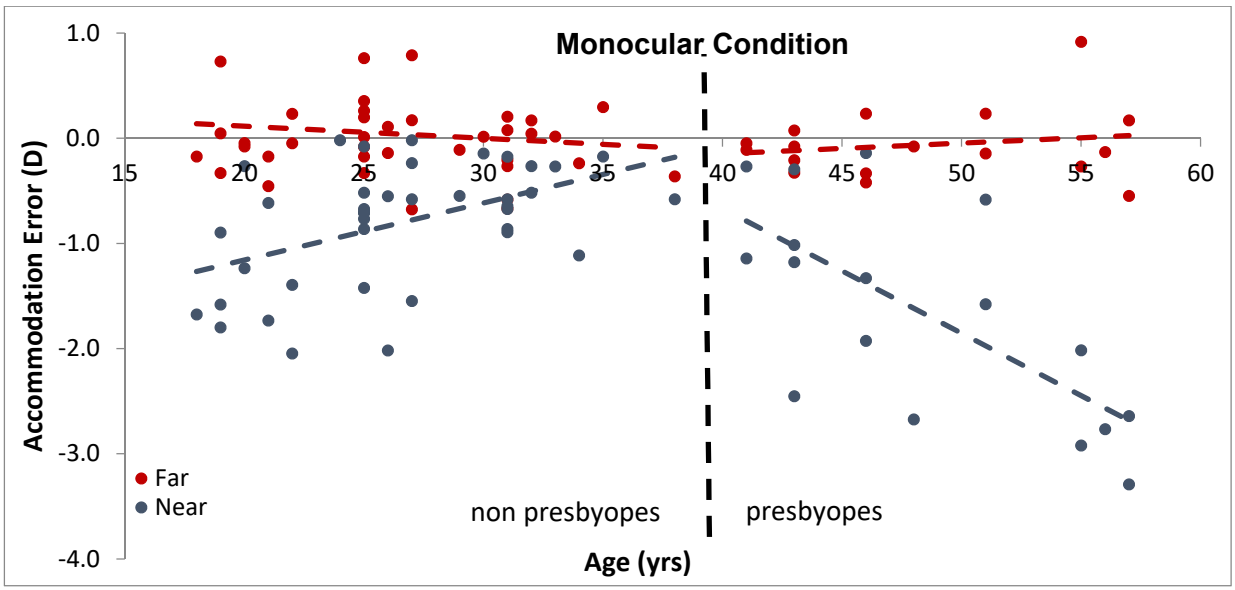

Figure 3.20. Accommodation error, for both far (-0.17 D) and near (2.67 D) targets, as a function of age under monocular viewing conditions.

		Accommodation Error			
		Binocular		Monocular	
		Far	Near	Far	Near
Age	Non-presbyopes	0.02	0.06	-0.13	0.47
	Presbyopes	0.21	-0.69	0.18	-0.69

Table 3.4. presents the findings after fitting the data to Pearson's linear correlation coefficient in terms of the relationship between accommodation error and age for the presbyopic and non-presbyopic group at the two target vergences. The cells highlighted in orange indicate a strong linear correlation (r≈0.7), while the yellow cells indicate a weak to moderate (r≈0.5) linear correlation.

3.6 Discussion

Within the present study, we have sought to extend our knowledge in terms of the advantages that are conferred through binocular vision, which presently extend to depth perception, visual acuity, colour vision and many other facets of human vision (Fletcher, 2011). To address the potential advantage of binocular over monocular vision in terms of accommodation performance, three target vergences were employed corresponding to far (-0.17 D), intermediate (1.67 D) and near (2.67 D) distances. Accommodation errors (lag and lead of accommodation) were also analysed for both non-presbyopic subjects (up to 40 years of age) and for presbyopes (who were over 40 years of age), an age at which the symptoms of presbyopia first appear (Grosvenor, 1987). The accommodation response was calculated from the spherical equivalent, as measured with an open-field autorefractometer, using external targets. Average values from the two eyes were obtained and analysed, although no significant difference was found between the two eyes, which is in agreement with a previous study where no difference was found between the dominant and non-dominant eye in the accommodation response (Ibi, 1997).

The intrinsic steady-state errors in the accommodation response (*i.e.* "lags" at high vergence stimulus levels, see Figure 3.15), which were previously reported by several authors (Charman, 2010; Plainis et al., 2005), were replicated in this study. Although the increasing errors in focus for ‘near’ targets were evident for all subjects tested, the exact value of the accommodative lag revealed large inter-subject variability, especially given that the participants were of different ages. For example, the average lag in accommodation under binocular viewing conditions for non-presbyopes was found to be about 0.28 D and 0.55 D for the intermediate and near targets, respectively, while for the early presbyopes the values were 0.61 D and 1.66 D, respectively.

Another interesting observation derived from the measurement of the magnitude of the focusing errors for the near target. When the analysis was performed for each subgroup, no difference was found for the non-presbyopic group, although a significant advantage was measured under binocular viewing conditions for the

presbyopes using the near target. However, no advantage was conferred by binocular viewing conditions for either group for the far and intermediate stimulus distances. The increased responsivity (and reduced error in focus) during binocular viewing is not altogether surprising, since the accommodation lag is known to be higher under monocular viewing conditions (Ibi, 1997; Jaschinski, 2001) when both retinal disparity and convergence, which also drive the accommodative response (Fincham & Walton, 1957), are not in play. This difference is expected to be more pronounced for the near as compared to intermediate target, given that an increased degree of convergence is required. Similar results were reported by Ibi (1997), who studied binocular advantage in the accommodation response among younger subjects aged 12-19 years.

The absence of a binocular advantage in the accommodation response in presbyopes aged over 40 *has not previously been reported*, given that the extant studies have tended to focus upon younger subjects with higher level of reserve accommodation. This may be due to the reduced average responses of presbyopes, leading to a higher level of lag (~1.00 D at 2.67 D vergence), which probably results in a significant degree of retinal blur. Thus, under these conditions, a 1.0 D of defocus may not be sufficient to drive an accurate convergence response and an increase in accommodative response under binocular viewing conditions.

Although a significant difference in the average accommodation response between the two age groups was observed, it is nonetheless obvious that a progressive decline in the accommodation response should occur with increasing age. For this reason, we correlated accommodative performance with the age of the participants. Upon examination of the binocular advantage at the two boundary distances (far and near), no advantage was found for the far target across all ages tested. However, a significant binocular advantage was found for the near distance within the non-presbyopic group. Moreover, this binocular advantage was largest for younger adults, an advantage that decreased progressively with age until there was no significant advantage by the early thirties.

Chapter 4. The effect of crowding on visual acuity

4.1 Introduction

4.1.1 Background

The effects of visual crowding are well known and were originally reported by researchers in the early 20th Century (Ehlers, 1936; Korte, 1923). The name “crowding” was first given to the phenomenon in which a pattern seen in isolation is more easily recognized than when in the presence of neighbouring patterns by Holger Ehlers in 1953 (Ehlers, 1953). Since its formative definition, the use of the term “crowding effect” has been expanded to describe an observer’s reduced visual performance in resolving and recognising objects when surrounded by other similar stimuli (Stuart and Burian, 1962).

Crowding was however long confused with the reduced resolution that is associated with rod-dominated peripheral vision (Strasburger and Wade, 2015). This phenomenon is called “masking” and its effect differs from that of crowding. The key difference between crowding and masking is that crowding involves simultaneously presented stimuli and primarily affects the recognition and identification of objects; whereas visual masking can also affect the detection of the stimulus itself (Pelli et al., 2004; Whitney and Levi, 2011; Levi et al*.,* 2002; Levi and Carney, 2009).

While the underlying mechanisms of crowding are keenly debated, there is substantial controversy as to whether masking is itself a form of crowding, and whether both do (or do not) occur at the level of the retina (Doron et al., 2015). This phenomenon may owe its existence, at least part, to the fact that the centre of the image is processed by the cone-dominated fovea while the periphery of the image is processed by the rod-dominated peripheral retina.

There is however, evidence that some target identity information is differentially processed in masking in a manner that remains unaffected by crowding. For example, when required to report all the letters present in a crowded display, the percentage of correct responses is higher when letters are not required to be included in the correct order (Whitney and Levi, 2011; Strasburger, 2005; Popple and Levi, 2005). Although the information about ‘location’ appears to be lost, some

information, such as semantic information, seems to survive the phenomenon of crowding (Huckauf et al., 2008).

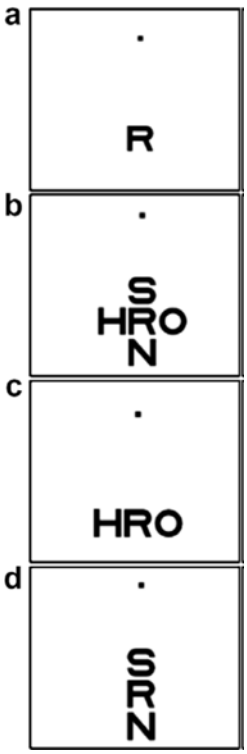

Figure 4.1. An illustration of the crowding effect. The reader can experience crowding by fixating upon the dot while trying to identify one letter either, (a) in isolation, (b) when surrounded by 4 random flanking letters; (c) when surrounded by 2 horizontally placed random flanking letters, or (d) when surrounded by 2 vertically placed random flanking letters. From Levi (2008).

Crowding might best be operationally defined as the inability to recognise objects in the midst of clutter. From a diagnostic point of view, crowding impairs identification rather than detection *per se*, whereas masking is the reduction in the visibility of a visual stimulus caused by the presentation of a second stimulus at the same time, or slightly before or after presenting the primary target stimulus (Whitney and Levi, 2011).

4.1.2 Effect of spacing and eccentricity

The crowding phenomenon has been studied across a variety of visual tasks, including letter identification (Flom et al., 1963a; Leat et al., 1999; Pelli et al., 2004; Flom et al., 1963; Liu and Arditi, 2000; Flom et al., 1963b), number identification (Strasburger et al., 1991), Vernier acuity (Levi and Klein, 1985; Levi et al., 1985; Westheimer and Hauske, 1975), stereoacuity (Butler and Westheimer, 1978; Greenwood et al., 2012), and orientation discrimination (Parkes et al., 2001; Solomon et al., 2004; Andriessen and Bouma, 1976; Wilkinson et al., 1997). The magnitude of the crowding effect may vary with the characteristics of the stimulus (*e.g.* spacing and eccentricity). The term *critical spacing* describes the distance between target and distractors; whereupon the distractor begins to have a negative effect upon the identification of the target image. Contrast discrimination thresholds tend to increase as the distractors come into closer proximity with the stimulus (Wilkinson et al., 1997; Chung et al., 2001; Liu, 2001; Tripathy et al., 2002). It has

been suggested that the critical spacing is proportional to eccentricity (Wilkinson et al., 1997; Pelli et al., 2004; Bouma, 1970). It has also been shown that the critical spacing is about half the viewing eccentricity (Andriessen and Bouma,1976; Pelli et al., 2004; Strasburger et al., 1991). The closer the distractors are to the stimulus, the harder therefore it is to discriminate the stimulus from the distractor. The decline in VA with eccentricity and the effects of crowding within the visual periphery have been investigated in many studies (Ehlers, 1953; Ehlers, 1936; Levi et al., 2002a; Loomis, 1978; Pelli et al., 2004; Toet and Levi, 1992; Wilkinson et al., 1997). In contrast, other studies have suggested little or no effect of crowding upon central vision (Flom et al., 1963a; Levi et al., 1985; Liu and Arditi, 2000; Toet and Levi, 1992), while some researchers have even postulated that crowding does not influence central visual performance at all (Bouma, 1970; Levi et al., 2002a; Strasburger et al., 1991). Levi and colleagues (2002a; 2002c) however demonstrated an elevated threshold at the foveal location, similar to that of simple contrast masking, whereas peripheral locations required much higher thresholds and therefore exhibited a crowding effect (Levi et al., 2001a; Levi et al., 2002c).

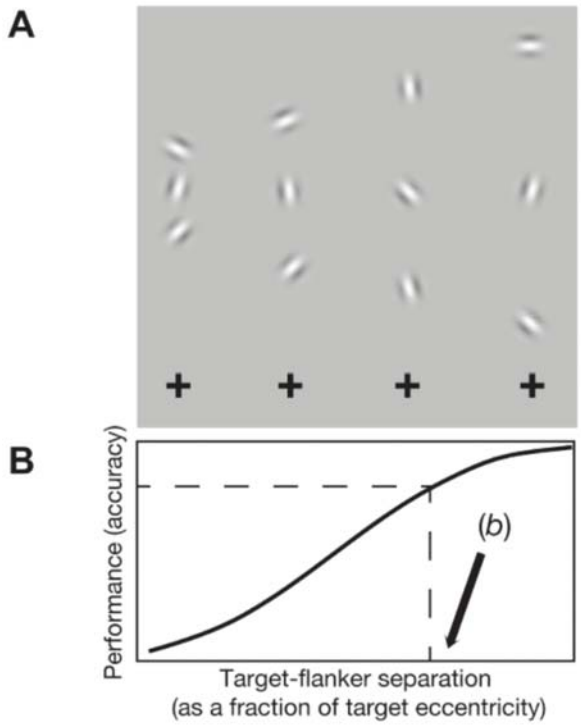

Figure 4.2. The critical spacing of crowding and Bouma's proportionality constant. A. Fixating the crosses along the bottom (note the target orientation with the central Gabor patch in each column is easier to recognize on the right). **B.** Performance accuracy increases as the target-flanker separation increases. Bouma's constant, ***b***, may be defined as the target-flanker separation (as a ratio of target eccentricity) that results in criterion performance (shown by the dashed line). Although the analytic methods and criteria used to compute b vary from study to study, it generally corresponds to the point at which performance begins to drop as flankers are advanced toward the target (from Whitney and Levi, 2011).

4.1.3 Effect of stimulus and distractor size

Levi and colleagues (2002c) highlighted the importance of stimulus size in relation to critical spacing in identifying targets at the fovea. Levi (2008) also went on to explain how the crowding effect may be connected to the receptive fields, the long-range horizontal connections, and the hypercolumns (i.e. the size of the targets and the distractors comprise an important factor; Levi, 2008). Strasburger and colleagues concluded that the stimulus and distractor size also have an influence on the critical spacing (Strasburger et al., 1991). Their study showed that, when the stimulus size was greater than 0.6 deg, the effect of crowding on contrast thresholds measured at the fovea was independent of the stimulus size. However, for stimulus sizes smaller than 0.6 deg, this was no longer the case and crowding caused increased contrast thresholds. Greater effects were demonstrated at larger eccentricities when, in addition to increased contrasts thresholds, larger stimulus sizes were also needed to carry out the task (Strasburger et al., 1991). These findings however remain somewhat controversial, as Tripathy and Cavanagh (2002) and Pelli et al. (2004) found little evidence to support their claim that, at larger eccentricities, the crowding effect depends significantly on stimulus size. In contradiction, Pelli and colleagues found that crowding scaled with eccentricity in a manner that was independent of size and also made similar observations for a range of distractor sizes (Pelli et al., 2004). Levi et al. (2002a, c) concluded that distractor size plays a significant role at foveal locations, but not in the periphery. It appears that stimulus size, however, could play a role in that it affects grouping. More recently, Manassi et al. (2012) found that, although the crowding effect increases with the number of flankers due to the interaction of flanker and target, a ‘pop out’ of the target occurs as soon as the flankers are perceived as a unit. It has also since been agreed that, when the targets and the distractors are dissimilar in size and shape, the crowding effect is reduced (Kooi et al., 1994; Nazir, 1992).

4.1.4 Origin of crowding

The question of where in the brain the phenomenon of crowding occurs has attracted considerable attention, and a number of psychophysical and neurophysiological experiments have been conducted to elucidate this issue. Neurophysiological studies have revealed the difficulty in isolating the underlying neural mechanism(s)

of crowding *per se*, while psychophysical studies have assisted in narrowing down the possible level(s) at which crowding occurs, as well as in guiding the design of more sophisticated neurophysiological experiments (Whitney and Levi, 2011).

Early studies demonstrated that crowding works under dichoptic conditions, in that it occurs even when the actual target is shown to the one eye and the distractors are shown to the other one (Flom et al., 1963b; Tripathy and Levi, 1994). This finding supports the opinion that the phenomenon of crowding arises in the visual cortex. Further studies have attempted to site the locus of crowding in V1 (Pelli, 2008; Millin et al., 2014); V2 (Freeman and Simoncelli, 2011); V3 (Tyler, 2007; Bi et al., 2009); V4 (Liu et al., 2009; Motter, 2006); or, according to some investigators, even later in visual processing (Aghdaee, 2005; Louie et al., 2007). Determining the ultimate locus, or loci, for the crowding effect is extremely difficult as the crowding effect is strongly affected by many factors such as the type of the stimulus, stimulus-distractor similarity, context, and so forth (Whitney and Levi, 2011).

4.2 Aim of the study

The aim of the present study was to evaluate the effect of crowding under both binocular and monocular viewing conditions. The crowding effect was measured using a Landolt C optotype with and without distractors. The stimuli were presented at three eccentricities; foveally and at ±2 degrees nasally and temporally to the foveal centre.

The magnitude of visual crowding under binocular viewing conditions was compared with monocular viewing conditions. The correlation of the magnitude of crowding with the ETDRS measurement of VA was also investigated for all three eccentricities.

4.3 Materials and methods

4.3.1 Subjects

A group of 25 subjects were recruited for the current study (14 females and 11 males). Their mean age (± SD) was 31 (± 8) years, with an age range of 20 to 62 years. Standard optometric eye examination tests were conducted for each subject, including a measurement of full refraction and of wavefront aberrations. Each subject

completed a questionnaire on their health history. Subjects with any ocular abnormalities were excluded from the study. Subjects were either examined with their habitual refraction (if needed) or with best-corrected VA. Written informed consent was received from all participating subjects, and the study was designed and conducted in accordance with the tenets of the Declaration of Helsinki.

4.3.2 Apparatus

The assessment of VA and the effects of crowding were investigated using the Contrast Acuity Assessment (CAA) test which was developed to assess functional visual performance in pilots (Chisholm et al., 2003). The test was implemented using the P_SCAN 100 system (Barbur et al., 1987), which includes a fully calibrated, 21" high resolution Sony Trinitron monitor (model 500PS). The library of functions developed for the P_SCAN system allows for the generation of any luminance colour combination with 10 bits per / gun within the limits imposed by the phosphors of the display.

4.3.3 Viewing conditions

The subject was seated in front of the screen at a distance of 3m. An ophthalmic instrument base unit fitted with a standard clinical chin and forehead rest was employed for easy and stable viewing. The experiments were carried out in a darkened room where the only light originated from a low power lamp placed so as to avoid direct illumination of the visual display. The illuminance of the stimulus display caused by the ambient mesopic lighting was less than 1 lux. While this arrangement contributes negligible additional light to the actual display, it serves to prevent peripheral dark adaptation. The luminance of the background field was 32 cd/m^2. Separate experiments were carried out using binocular and monocular viewing conditions. The subject's pupil at high magnification was visually monitored by the experimenter to ensure that the subject could maintain steady fixation during the presentation of the stimulus.

4.3.4 Experimental procedure

In order to adapt to the uniform field, the subject was seated in front of the screen for a period of around 3 minutes. In the meantime, the experimental procedure was

explained to the subject and a short trial was carried out to familiarise the subject with the test. We elected not to use a Landolt ring as the distractor target, because this could lead to falsely naming the flanker rather than the target orientation (Greenwood et al., 2009). As crowding is usually increased with flanker-target similarity circles, full rings were used as flankers in this study (Nazir, 1992, Toet and Levi, 1992, Parkes et al., 2001). Preliminary experiments were carried out by Dr. Franziska G. Rauscher (the results still remain unpublished) on a group of subjects, using spacing as the variable, showed that crowding effects start for spacing as far away as 2.4 times the diameter of the Landolt ring (foveally) and 5 times (in the periphery) and continue to increase as the inter-spacing distance decreases. Based on these initial findings a spacing of 1.5 times the diameter of the Landolt ring was selected for the purposes of this study to ensure a significant effect in all subjects tested.

The four distractor rings were placed on oblique axes around the target, with one of the four distractors in each quadrant at 45, 135, 225 and 315 degrees around the target. Results from other studies in our laboratory investigated horizontal and vertical directions (0, 90, 180, 270 degrees on a circle around the target) but found that those confounded the results for the eccentric locations, as the distractor has the potential to encroach on the foveal location. To rule out these potential side effects and, in line with previous findings, oblique distractor locations were chosen (after Toet and Levi, 1992).

Earlier studies in our laboratory (Dr. Franziska G. Rauscher, private communication) showed that crowding affects both negative and positive contrast targets, although at a given eccentricity there is no significant difference between the two conditions As the great majority of high contrast test charts employ negative contrast, we decided to use a stimulus of negative contrast (-100%) for the current study (*i.e.* black letter on a “white” background). During the test, the size of the stimulus was varied, so as to measure the subject’s VA. A four-alternative, forced-choice procedure with multiple, interleaved staircases was employed. Each staircase was based on 16 reversals; the subject being required to respond correctly twice in succession before implementing a step reduction in stimulus size. The stimulus

appeared for 75ms with a Gaussian temporal weighting of ± 2σ (σ = 50ms). The stimulus appeared randomly at each of the following eccentricities (degrees):

-2, 0, 2

The outcome of the test (*i.e.* the threshold gap size at each eccentricity investigated) was calculated by averaging the last 10 reversals.

The initial experimental condition employed binocular viewing. Initially, a single Landolt 'C' ring was shown on the screen and then the Landolt C stimulus was surrounded by four distractor rings as shown in Figure 4.3. The rings had the same size as the stimulus throughout the test. The subject had to fixate a dot in the middle of the screen throughout the test, and the fixation point was surrounded by four guides (Figure 4.3) which remained permanently on the screen, helping the subjects to maintain fixation at the centre of the screen. This was important as the central fixation dot disappeared some 0.8 s before the onset of the test stimulus. The guides had a contrast of -35%, and the stimulus gap in the Landolt C optotype had one of four randomly selected, diagonal locations (*i.e.* top right, top left, bottom right, bottom left). The subject pressed one of four response buttons arranged as the corners of a square to indicate the position of the gap using a four alternative, forced-choice procedure (Chisholm et al., 2003).

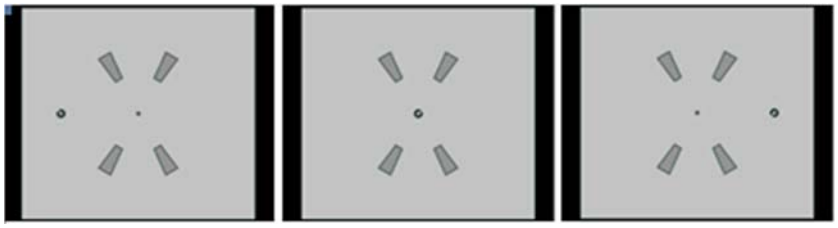

Figure 4.3. Screenshots showing the appearance of the single Landolt ring stimulus at the eccentricities investigated. The grey fixation guides (-35% contrast) aided fixation but are highly unlikely to have further contributed to the crowding effect as they are of low visibility and crowding depends on the visibility of the distracting material (the guides have been made darker in the figures).

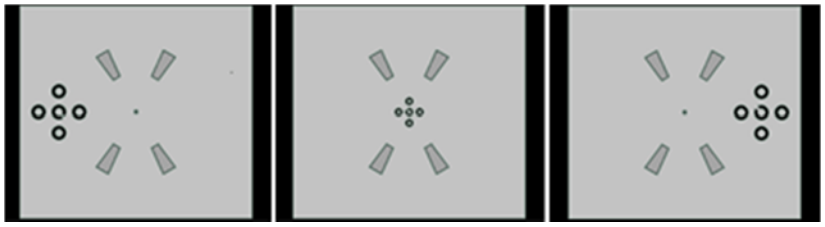

Figure 4.4. Screenshots showing the appearance of the Landolt C stimulus surrounded by distractor rings.

The second viewing condition employed monocular viewing and the same procedure was conducted. The best corrected eye was chosen (17 right eyes, 8 left eyes). Again, first a single Landolt C stimulus was presented and then the Landolt C stimulus was surrounded by four distractor rings (Figure 4.4).

4.4 Results

4.4.1 Binocular viewing

The threshold gap size of the Landolt C in minutes of arc (minimum angle of resolution, MAR) was converted to logMAR VA for each subject. Mean values (±SEM) were calculated for each eccentricity (-2°, 0° and +2°) and condition (with or without distractors). VA data for binocular viewing are summarized for all subjects (n=25) in Table 4.1.

Eccentricity (deg)	No distractors		With distractors	
	VA (logMAR)	SEM (logMAR)	VA (logMAR)	SEM (logMAR)
-2	0.26	0.02	0.58	0.03
0	-0.01	0.02	0.15	0.03
+2	0.23	0.02	0.55	0.03

Table 4.1. First viewing condition; binocular viewing. Mean visual acuity and standard error of the mean, with and without distractors in all three eccentricities. Paired-sample t-test analysis showed a significant difference in VA at all eccentricities tested between the with- and without distractors condition (paired sample t-test; $p<0.001$).

4.4.2 Monocular viewing

The threshold gap size of the Landolt C in minutes of arc (minimum angle of resolution, MAR) was converted to logMAR visual acuity for each subject. Mean values (±SEM) were calculated for each eccentricity (-2°, 0° and +2°) and condition (with and without distractors). VA data under monocular viewing conditions are summarized for all subjects in Table 4.2.

Eccentricity (deg)	No distractors		With distractors	
	VA (logMAR)	SEM (logMAR)	VA (logMAR)	SEM (logMAR)
-2	0.31	0.02	0.68	0.02
0	0.07	0.02	0.22	0.03
+2	0.26	0.02	0.61	0.02

Table 4.2. Second viewing condition; monocular viewing. Mean visual acuity and standard error of the mean, with and without distractors in all three eccentricities. Paired-sample t-test analysis showed significant difference in visual acuity in all eccentricities between the with- and without distractors condition (paired sample t-test; $p<0.001$).

4.4.3 Binocular vs monocular

The ETDRS VA was first evaluated for binocular and then monocular viewing conditions. The mean (±SEM) VA was found to be -0.12 (±0.02) logMAR and -0.11 (±0.01) logMAR under binocular and monocular viewing conditions, respectively. No significant difference was found between the two conditions (paired t-test; p=0.49). Figure 4.5 shows foveal VA data for all 25 subjects, measured in logMAR, with and without distractors under both binocular and monocular viewing conditions.

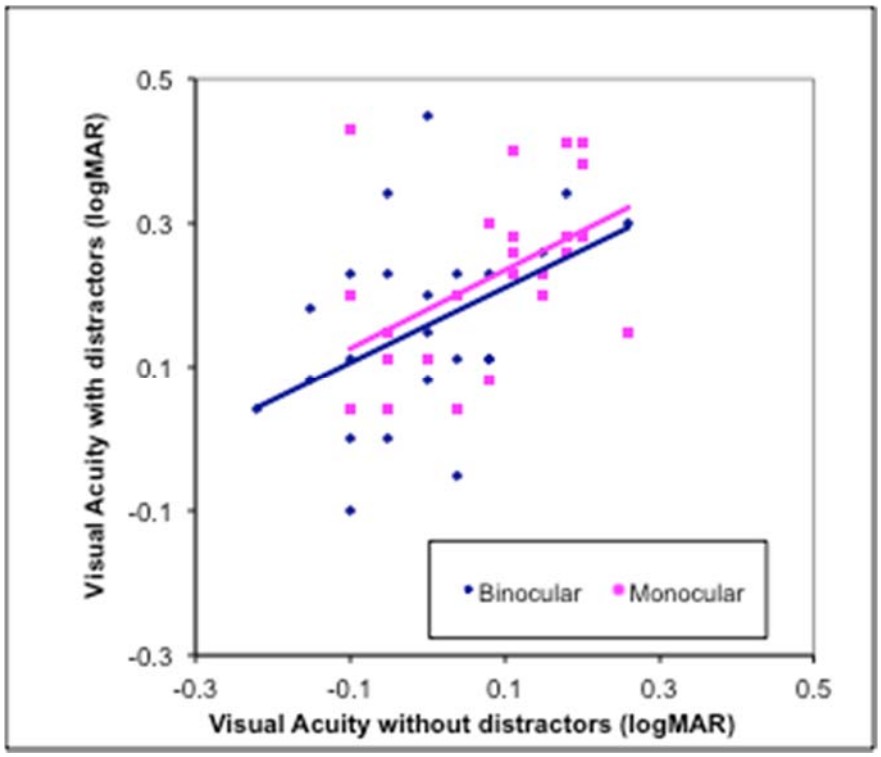

Figure 4.5. Visual acuity data for binocular and monocular viewing with distractors and as a function of visual acuity without distractors. This method of assessing the effect of distractors on visual acuity using Landolt ring optotypes is novel and needs to be explored further since the results suggest that even letter acuity could improve when assessed with single letters.

Figure 4.6 presents VA data as a function of eccentricity under both viewing conditions (binocular and monocular), with and without distractors. A statistical analysis reveals significant differences in VA at eccentricities of 0° and -2° between monocular and binocular conditions both with and without distractors (paired sample t-test; $p<0.01$). For the +2° eccentricity condition, the differences approached significance under monocular and binocular conditions, both with and without distractors (paired sample t-test; p=0.055 and p=0.041).

Visual acuity values were converted from logMAR to a decimal scale, and the ratio of VA with crowding to VA without crowding was calculated, so that the magnitude of visual crowding could be measured. Mean values (±SD) for binocular viewing were 51% (±11.0), 29% (±17.4) and 50% (±16.1) for eccentricities -2,0, 0.0 (fovea) and +2 degrees, respectively. For monocular viewing, mean values (±SD) were 57% (±7.9), 26% (±15.3) and 54% (±12.1) respectively. However, a statistical analysis revealed no significant difference in the magnitude of visual crowding between binocular and monocular viewing conditions at any eccentricity tested ($p>0.20$ in all cases).

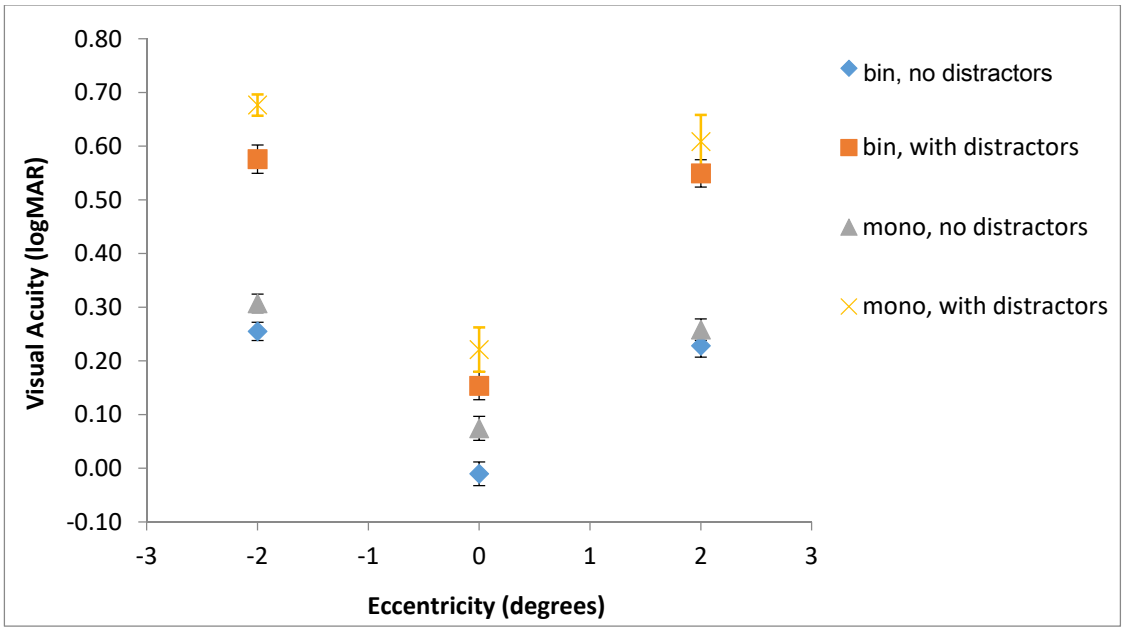

Figure 4.6. Mean visual acuity of all subjects (in logMAR) for binocular and monocular viewing condition, with and without distractors, for all three eccentricities (0°, ±2°). Error bars represent Standard Error of the Mean (SEM).

Figure 4.7 plots the crowding effect (percentage decrease in VA) as a function of eccentricity and viewing condition. Data with blue squares represent the percentage difference of VA with distractors to VA without distractors under binocular viewing conditions. The red squares denote monocular viewing conditions, indicating no significant difference.

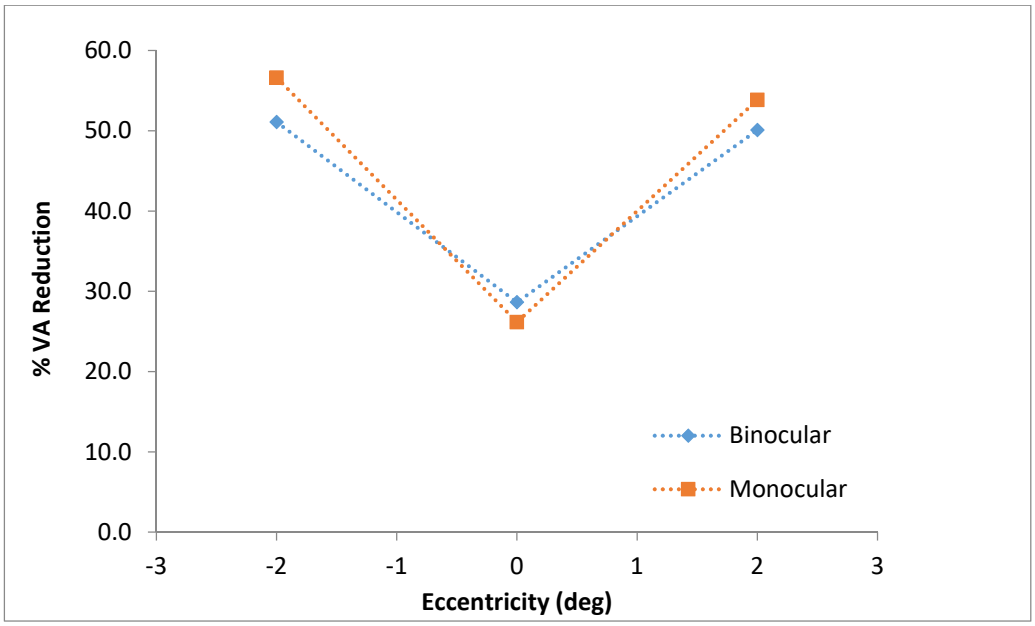

Figure 4.7. The percentage decrease in visual acuity (decimal scale) caused by crowding for all three eccentricities tested (0°, ±2°) under binocular and monocular viewing conditions.

Figure 4.8 presents the correlation between the percentage decrease in VA (i.e. the crowding effect) as a function of ETDRS visual acuity (converted into a decimal scale), under both binocular and monocular viewing conditions for all three eccentricities tested. The decimal scale was selected simply because VA values on this scale increase as acuity improves. The Pearson correlation coefficient for binocular viewing was found to be -0.105, -0.065 and 0.41 for eccentricities of -2, 0 and 2 degrees, respectively. No correlation between ETDRS visual acuity and the percentage decrease of visual acuity was evident that could be attributed to the crowding effect at any of the eccentricities tested under binocular viewing conditions. The values for monocular viewing were found to be 0.010, -0.337 and 0.252 for eccentricities -2, 0 and 2 degrees respectively. Under monocular viewing conditions, a weak to moderate correlation was evident at the foveal location.

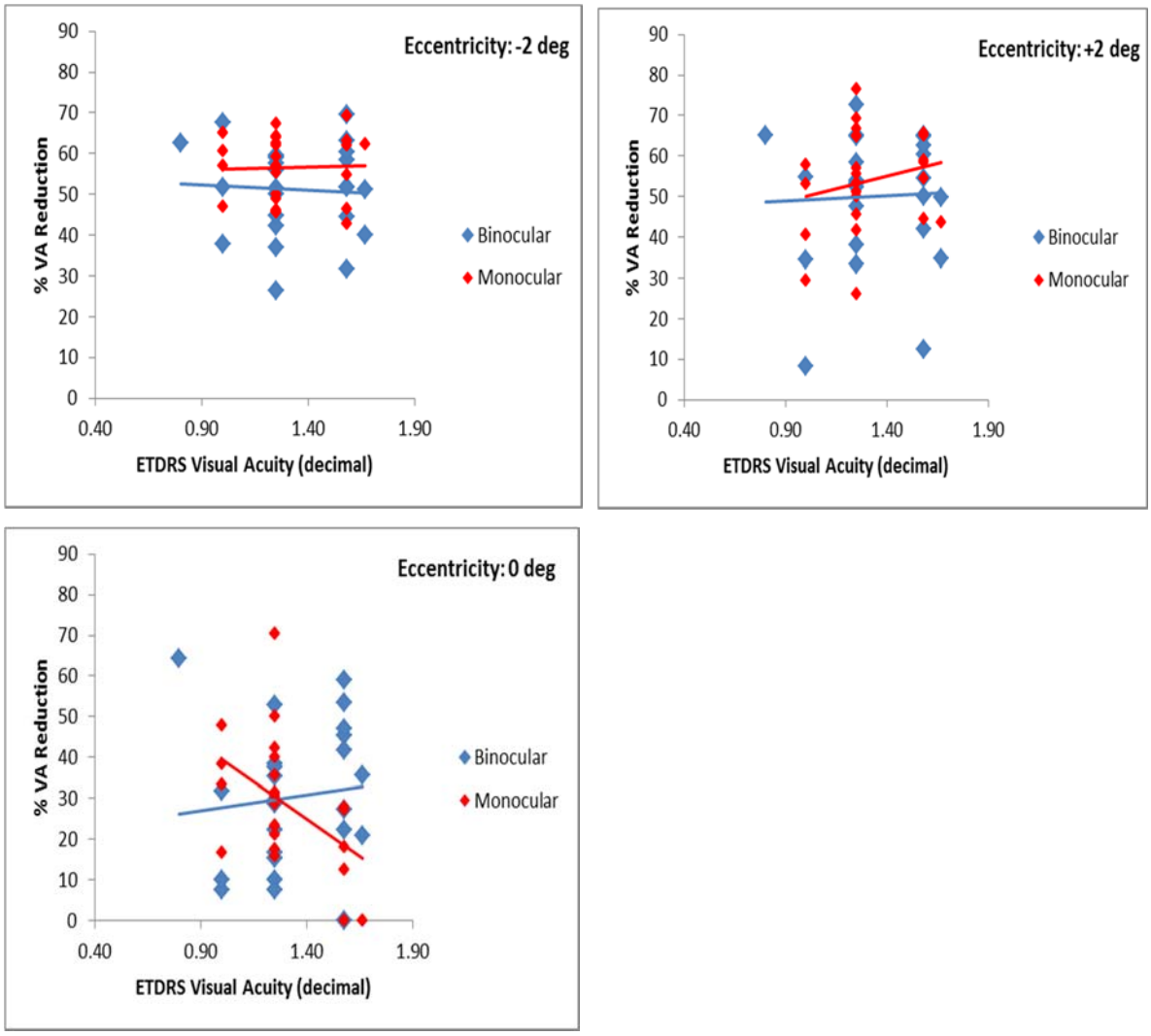

Figure 4.8. The percentage decrease of visual acuity (decimal scale) caused by crowding for all three eccentricities tested (0°, ±2°) under binocular and monocular viewing conditions as a function of ETDRS visual acuity.

4.5 Discussion

The primary goal of this study was to establish any clear binocular advantage that may be conferred in terms of the magnitude of the crowding effect. To this end, a Landolt C optotype, presented either with or without distractors, was used to measure VA at three different eccentricities (namely 0, ±2 deg). VA determined using an ETDRS test chart were found to be superior when compared to the test employing the Landolt C optotype, in broad agreement with previous findings (Plainis et al., 2013; Ruamviboonsuk et al., 2003). When measuring VA with the Landolt C optotype, the objective is to resolve and hence locate the gap in the Landolt C, whereas using the ETDRS chart the task is to recognise a specific letter within a set of letters. To date, most published studies are in agreement with the interpretation of letter optotypes involves compensatory cognitive mechanisms, thereby resulting in a higher level of VA as compared with the Landolt C method (Wittich et al., 2006).

Crowding is currently thought to have a greater effect within the periphery given that the spatial extent and intensity of the interaction are greater in peripheral than central vision (Loomis, 1978; Jacobs, 1979). This phenomenon may well be attributable to the reduced cortical representation, in terms of cortical volume and therefore presumably the number of associated neurons and synapses, that is dedicated to processing more peripheral stimuli (Azzopardi and Cowey, 1993). Our results are in a good agreement with these studies, both under binocular and monocular viewing conditions. Generally speaking, changes in foveal visual acuity due to crowding are relatively small for stimuli with a higher degree of contrast, given that Flom et al. (1963) found a decrease of 0.12-0.20 logMAR; whereas Jacobs (1979) reported a decrease of 0.18 logMAR with flanked Landolt C's; and Simmers and colleagues (Simmers et al., 1999) postulated a decrease of 0.12 logMAR with letters flanked by bars. In concordance with the extant literature, our study indicated a decrease of 0.16 logMAR under binocular viewing conditions and 0.15 logMAR under monocular viewing conditions (please see Tables 4.1 and 4.2).

In order to evaluate the magnitude of the crowding effect we measured the percentage decrease in VA. As expected, the magnitude of the crowding effect was found to be greatest within the periphery, in accordance with previous findings (Flom

et al., 1963a; Hess et al., 2000; Levi et al., 2002c; Loomis, 1978; Strasburger et al., 1991).

The correlation between ETDRS VA and the percentage decrease in VA attributable to the crowding effect was evaluated. Under binocular viewing conditions, no correlation was found at any of the eccentricities tested while, under monocular viewing conditions, a weak to moderate correlation was observed at the foveal location. Although these data would tend to suggest that individuals with better VA exhibit a reduced crowding effect under monocular viewing conditions, it is of course impossible to extrapolate these findings to all levels of VA across all individuals. However, it might be suggested that individuals with reduced VA may experience a greater crowding effect, although the subject group did not include participants with low vision.

This study did, however, demonstrate better VA in the rightward eccentricity than in the leftward, both under binocular and monocular viewing conditions. This finding remained unchanged, even when distractors were present. The magnitude of the crowding effect is also smaller for the rightward eccentricity, both under binocular and monocular viewing conditions. The literature has investigated such aspects of reading and word detection and, in societies reading from left to right (including the English language), the visual span extends further to the right than to the left (Legge et al., 2001; Rayner, 1998), although the converse is true for those societies reading from right to left (*e.g.* Hebrew; Pollatsek et al., 1981). These findings may reflect underlying neuronal processes favouring this directionality.

The results from this study revealed no significant difference in the magnitude of the crowding effect between binocular and monocular viewing conditions at any eccentricity tested in those subjects presenting with normative vision. The absence of any significant difference may have arisen owing to the use of high contrast stimuli which lie far from the threshold for detection. It has however been shown that, under binocular conditions of stimulation, cells within the cat's striate cortex exhibit an enhanced contrast sensitivity and that for lower (*i.e.* close-to-threshold) contrast a greater number of cortical neurons showing facilitatory interactions are activated (Anzai et al.,1995). Further, a facilitatory interaction between the signals from the

two eyes has been demonstrated through both electromyography studies (Plainis et al.,2006), and single-cell electrophysiology (Hubel and Wiesel,1962), demonstrating not only that binocular interactions exist at the level of single cortical cells, but also that a larger population of neurons contribute to contrast detection under binocular stimulation (Anzai et al.,1995). Binocular facilitation has also been reported under conditions of retinal blur (Plainis et al., 2011). However, such studies only consider the impact of binocular advantage upon VA rather than that of visual crowding per se. The findings presented within this chapter indicate that the involvement of binocularly driven neurons is not a necessary condition to cause visual crowding.

Based upon this reflective review of the literature, we have one potential explanation as to why, owing to the use of high contrast stimuli in this study, fewer cortical neurons were potentially activated, thereby occluding any potential advantage of binocular summation in the magnitude of the crowding effect. These observations also suggest that visual crowding can be achieved without the involvement of binocularly driven neurons. This implies that visual crowding arises due to lateral interactions amongst monocularly driven neurons that map the same region of the visual field with receptive fields that vary in size, but are spatially coextensive. Further research is needed to reconcile the difference between the findings presented within this thesis and other reports which have suggested that crowding effects may be observed during the dichoptic viewing of target and distractors (Masgoret et al., 2011; Kim et al., 2013). Thus, evaluating the magnitude of the crowding effect under both binocular and monocular viewing conditions across a range of stimulus contrast levels may serve to elucidate the neural mechanisms underlying the crowding effect and any effects that binocular summation may have upon them.

Chapter 5. Optical and retinal factors influencing aspects of spatial vision in aging and disease

5.1 The effect of stimulus presentation time upon visual acuity in normal subjects and patients presenting with AMD

5.1.1 Background

The measurement of VA remains the standard and most common psychophysical method for assessing the quality of spatial vision. Among a range of stimulus parameters, including contrast, background luminance and so forth, the stimulus presentation time plays an important role in determining VA. For example, it has been found that increasing the stimulus exposure duration up to 400ms causes a significant improvement in acuity thresholds in healthy subjects, particularly when there are surrounding letters and the effect of visual crowding becomes an influential factor (see Figure 5.1; Baron and Westheimer, 1973). Moreover, the combination of stimulus contrast with stimulus fixation duration dramatically affects VA. More specifically, a reduction in either contrast, stimulus presentation time, or both, worsens VA (Adrian, 2003). Although there is a critical presentation time (CPT), which may be less than 50ms to recognize an item in some cases (Thorpe et al., 1996), the CPT will ultimately depend on the optical characteristics of the stimulus, including its contrast and size, as a longer exposure duration leads to more efficient processing. This may be due to the fact that a longer exposure time leads to more fixations, given that a typical glimpse duration is in the range 150-200ms, resulting in additional retinal responses from adjacent retinal regions, thereby making visual processing more efficient. On the other hand, Keesey (1960) demonstrated that VA is neither enhanced, nor impaired by involuntary eye movements which occur during the inspection of a test object.

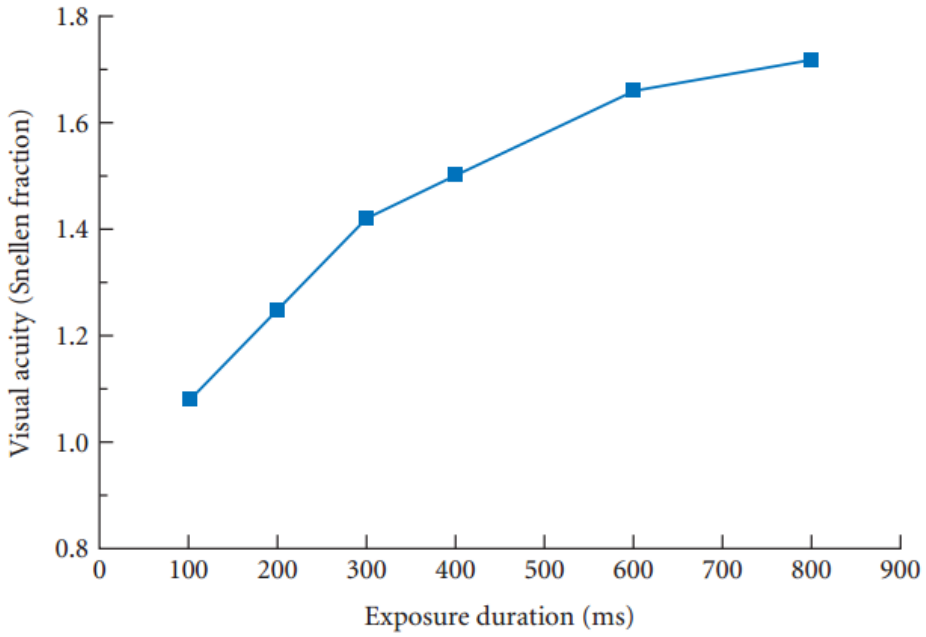

Figure 5.1. Visual acuity as a function of exposure duration (from Baron and Westheimer, 1973).

5.1.2 Visual acuity in Age-related Macular Degeneration (AMD)

Age-related Macular Degeneration (AMD) is a clinical condition which commonly affects older adults and may result in a loss of vision due to maculopathy. When the damage to the retina affects the macula, the loss of spatial vision becomes much more apparent and is associated with a notable decline in visual performance. The stimulus exposure duration becomes very important when the damage to the macula is anisotropic in nature. Consequently, AMD patients require longer stimulus presentation times to find an appropriate central fixation point that may be less affected by the lesion. The retina may also require more time to process edges and contours, and letter contrast becomes more important, even when suprathreshold contrasts are involved. Moreover, such patients may also present with unusual tremor or unstable fixation and eye movements. Generally, VA scores vary widely depending on the test that is used, with such effects being more pronounced in affected individuals, especially those suffering from AMD. Other important factors include the type of the test that is used (*e.g.* letter recognition or resolution tasks), background luminance, visual crowding, and stimulus contrast (Falkenstein et al., 2008; Fosse et al., 2001).

5.1.3 Visual acuity and contrast acuity charts

VA has become the standard means of assessing the overall functionality and therefore ‘health’ of the visual system. However, a decreased stimulus contrast can have a large effect upon VA. For instance, letter recognition can become more difficult under low contrast conditions. The undisputed advantage of employing contrast sensitivity measurements is that it can reveal several latent visual abnormalities in subjects who otherwise present with satisfactory levels of simple VA, including patients in the early stages of glaucoma, cataract, AMD, and multiple sclerosis (Hawkins et al., 2003; Jindra and Zemon, 1989; Wilkinson, 2010).

Although, in general, VA charts seek to assess spatial vision under conditions of high contrast (i.e. 100% black and white contrast); contrast sensitivity charts employ letters (or gratings) that vary in both size and contrast. The most widely known contrast sensitivity charts that use sinusoidal gratings are the FACT and Vistech charts (Ginsburg, 1984) which use a number of spatial frequencies and nine fixed levels of contrast, whereas the Pelli-Robson chart uses large letters of varying contrast to assess contrast sensitivity, while Regan charts (also a feature of Bailey-Lovie low contrast charts) feature a standard contrast level with letters of different sizes (see Figure 5.2).

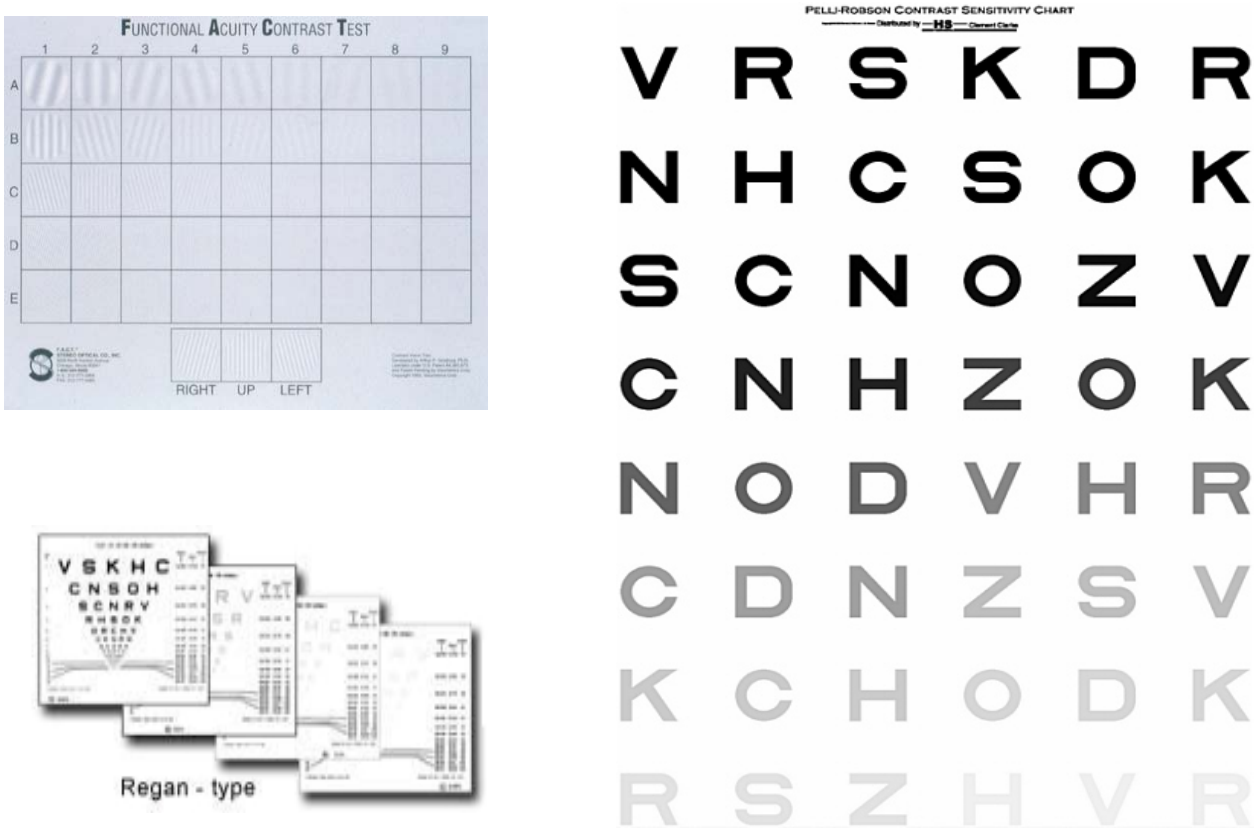

Figure 5.2. Contrast sensitivity grating and letter charts. The FACT chart is depicted in the top left corner, while the Regan charts is located in the bottom left corner. A Pelli-Robson chart is illustrated in the right panel.

In addition to such printed charts, a range of computer tests have been developed to assess both contrast sensitivity and VA. These tests use visual displays with high graphical resolution and employ psychometric methods to measure thresholds for contrast or size detection. One example is the Freiburg Visual Acuity & Contrast Test (FrACT; Bach, 1996). For both contrast and VA measurements, a Landolt-C array is employed as target, where the gap of the C can have any one of four or eight orientations. For the measurement of VA, the size of the letter is varied while the contrast remains high. For determination of contrast sensitivity, the contrast is varied while the size of the target is fixed as large.

The Contrast Acuity Assessment (CAA) test, developed at City, University of London by Chisholm and colleagues (2003; Figure 5.3), is based on the measurement of the

threshold contrast needed to resolve the presence of a gap in a Landolt C letter when projected at different sizes across a number of discrete eccentricities in the presence and absence of crowding and under a range of luminance levels that fall within either the photopic or the mesopic range. In the CAA test there is also the option to change the stimulus presentation duration and contrast polarity, as it has been found that these parameters can play an important role in VA in some patients.

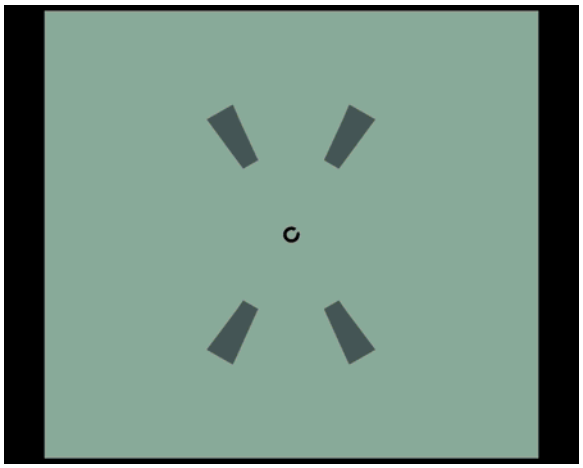

Figure 5.3. Screenshots showing the Landolt C stimulus as presented in the CAA test at the fovea. For the purposes of these experiments, only foveal testing was performed.

5.1.4 Aim of the study

Preliminary studies in patients with early stage AMD have revealed large differences between measurements of VA using either clinical EDTRS test charts (i.e. static presentation of high contrast optotypes) or similar measurements of high contrast acuity using single, high contrast Landolt rings presented briefly on a visual display. These two techniques will be referred to as the logMAR and the Contrast Acuity Assessment (CAA) tests, respectively. The differences in VA scores between these two techniques arise for several reasons. The CAA test employs a short stimulus presentation time to avoid multiple fixations over the stimulus and also uses a single optotype with no crowding. As such, it is conducted at a luminance of ~ 26cd/m^2, whereas the logMAR test employs a much higher luminance, with the subject having sufficient time to view the stimulus across a number of retinal areas around the point of regard. The final measurement of acuity in this second test is therefore likely to

reflect the performance the subject achieves with the least affected region of the retina.

During the CAA test, the subject's point of regard is drawn by briefly flashing the fixation target, which is then followed by the Landolt ring stimulus. Since the presentation time is less than 200ms, only one fixation is thus possible. On the other hand, the estimated threshold involves a large number of stimulus presentation times during a 'staircase' procedure. Therefore, each stimulus may end up over a slightly different region of the retina and hence the estimated acuity or contrast threshold may still reflect the average performance of the retina over a region that corresponds to the preferred point of regard. A more severe temporal filtering of the retinal image in AMD patients may also serve to reduce the 'effective' contrast of the briefly presented optotype. Since spatial contrast affects VA, even with longer duration stimuli, the difference between the LogMAR and CAA measurements of VA may reflect differences in the temporal processing of signals in AMD patients.

In order to understand the differences between the two tests, a number of experiments have been designed to test both normal subjects and AMD patients using VA and contrast sensitivity as the measurement variables. The aim of the study was to evaluate the effect of presentation time and binocular summation on VA and contrast sensitivity for both healthy and AMD subjects. Finally, for four normal subjects, the effect of presentation time on high contrast gap acuity and on functional contrast sensitivity was determined for six different levels of background luminance.

5.1.5 Materials and methods

5.1.5.1 Study population

Twenty-two (22) AMD patients were recruited for the study from King's College Hospital, whilst eighty-two (82) subjects with a healthy ocular status were recruited from amongst staff and students at City, University of London. Only early stage AMD eyes were analysed from the patient group (dry and wet form; while the exclusion criteria for the normal subjects were any binocular abnormalities that compromised binocular function, including strabismus or amblyopia, or the existence of other ocular diseases). Healthy subjects were also required to have a minimum best

corrected VA of 6/12 which was measured using a high contrast Bailey-Lovie logMAR back-illuminated chart. After assessing their compliance with the inclusion criteria, thirteen had to be excluded leaving a final group of sixty-nine who participated in the actual study. From amongst the AMD group, seven subjects were excluded from the final study owing to the advanced stage of their AMD.

The age range for the AMD group varied from 49 to 82 years, with an average age being of 70.3 (±8.5) years; while for the normative group, the age range varied from 19 to 58 years with the average age being 35 (±10.9) years. Although the age ranges of the two populations were significantly different, the aim of the study was not to compare specific age-related differences, but rather to establish how stimulus presentation time, adaptation luminance, and contrast affect AMD patients and to determine the extent to which the similar results can also be observed for the eyes of the healthy control population.

For the assessment of high contrast gap acuity as a function of stimulus presentation time and background luminance, four subjects with normative vision were recruited from City, University of London. Their age range was 28 to 33 years, with a mean age of 31.3 (±2.4) years.

The subjects participating in this study had varied ethnic backgrounds, including Caucasian, British Asian, East Asian African, and Middle Eastern. All experimental procedures were conducted in accordance with the City, University of London Research and Ethics guidelines. The aim of the project and the procedures involved were thoroughly explained to subjects before informed consent was obtained.

5.1.5.2 Experimental procedure

LogMAR VA was assessed for all subjects using an ETDRS test chart at a distance of 6m. Participants were allowed to spend as much time as they required to complete this task. After the logMAR VA measurement, subjects were moved to another room to perform the CAA test. Each subject was handed a remote control with response buttons (as depicted in Figure 5.4). The four-button array formed a square and was used in the test. The subject sat in a darkened room at a distance of 3m from a computer screen. The CAA test was configured to present a Landolt C at 100%

contrast and at a fixed duration in the middle of the screen (Figure 5.4), with the gap orientated either top left (TL); top right (TR); bottom left (BL); or bottom right (BR).

The subject's task was to determine the spatial position of the gap in the Landolt C and then to press the corresponding button to indicate its location. The acuity threshold was then measured using a four-alternative, forced-choice staircase procedure with variable step sizes. Fourteen reversals were employed, and the threshold was estimated by averaging the final eight reversals. Each eye was tested separately, with the assessment of binocular VA conducted last. The first presentation time to be tested was for 80ms; thereafter the presentation time was progressively changed to 250, 500, 1172, and finally 3000ms. The same procedure was also used later in the study to measure high contrast gap acuity and the functional contrast sensitivity (FCS) using the Acuity-Plus test (City Occupational Ltd) with six different background luminance values of 2, 4, 8, 16, 32, and 64 cd/m^2, but only for short (160ms) and long (1200ms) presentation times. In both tests, positive and negative stimulus contrast polarities were used for binocular viewing at a distance of 3m for further description on the test (http://www.city-occupational.co.uk/acuity-plus/).

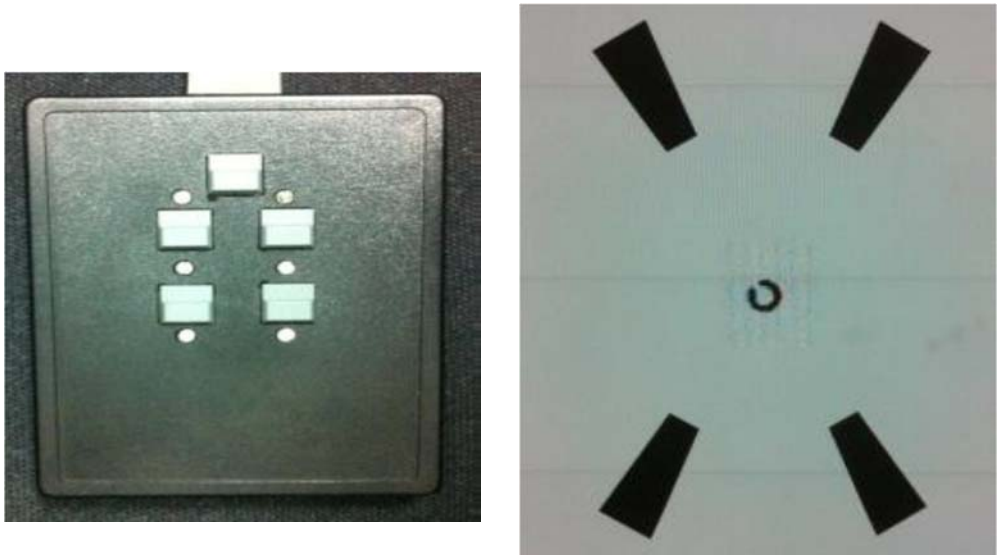

Figure 5.4. Remote control (left) and photograph of target stimulus as shown to subjects in the CAA test.

5.1.6 Results

5.1.6.1 Effect of stimulus presentation time on acuity

Figure 5.5 plots the gap acuity threshold, as measured with the CAA test, as a function of presentation time for both groups. The results indicate that, on average, patients within the AMD group require a gap size that it is twice as large as for the normal group. Although the effect is more pronounced for short stimulus durations, a significant worsening of VA is also observed for the longest presentation times. The AMD patients require, on average, gap sizes that are 2.3x at 80 ms, 2.1x at 250 ms, and 2.0x at both 500 and 1172 ms larger, relative to the control population with normative vision. This ratio was slightly reduced to 1.85x for the longer 3000 ms presentation time. The difference between the two groups reached statistical significance (two-sample unequal variance t-test; $p<0.001$) for all conditions tested. Moreover, the average acuity threshold, as measured with logMAR test chart and expressed in min arc, was found to be 0.82 (±0.12) for normal subjects as compared to 1.39 (±0.55) for AMD patients. The ratio of the mean values for the two groups yields a gap size ratio of ~1.7, a Figure that is significantly smaller than for the corresponding ratios derived using the CAA test, even for the longest presentation time of 3000ms (which yields a corresponding ratio of 1.85).[1]

[1] *Nota bene*. During the ETDRS task (logMAR acuity), participants could spend as much time as they needed.

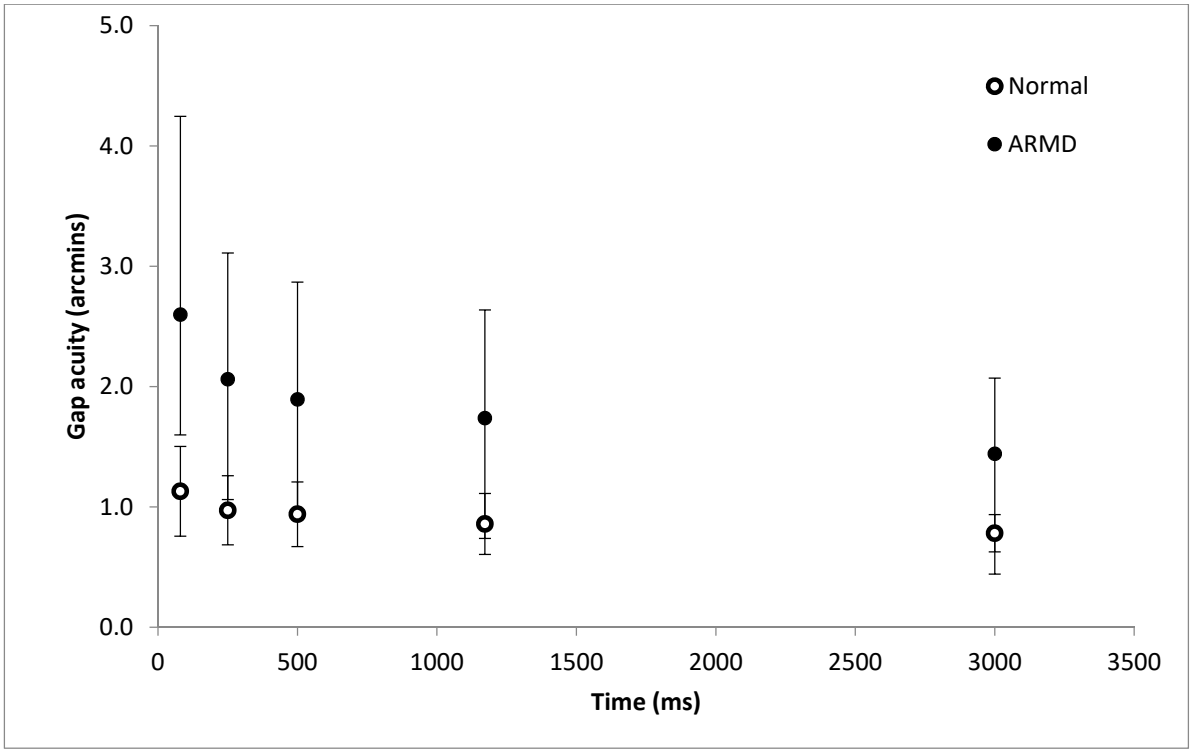

Figure 5.5. Average CAA gap acuity for AMD (ARMD) and normal patients plotted as a function of stimulus presentation time. *Error bars (+/-) represent standard deviation of the mean.*

Figure 5.6 shows the difference in VA as measured on the logMAR chart and the CAA tests for each presentation time in both AMD and healthy groups. Mean values for the left and right eyes are shown for each of the two groups as the correlation between the two eyes was significant (AMD group r^2= 0.56; normative group r^2 = 0.66). As expected, the ETDRS test chart yields significantly higher levels of VA when compared to the CAA test for all but the longest presentation time of 3000ms, at which point the measured difference in VA was no longer significant. The difference is however more pronounced for the AMD group, and is statistically significant for each presentation time from 80ms through to 1172 ms. The ETDRS-measured acuity in the normal group was however only marginally better than for the CAA-measured acuity for the two shortest presentation times. In contrast, the ETDRS-measured acuity within the AMD group is better than the CAA acuity for every stimulus presentation time, although the difference was statistically less significant for the 3000 ms duration. More specifically, the mean difference between ETDRS and CAA measured acuity for the AMD group at each presentation time was -1.21 ($p<0.001$), -0.65 ($p=0.01$), -0.48 ($p=0.01$), -0.32 ($p=0.045$) and -0.07 arcmin

(p=0.66). The corresponding stimulus presentation times were 80, 250, 500, 1172 and 3000 ms, respectively.

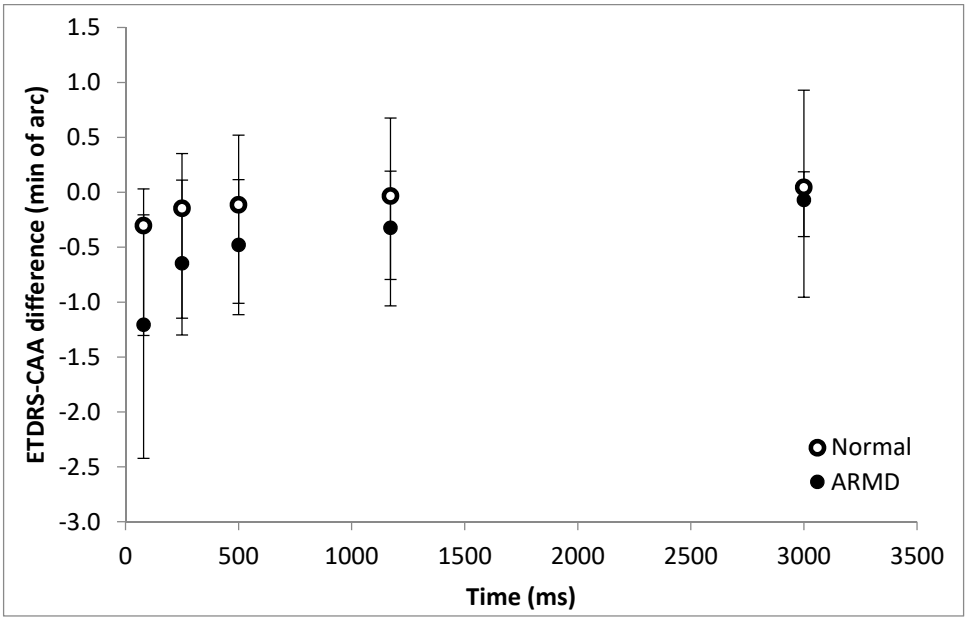

Figure 5.6. Plot of the difference between ETDRS and CAA acuity for AMD (ARMD) and normal patients. Error bars (+/-) represent the standard deviation of the mean.

For the control group, the observed difference in the results between two tests gradually decreases as the stimulus presentation time of the CAA test increases. A statistically significant difference between the two tests was however found for the 80ms (-0.30 arcmin, $p<0.001$), 250ms (-0.15 arcmin, $p<0.001$) and 500ms (-0.11 arcmin, $p<0.001$) stimulus duration times. There is however no statistically significant difference for the 1172ms (-0.03 arcmin, $p=0.22$) presentation time, while at the 3000ms stimulus presentation time, the ETDRS-measured acuity was demonstrably worse than for that derived from the CAA test (0.04 arcmin, $p=0.01$).

5.1.6.2 Effect of stimulus presentation time on acuity and the contribution of binocular summation

Figures 5.7 and 5.8 present gap acuity results (as measured with the foveal CAA test) for various stimulus presentation times under both binocular and monocular

viewing conditions. Data from both groups (AMD and normal subjects) are presented. For the normal group, monocular gap acuity values are presented as mean values from both eyes (left and right), given that non-significant statistical differences were found between the two eyes ($p>0.26$ in all conditions, except at 80ms presentation time, $p=0.02$). Data from 28 subjects are presented for the control group. For the AMD group, data were as derived from only four subjects collected under binocular viewing conditions.

Binocular viewing evidently improves VA for all stimulus presentation times within the normative group ($p<0.001$ for all conditions tested). The degree of binocular improvement varied between 1.17-fold to 1.21-fold independently of the stimulus presentation time. For the AMD group, there was also a marked improvement when acuity was measured binocularly, which was even more pronounced when compared to the worst eye. However, with only 4 patients tested, this apparent trend did not reach statistical significance. Notably, the measured binocular VA within the AMD patients was not significantly better than that measured in the least affected eye.

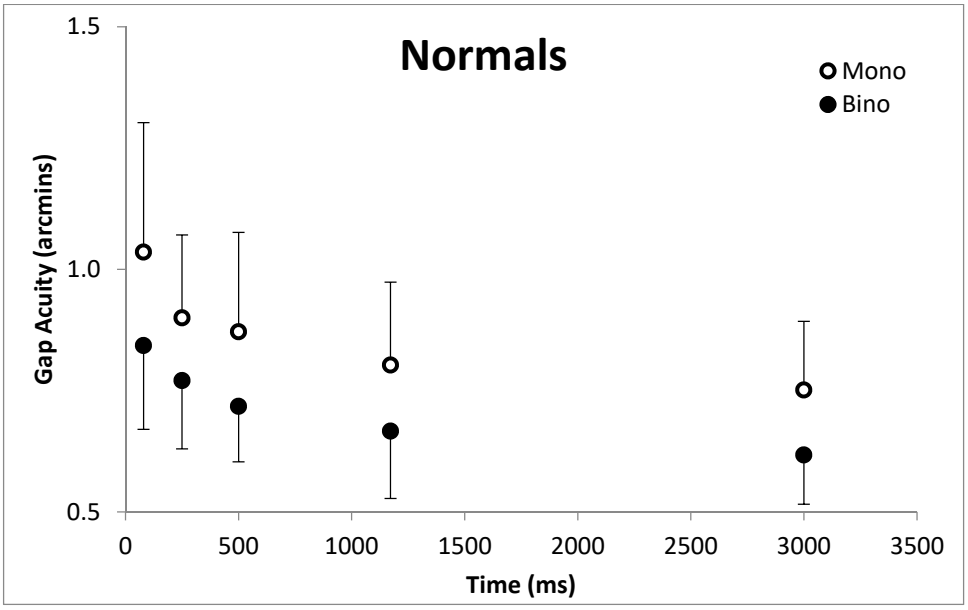

Figure 5.7. Binocular and monocular gap acuity as a function of stimulus presentation time. Error bars are presented +/- standard deviation of the mean (n=28).

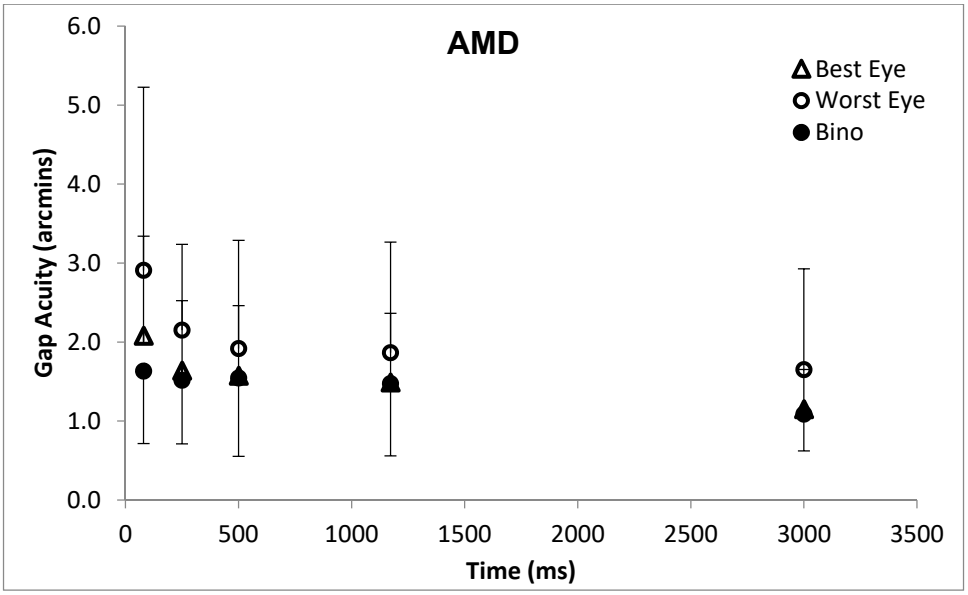

Figure 5.8. Binocular and monocular (best vs. worst eye) gap acuity as a function of stimulus presentation time in AMD patients. Error bars represent the standard deviation of the mean. Data taken from four AMD subjects.

5.1.6.3 Effect of luminance upon acuity and functional contrast sensitivity

Figures 5.9 and 5.10 plot the results from the high contrast gap acuity tests for the 160ms and 1200ms presentation times, respectively, as a function of background luminance and for a stimulus of either positive or negative contrast polarity. Figure 5.11 compares high contrast gap acuity for the 160ms and 1200 ms presentation times, but only for a stimulus of negative contrast polarity.

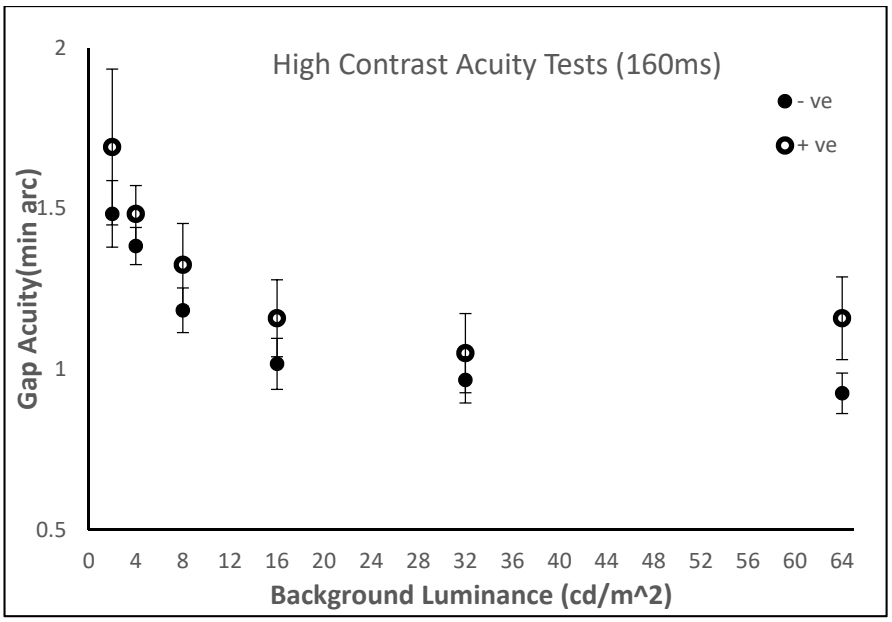

Figure 5.9. High contrast gap acuity as a function of background luminance for a stimulus with a 160ms presentation duration at both positive and negative contrast polarities. Averaged data from 4 normal subjects are presented. Error bars represent the standard deviation (+/-) of the means.

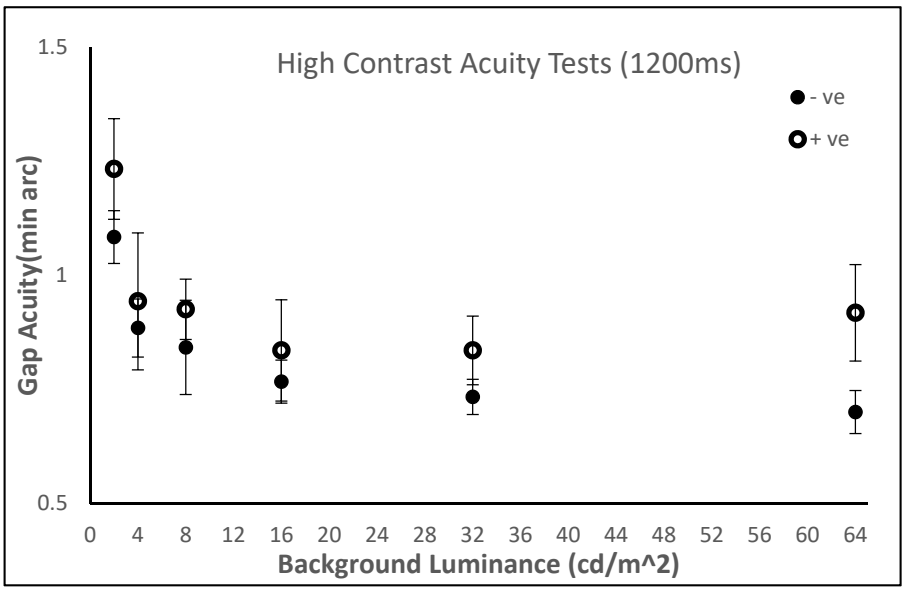

Figure 5.10. High contrast gap acuity as a function of background luminance for a stimulus with a 1200ms presentation time at both positive and negative contrast polarities. Averaged data from 4 normal subjects are presented. Error bars represent the standard deviation (+/-) of the means.

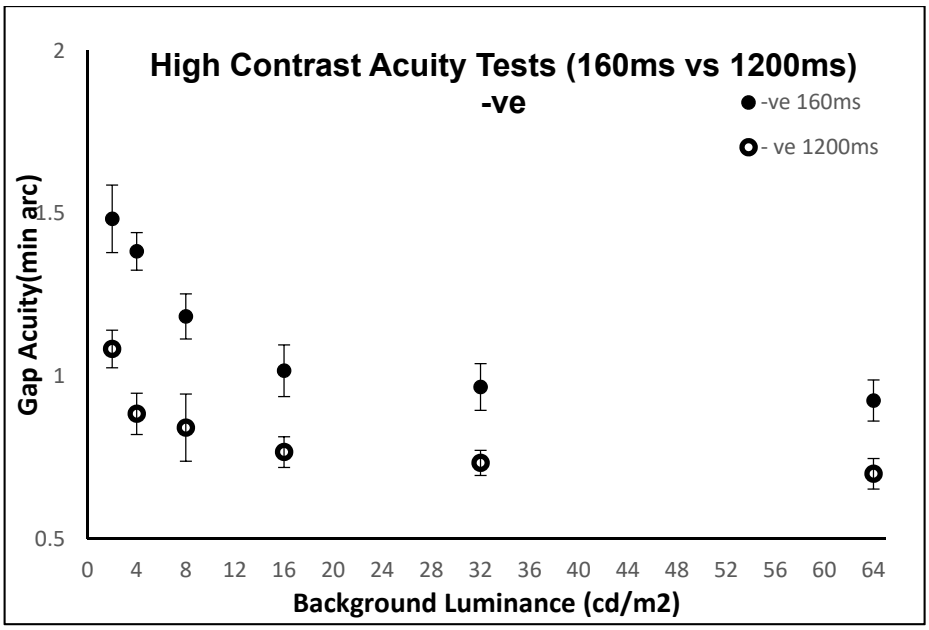

Figure 5.11. Comparison of high contrast acuity as a function of background luminance for two stimuli of 160ms and 1200ms presentation durations and a negative contrast polarity. Error bars represent the standard deviation (+/-) of the means.

It is evident from these findings that, independently of stimulus duration and background luminance, high contrast gap acuity is always better when a negative polarity stimulus contrast is used. More specifically, for both the 160 and 1200 ms stimulus presentation times, there is an improvement of approximately 1.14-fold when negative contrast is used at all background luminance levels, although the sample was again too small to achieve statistical significance. On the other hand, there is a remarkable improvement in high contrast gap acuity as the background luminance level is increased from 2cd/m^2 to 8cd/m^2, especially for the 160ms stimulus presentation time, although at higher background luminance levels (>16 cd/m^2) gap acuity does not further improve. These effects, as expected, are more pronounced for the shorter (160ms) presentation time.

Figure 5.12 shows the Functional Contrast Sensitivity (FCS) as a function of background luminance at both stimulus contrast polarities for a presentation time of 160ms. Once again, a striking difference in FCS was found only for luminance levels below 8cd/m^2 at both stimulus contrast polarities tested. It appears that FCS is superior with a negative contrast polarity, especially for background luminance levels below 8cd/m^2, the improvement being 20% over a positive contrast polarity.

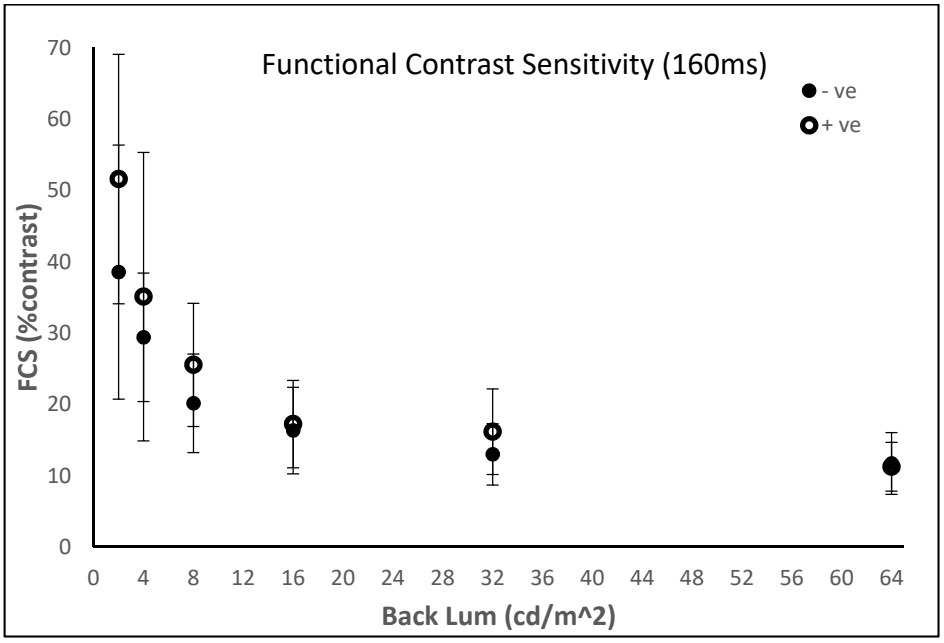

Figure 5.12. Functional Contrast Sensitivity as a function of background luminance. Filled circles represent values obtained with a negative contrast polarity, while the data presented as white circles were obtained with a positive contrast polarity. Error bars represent standard deviation (+/-) of the means.

5.1.7 Discussion

The findings presented in this section indicate that the presentation time during a classical VA task is an important parameter. Although the ETDRS (logMAR) acuity test affords subjects sufficient time to make use of any spatial cues to aid them in the recognition of specific letters, this is not possible during a shorter presentation task such as gap acuity as measured with the CAA test. This is evident from an internal comparison of the ratio of VA as measured within each of the two groups.

Further, when the difference in acuity threshold between the two tasks is plotted (Figure 5.6) a significant effect of presentation time was observed for both those with normal vision and for the AMD patient group, although neither test yielded a significant difference in VA when the Landolt C presentation time was high (3000 ms), with the difference in acuity threshold increasing with decreasing presentation time within the gap acuity task. It is apparent that AMD patients benefit from a longer stimulus presentation time which would allow for a greater degree of temporal integration and more fixations, thereby reducing the overall effect of poor temporal responses in AMD patients and enhancing the benefit of multiple fixations. Under binocular viewing conditions, a significant 30% improvement in gap acuity was demonstrated among the younger, normative group using the CAA test, a gain which was independent of the stimulus duration (Figures 5.6 and 5.7). These values are somewhat higher than those reported within the extant literature, where the binocular summation advantage in high contrast letter acuity ranges from 5% to 13%. This might be explained by the fact that monocular viewing acuity is commonly overestimated for longer stimulus presentations, given that the subjects have sufficient time to make as many fixations as they need for letter recognition, whereas this is not possible with the relatively short presentations of the Landolt C letters. Although the binocular improvement in gap acuity for AMD subjects was less striking, this might be accounted for by the small number of subjects tested. However, it has already been widely established that AMD often shows a differential rate of progression in the two eyes, and this might lead to reduced stereoacuity which would be expected to affect the process of binocular summation.

Gap acuity was also affected by background luminance as acuity declines with reduced cone illumination within the fovea (see Figures 5.8 and 5.9), with the effect being accentuated at lower levels of luminance (a significant improvement between 2 and 8 cd/m^2), while such effects are statistically negligible for luminances greater than 8 cd/m^2. Finally, an interesting observation, in broad agreement with the literature (Owsley, 2003), is that negative contrast (“black” letter on a “white” background) leads to lower thresholds (better sensitivity) as compared to positive contrast (*i.e.* a “white” letter on a “black” background). Similar findings were obtained when comparing the effects of luminance upon functional contrast sensitivity, with

negative contrast resulting in a 20% improvement when compared to positive contrast. This effect was more pronounced at lower levels of background luminance.

5.2 Effect of AMD on colour vision

5.2.1 Background: Colour vision, function and assessment

Colour vision is the ability to distinguish the appearance of objects based upon the wavelength composition of the light they reflect, transmit, or emit. Trichromatic colour vision begins in the retina when light is absorbed by the three different types of cone photoreceptor (L-, M- and S-cones), each of which contains a specific photopigment with a characteristic spectral sensitivity. As there is a significant overlap between the spectral responsivities of the three classes of cone photoreceptor, trichromatic colour vision is achieved via the recombination of cone responses within the retina and their subsequent reconstruction within the LGN and visual cortex ('trichromatic colour theory' first postulated by Young, 1802). Two post-receptoral colour channels arise at the ganglion cell level. These are based upon colour opponent input from the photoreceptors and are the Red/Green (RG) channel, based on (colour) antagonism between L-cones and M-cones, and the Yellow/Blue (YB) channel, based on (colour) antagonism between S-cones with respect to the sumlargely cmed input of L- and M-cones. Within the cortex, colour information is subsequently decoded through a multitude of complex mechanisms which may result in narrower wavelength tuning (Engel et al., 1997).

Various chromatic vision tests have been developed to assess the functionality of colour vision, including the plate test, which are widely used owing to their low cost and comparative ease of use (Lakowski, 1969). Most of these tests assess only RG congenital deficiency although the AO-HRR plates also tests for YB loss (LeGrand et al., 1954). In these tests the observer is usually required to identify a figure of a given colour which is embedded within a textured background with discrete elements that vary randomly in their luminance and colour. There are many plate tests available, some of which are slightly better than others, but all seek to achieve the same goal, which is to screen for a loss or absence of colour vision (Birch, 1997).

The Ishihara test remains one of the most widely used screening tests and serves specifically to detect red-green colour deficiencies (see Figure 5.13). However, the results from this test tend to be noisy and conventional protocols often pass colour deficient subjects, some with severe loss of colour vision (Barbur et al., 2017) with poor classification of the type of colour vision loss.

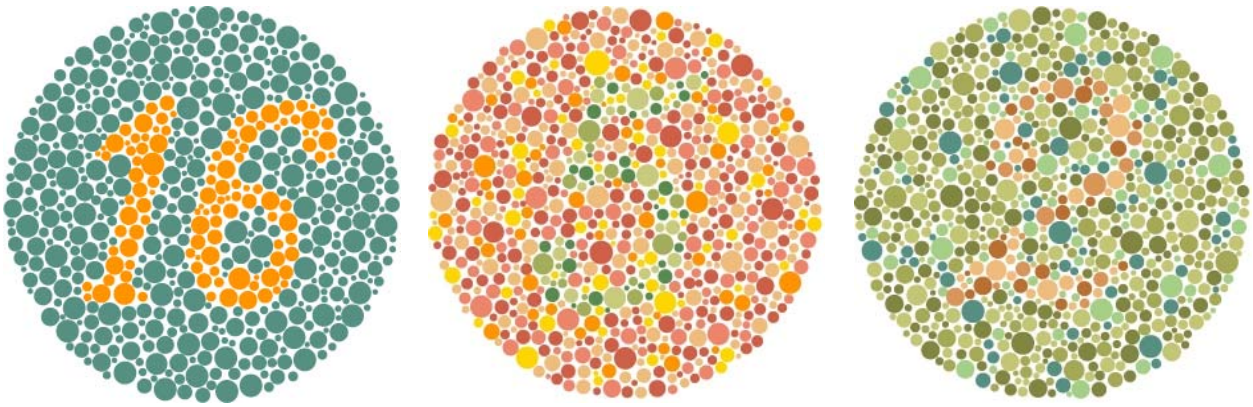

Figure 5.13. Ishihara pseudoisochromatic plates.

Arrangement tests are also commonly used, in which the patient has to place colour samples (caps) in their order of minimum differences, based largely on hue or saturation. The most common tests are the Farnsworth-Munsell 100-hue test (FM 100-hue), which comprises a range of 80 colours divided into 4 boxes and the Farnsworth dichotomous test for colour blindness (Panel D-15), which only requires 15 colours to be placed in a “natural” colour order beginning from a reference colour (Farnsworth,1947).

In contrast, the Nagel anomaloscope relies on a dichromatic colour match and differentiates well deutan from protan-like deficiencies. The test does, however, fail to achieve this aim in that a small percentage of colour deficient subjects may rely upon variant L and M cones (Barbur et al., 2008). In normal trichromats (and also in mild anomalous trichromats), the size of the matching range is also a very poor measure of the severity of colour vision loss (Barbur and Konstantakopoulou, 2012).

5.2.2 The Colour Assessment and Diagnosis (CAD) test

The colour assessment and diagnosis test is a computer-based test designed to isolate the use of colour signals and to detect both RG and YB associated losses in terms of chromatic sensitivity. The test detects and quantifies the severity of colour vision loss by isolating and measuring RG and YB thresholds. As it is used to diagnose colour deficiency in individuals, it removes all additional cues other than colour signals, including luminance contrast cues, by employing spatiotemporal luminance contrast masking techniques. The CAD test is designed to produce a numeric threshold for RG and YB chromatic evaluation which is expressed in 'standard normal units' (SNU). The chromatic sensitivity of the average, young, healthy individual with normal trichromatic colour vision is given as 1SNU, with deficient subjects scored on a representative scale. Thus, for instance, a RG threshold of 2SNU would indicate a deficiency in RG chromatic sensitivity, as the individual requires twice the average RG colour signal strength to give a correct response to the test, whilst a threshold below 1SNU indicates a superior chromatic sensitivity.

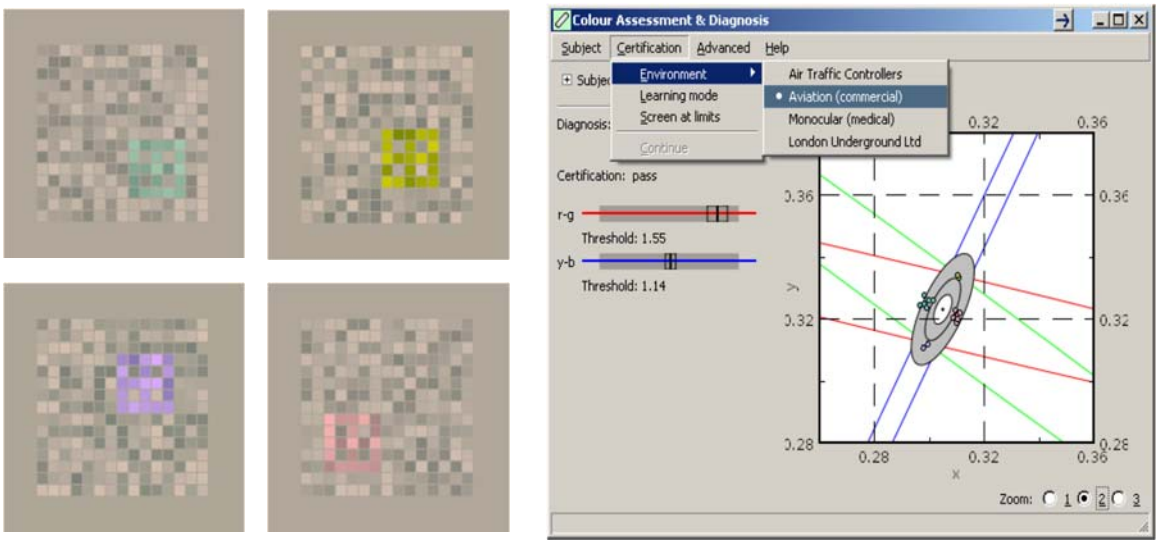

Figure 5.14. Screen captures showing typical stimuli employed in the Colour Assessment and Diagnosis (CAD) test. The stimuli are presented (left) and the results (right) show a plot for both RG and YB thresholds.

5.2.3 Colour vision loss in AMD patients

Age-related macular degeneration causes a general impairment in visual function. VA is often the least informative measure, given that many patients with AMD and drusen can present with normal acuity when the foveal region of the retina is spared. Rapid flicker sensitivity, functional contrast sensitivity and colour vision, on the other hand, may reveal a loss of sensitivity before the onset of other recognizable clinical signs of a decline in VA (Yioti et al., 2012). Other common symptoms include visual distortion, blindspots, central viewing scotoma, photostress and photophobia, decrease in depth perception, and a loss of peripheral vision sensitivity, particularly at lower light levels (Arden and Wolf, 2004). Both RG and YB chromatic sensitivity can be affected in AMD patients, although the YB loss is somewhat more pronounced during the early stages of the disease (O'Neill-Biba et al., 2010). The loss of colour sensitivity affects the whole retina and is also present in the unaffected fellow eye. Thus, a suitable technique which can evaluate RG and YB colour discrimination thresholds would be ideal tool with which to detect and quantify deficits in colour vision during the very early stages of disease. Generally, abnormalities in cone and rod photoreceptor function have been reported in aging retinas in the absence of any other associated pathology, and thus such a measure can reveal the presence of the very early stages of retinal disease. On the other hand, most diseases exhibit specific patterns in terms of RG and YB colour discrimination thresholds, despite similarities in any structural changes to the retina itself, and so these patterns can be used to distinguish the different diseases (O'Neill-Biba et al., 2010). The establishment of age-specific, normal upper threshold limits for both RG and YB colour vision helps separate changes that can attributed to disease from effects of normal aging (Barbur & Rodriguez-Carmona, 2015).

It is therefore possible to distinguish the progression of normal aging from that of actual retinal disease processes. Useful, clinical information can now be obtained by examining any loss in chromatic sensitivity at various light levels, especially in light of the fact that AMD patients are known to exhibit a more pronounced degradation in visual performance at lower luminance levels and also within the YB channel when compared to RG chromatic sensitivity (Barbur and Konstantakopoulou, 2012).

5.2.4 Aim of study

The aim of the study was to assess the loss of both RG and YB chromatic sensitivity in patients with AMD. Preliminary findings suggested that there is a substantial decrease in chromatic sensitivity in both chromatic channels, especially at lower luminance levels, with a slightly greater loss of sensitivity in the YB chromatic channel. Any differences in RG and YB sensitivity between AMD and age-matched normals are also evaluated as a function of age. Finally, the question as to whether there are any correlations between VA and RG and YB sensitivity is addressed.

5.2.5 Materials and methods

5.2.5.1 Study population

Twenty-two AMD patients were recruited for the study from King's College Hospital. Only patients with early stage AMD were included for the purposes of measurement and analysis. Seven subjects were excluded due to the advanced stage of their AMD or the absence of complete data. The age-matched normal limits for monocular CAD thresholds was established in a previous study (Barbur and Rodriguez-Carmona, 2015) and is already included in the CAD test.

The age range of the AMD group (a total of 15 subjects) was 49 to 82 years, with the average age being 70.3 (±8.5) years.

5.2.5.2 Experimental procedure

Chromatic sensitivity was measured using the Colour Assessment and Diagnosis (CAD) test which measures chromatic sensitivity in 16 directions within the CIE 1931 chromaticity chart, using multiple randomly interleaved staircases with variable step sizes and a four alternative forced choice procedure. The stimulus is generated with 30-bit resolution in the centre of a large uniform background field on a visual display (LaCIE Electron Blue, 20" CRT monitor). The stimulus consists of a square array of 15 x 15 achromatic checkers, subtending a horizontal visual angle of approximately 3.3deg x 3.3deg. The background chromaticity was set as MacAdam 'white' in the 1931 CIE-x,y chromaticity coordinates x=0.305 and y=0.323. The luminance of each checker scintillates every 33 to 66 ms, with equal probability, within a range defined

as a percentage of background field luminance; the CAD test employs a range of ± 45% luminance contrast noise. The variation of the checks is such that the average luminance over the stimulus is constant and equal to that of the background, thus providing a steady state of light adaptation independently of any chromatic displacement. This random luminance modulation (RLM) is applied spatially and temporally, thereby creating achromatic dynamic luminance contrast (LC) noise which masks the detection of luminance contrast signals and isolates the use of chromatic signals (Barbur and Ruddock, 1980; Barbur et al., 1981; Barbur et al., 1994; Rodriguez-Carmona et al., 2005). The 45% noise level was selected as it ensures that the colour detection thresholds of those dichromats tested during the development of the CAD test reach the limits of the phosphors of the display (Rodriguez-Carmona, 2006). A smaller, colour-defined test stimulus, which comprises 5 x 5 checkers (subtending a visual angle ~ 0.5 deg at a viewing distance of 1.4m) is buried in the larger array of LC checkers. The test stimulus moves diagonally at a speed of ~4 deg/s from one corner of the flickering square towards the opposite corner, and the subject's task is to indicate the direction of movement of the coloured stimulus by pressing one of the four buttons in an appropriate geometrical spatial array. If no coloured stimulus is seen, the subject is asked to guess by pressing any one of the four buttons. The chance probability of a correct response is 1 in 16, as the correct direction has to be reported twice in succession (before the colour signal employed is decreased according to the interleaved staircase procedure. The initial step size is 0.025 units, reducing exponentially to a final step size of 0.001 units. The test is terminated after 11 reversals, and the mean of the last 6 reversals is taken as a threshold estimate for colour direction.

The CAD test algorithm used within this study averages the chromatic signals measured at each of the 16 chromaticity directions tested to compute the mean RG (140, 145, 170, 175, 320, 325, 350, 355 deg) and YB (56, 60, 64, 68, 236, 240, 244, 248 deg) thresholds.

Subjects were positioned 1.4m away from the centre of the visual display with the optimal refractive correction in place. Each subject was adapted to the uniform background field for three minutes before the onset of the test. They were instructed

to view the centre of the visual display and to notice the direction of the moving target. The learning procedure employed an outline square defined by both colour and luminance contrast signals which is normally seen by all colour deficient subjects. Subjects were asked to identify verbally the corner in which the coloured square ended. Upon oral response, they were directed to press the corresponding spatially located button on the response box. This was repeated until the subject was familiar with the task and motor response (by securing 100% correct responses). Very few subjects required a second repeat in order to achieve 100% correct responses during the 'learning' mode. We can therefore be sure that subjects understood the task. Each presentation of the coloured stimulus was followed by a brief auditory cue to inform the subject to make a response. The subject was now ready to carry out a full CAD test. Two correct responses were required to reduce the saturation of the chromatic stimulus while one incorrect response increased the saturation level. If the subject was unable to detect the moving coloured stimulus, a 'guess' response was still required. On average, the full CAD test takes approximately 10-14 minutes to complete.

The test was repeated at two background luminance levels, one within the photopic range (26 cd/m^2), and the other in the high mesopic range (2.6 cd/m^2).

5.2.6 Results

5.2.6.1 Effect of background luminance on colour sensitivity.

Prior to analysis, a two-sample t-test, assuming unequal variances of CAD threshold values, was performed between right and left eyes for both luminance levels and chromatic channels ($p>0.05$). However, considering the two eyes as being better or worse (depending on the CAD threshold value for each subject) a statistically significant difference was found for all four testing conditions. Figure 5.15 demonstrates the colour thresholds for RG and YB chromatic channels at luminance levels of 26 and 2.6 cd/m^2, respectively. Note that a threshold higher than 1.76 and 2.3 CAD units, depending on age, denotes a significant loss of chromatic sensitivity as compared to subjects with normal colour vision. More specifically, for the YB chromatic channel the average threshold was 4.8 vs. 10.0 SN units for the better and the worse eye, respectively, at photopic light levels; while the thresholds were

11.0 vs. 14.6 SNU for the better and the worse eye, respectively, at mesopic light levels. For the RG chromatic channel, the average threshold was 3.7 vs. 10.0 SN units for the better and the worse eye, respectively, at photopic light levels, while the thresholds were 6.1 vs. 14.0 SN units for the better and the worse eye, respectively, at mesopic light levels.

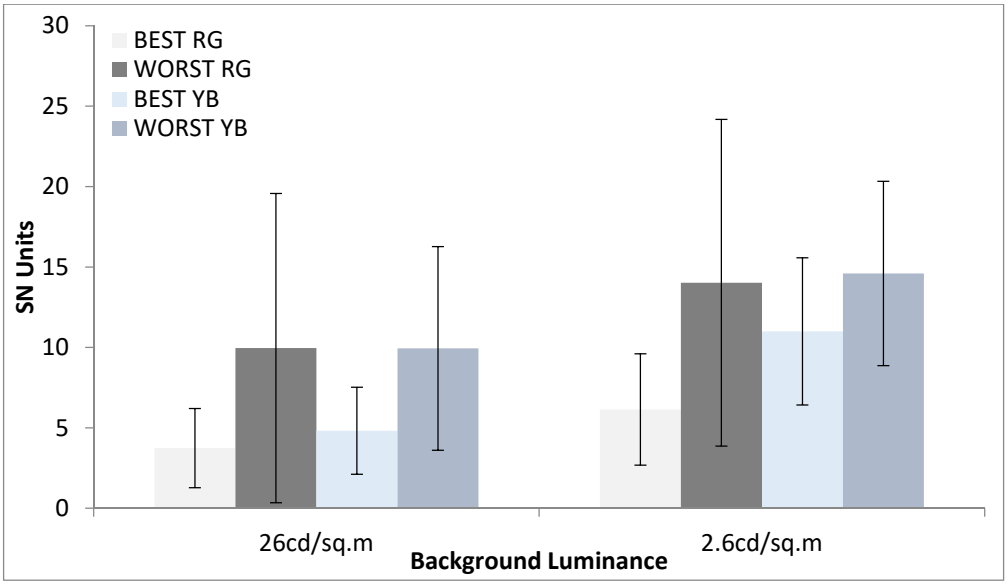

Figure 5.15. RG and YB thresholds for the better and the worse eye at photopic (left) and mesopic (right) light levels (26 vs. 2.6cd/m^2). Error bars represent standard deviation of the mean.

Moreover, at both luminance levels the YB colour sensitivity for the better eye is lower (threshold is higher) as compared to RG, with the difference being more pronounced for the mesopic condition. The difference between the two chromatic channels (RG-YB) was found to be 1.1 ($p=0.24$) and 0.0 ($p=0.99$) SNU for the better and the worse eye, respectively, under the photopic condition and 4.9 ($p<0.01$) and 0.6 ($p=0.77$) SN units, respectively, under the mesopic condition. Thus, the only statistically significant difference was found between the RG and YB threshold for the better eye at mesopic light levels.

It is evident that colour thresholds are impaired at mesopic as compared to photopic light levels. Performing a paired sample t-test for chromatic thresholds observed between the two light levels, a statistically significant difference ($p<0.001$) was found for both RG and YB chromatic channels for both eyes.

5.2.6.2 AMD and normal age colour sensitivity comparison

Taking into consideration the effects of aging, the RG and YB thresholds for the best and worst performing eye for each patient are compared with corresponding upper age-matched normal thresholds reported in previous studies (O'Neill-Biba et al., 2010; Barbur and Rodriguez-Carmona, 2015), in order to establish whether these thresholds were within the normal age-matched range. The following tables detail the differences in colour sensitivity measured for the RG and YB colour channels. The values presented in the final two columns depict the difference for each AMD subject threshold from the corresponding upper normal threshold value (which corresponds to the lower normal sensitivity). Please note that negative values indicate normal colour vision, as a patient's threshold falls between the upper and lower age normal values. Moreover, no subject had a threshold lower (i.e. a higher sensitivity) than the corresponding age-matched lower threshold for normals.

Age	Lower age normal RG threshold	Upper age normal RG threshold	Best Eye RG threshold	Worst Eye RG threshold	Diff of best	Diff of worst
49	0.945	2.545	1.065	1.236	-1.480	-1.309
54	1.026	2.626	2.426	27.895	-0.200	25.269
65	1.206	2.806	1.516		-1.290	
65	1.206	2.806	4.137	9.374	1.331	6.568
68	1.255	2.855	5.296	15.252	2.441	12.397
69	1.271	2.871	3.513	6.008	0.642	3.137
70	1.288	2.888	10.070	17.596	7.183	14.709
71	1.304	2.904	1.640	1.773	-1.265	-1.132
72	1.321	2.921		2.965	0.044	
73	1.337	2.937	6.201	6.282	3.264	3.345
74	1.353	2.953	2.454	3.900	-0.499	0.947
76	1.386	2.986	2.140	4.410	-0.846	1.424
77	1.403	3.003	3.163	3.224	0.160	0.221
78	1.419	3.019	1.855		-1.164	
82	1.485	3.085	1.805	2.429	-1.279	-0.655
				Mean	0.469	5.403

Table 5.1. Differences between AMD and age-matched RG thresholds for the best and worst performing eye. *Changes in retinal illuminance, particularly in older patients with smaller pupil size may have contributed to some of the observed threshold differences. Some patients failed to complete every test, hence the missing data in some of the cells.* The normal subject group did not include any subjects with congenital colour deficiency (Barbur and Rodriguez-Carmona, 2015)

It is evident that there is a notable and statistically significant difference arising in RG threshold between the best and worst performing eyes, although there is no correlation between the age of the subject and the difference in threshold arising between AMD and age-matched control subjects (the correlation coefficient was calculated to be r=-0.11 for the best and r=-0.52 for the worst performing eyes; see table 5.1).

Age	Lower age normal YB threshold*	Upper age normal YB threshold	Best Eye YB threshold	Worst Eye YB threshold	Diff of best	Diff of worst
49	0.951	2.691	1.106	1.110	-1.584	-1.581
54	1.067	2.807	5.256	18.478	2.449	15.671
65	1.325	3.065	2.272		-0.793	
65	1.325	3.065	9.790	15.671	6.725	12.606
68	1.395	3.135	14.390	17.843	11.254	14.707
69	1.419	3.159	2.809	3.079	-0.350	
70	1.442	3.182	3.598	9.841	0.415	6.659
71	1.466	3.206	2.943	3.113	-0.263	-0.093
72	1.489	3.229	3.152		-0.077	
73	1.513	3.253	9.429	9.643	6.176	6.390
74	1.536	3.276	1.979	4.949	-1.297	1.673
76	1.583	3.323	5.056	14.813	1.733	11.490
77	1.607	3.347	5.822	8.207	2.475	4.860
78	1.630	3.370	3.761		0.390	
82	1.724	3.464	1.854	2.152	-1.610	-1.312
				Mean	1.694	6.461

Table 5.2. Difference between AMD and normal age YB threshold values for best and worst performing eye.

The differences observed between best and worst performing eyes in terms of YB threshold was found to be statistically significant (p=0.006), with the effect being more pronounced than for the RG channel measurements. Again, no significant correlation was found between age and the difference between AMD and normal age threshold values (r=-0.15 and r=-0.54 for the best and worst performing eye, respectively) (see table 5.2).

It is evident that the differences arising between the AMD colour threshold and the corresponding age-matched values for subjects with normative vision are independent of their age. This would also suggest that the differences in colour sensitivity observed between AMD patients and age-matched normative subjects is largely correlated with the stage of progression of the AMD disease process rather than age. This observation has now been confirmed in a more extensive study which involved ~ 80 patients (Vemala et al. 2017).

5.2.6.3 Visual acuity and colour sensitivity correlation

The correlation between RG and YB colour sensitivity with VA was ascertained for AMD subjects at two divergent stimulus presentation times (80ms and 3000ms). The resulting data are presented in Figures 5.16 through to 5.19. The data are plotted and fitted to a Pearson correlation coefficient with associated R^2 values to determine the significance of each underlying trend.

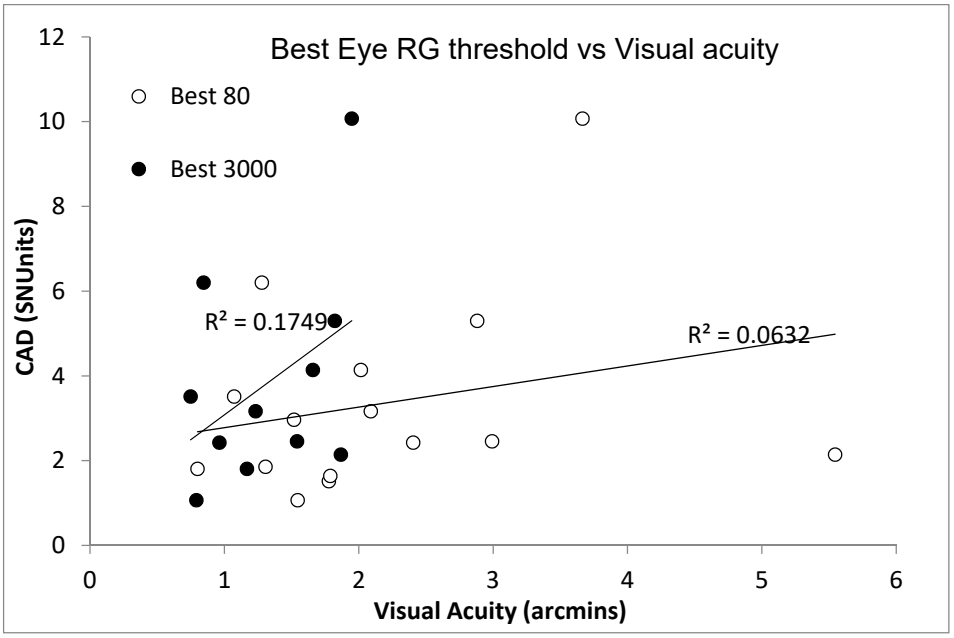

Figure 5.16. Best eye RG threshold correlation with visual acuity. White circles represent 80ms presentation times, while black circles denote 3000ms stimulus presentation times. The results illustrate the poor correlation between RG colour thresholds and VA in AMD patients.

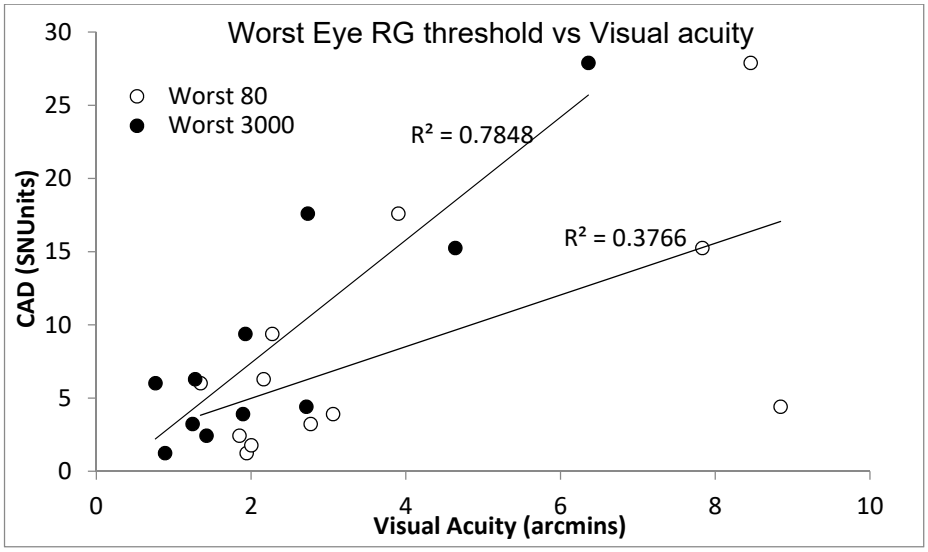

Figure 5.17. Worst eye RG threshold correlation with visual acuity. White circles represent 80ms presentation times, while black circles denote 3000ms stimulus presentation times.

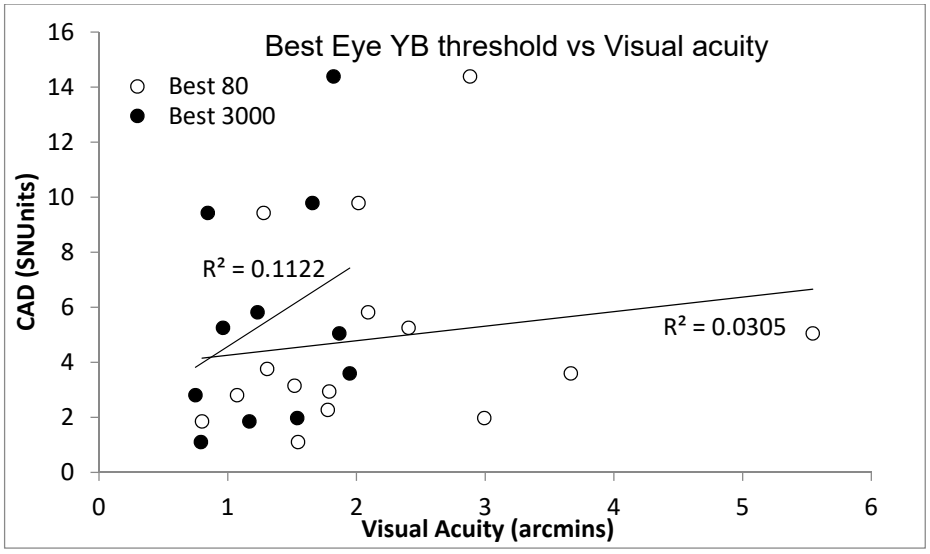

Figure 5.18. Best eye YB threshold correlation with visual acuity. White circles represent 80ms stimulus presentation times, while black circles denote 3000ms stimulus presentation times.

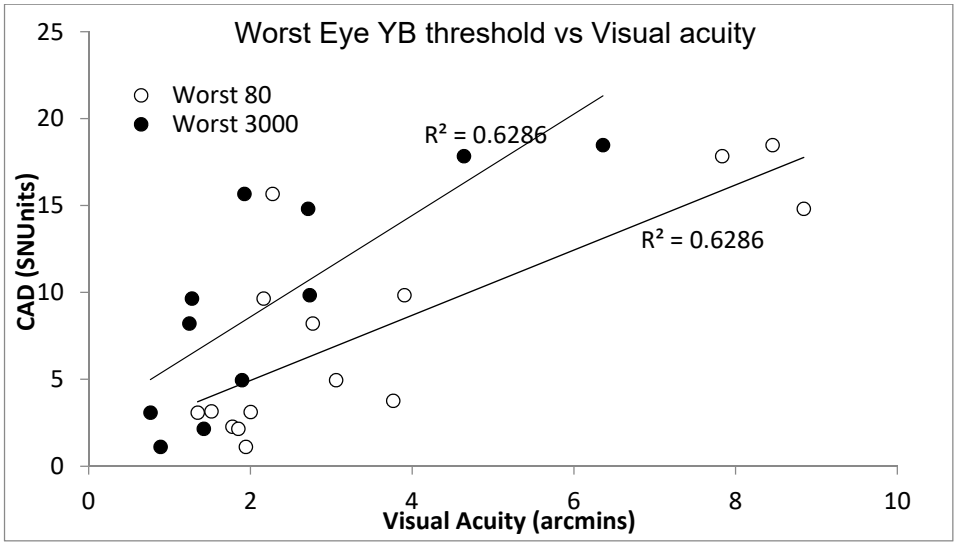

Figure 5.19. Worst eye RG threshold correlation with visual acuity. White circles represent 80ms presentation times while black circles denote 3000ms stimulus presentation times.

It is evident that, for both RG and YB thresholds, there is a stronger correlation between VA and CAD thresholds for the worst performing eye, in which VA is more significantly affected. On the other hand, in all experimental cases tested, the R^2 value was higher for the 3000ms than for the 80ms stimulus presentation time, indicating a higher correlation between VA and colour sensitivity when presentation times are greater.

5.2.7 Discussion

In this study, the chromatic sensitivity of AMD patients was assessed using the CAD test which serves to quantify the severity of colour vision loss within RG and YB chromatic channels. The test is purposely designed to isolate the use of RG and YB colour signals, yielding a linear scale[2,3] with an SNU of 1 for a normative subject[3].

The results obtained indicate that, at photopic light levels, AMD patients experience an average threshold of 3.7 and 10.0 SNU in their RG pathway within their better

[2] A RG threshold of 2 SNU units indicates a halving in RG chromatic sensitivity, while values below 1 SNU correspond to better than the average sensitivity.
[3] *i.e*. an average, young individual with normal trichromatic colour vision in both RG and BY chromatic channels.

and their worse performing eye, respectively. The corresponding loss within the YB colour pathway is found to be slightly more pronounced in the better eye (4.8), whereas it is similar in the worse eye (10.0). These changes may be attributed only in part to the effects of normal aging since the measured thresholds are well above the upper normal limits, even for subjects above 80 years of age (i.e., ~ 3 CAD units for RG and 3.4 CAD units for YB (Barbur & Rodriguez-Carmona, 2015).

Chapter 6. Vision in subjects with hyperawareness of afterimages and visual snow

6.1 Introduction

Visual snow (VS) refers to a transitory or permanent visual experience of flickering achromatic noise-like dots covering either part or the whole of the visual field, notably against darker backgrounds. Hence it is thought to resemble the dynamic noise or ‘snow’ present on a badly-tuned analogue television (Gersztenkorn and Lee, 2015, see Figure 6.1). Aside from its intriguing and unusual characteristics, the condition is extremely rare, and its prevalence is difficult to estimate, given that many patients are unaware that they have the condition. The precise frequency of VS arising within the population is therefore unknown.

Figure 6.1. Normal vision vs. visual snow (from quora.com).

The severity of the perceived "snow" differs from one person to another. In some cases, it can have a negative impact upon daily life, making it difficult to read and focus correctly. VS should not be confused with normal entopic phenomena or the presence of vitreous floaters, although these two conditions also cause spots and floating objects to appear over the field of view.

The symptoms are continuous and can last for many years. Despite the attention of ophthalmologists, neuroscientists and neurologists, many of whom have encountered and studied patients presenting with VS symptoms, the aetiology of the condition remains unclear. Moreover, the symptoms of VS often occur together with other visual dysfunctions, including photopsia, nyctalopia, palinopsia[4], constant blue

[4] The prevalence of an afterimage, i.e. the persistence of a previously viewed stimulus.

field entoptic phenomenon (Zambrowski et al., 2014), as well as with other symptoms such as migraine, migraine aura, tinnitus and tremor, all of which may serve to conceal or effectively mask other perceptual disorders. Although in some case studies researchers have provided valuable new insights into the phenomenon of VS, such as its association with occipital bending, and have proposed effective treatments that decrease the frequency of migraine attacks and VS symptoms (Unal-Cevik and Yildiz, 2015), as yet no general consensus as to its aetiology or treatment have emerged, given that VS can also be associated with stress or depression. While the latter relates to occipital bending (Maller et al., 2014) and the previous use of illicit drugs (Abraham, 1983; Halpern and Pope, 2003), no clear causative agent or disease process has been identified, further heightening scientific curiosity and debate.

Schankin et al. (2014) have suggested that VS is a unique visual disturbance, one which is clinically distinct from the disabling phenomenon of migraine aura and also from Hallucinogen Persisting Perception Disorder (HPPD). Thus, the authors proposed a set of diagnostic criteria in an attempt to demarcate the syndromic nature of this condition. According to these criteria, a diagnosis of VS syndrome can be made when a patient presents with at least one of the following associated symptoms, comprising palinopsia, photopsia, nyctalopia and entoptic phenomena (*but excluding those who have a history consistent with migraine aura or drug abuse*; Schankin et al., 2014). Moreover, their findings suggest that “visual snow,” migraine, and typical migraine aura are in fact distinct syndromes despite their common pathophysiological mechanisms, thus necessitating further research (Schankin et al., 2014). Recent studies have reported some relief from the symptoms of VS in those patients who wear tinted lenses. Intuitive colourimetry has been used in the past to alleviate the symptoms of perceptual disorders and visual stress as reported by patients presenting with dyslexia, migraine or photosensitive epilepsy. Lauschke et al. (2016) followed up these findings and identified a pattern of symptomatic relief arising from coloured tinted filters, particularly those within the YB spectrum. The authors thus proposed that VS arises as a result of an imbalance of koniocellular and magnocellular pathway functions, thereby creating a thalamocortical dysrhythmia that results in a visual processing disorder (Lauschke et al., 2016).

However, in summary, the causes of VS remain as yet largely undiscerned, and thus further research is required, especially given that many patients have no clinically detectable signs of disease and are thus mistakenly classified as having normal vision.

6.2 Visual Snow and after images

The most common symptom of VS patients is the persistence of after images, lingering within the field of vision after the gaze is averted or the image presented is changed (Bessero and Plant, 2014). Therefore, the condition requires a more extensive set of diagnostic tests and criteria to be developed to ensure its widespread recognition. Given that the assessment of after image strength is a common and widespread psychophysical method, this presents at least one experimental tool to enable us to decipher the origin of VS, as the persistence of after images has been shown to be dependent upon stimulus intensity and contrast as well as the time of fixation (Durgin and Hammer, 2001). While the time of fixation primarily concerns the manifestation of physiological after image phenomena in pathological cases, both illusory and hallucinatory palinopsia have also been reported (Gersztenkorn and Lee, 2015), although illusory *(and not hallucinatory)* palinopsia is also strongly affected by stimulus psychophysical characteristics, and thus has to be separated from physiological after image effects, although there are no clear operational clinical criteria that define whether the persistence of after image is pathological or physiological in nature. Of particular interest, are the persistence of chromatic after images.

Chromatic after images fall into two categories, namely positive and negative after images. Perceptually, positive after images have the same colour as the original colour, whereas negative afterimages have the complementary colour. The neural processes underlying the formation of positive after images is however less well understood, although some studies suggest that the mechanism relates to neural adaptation (Barlow and Sparrock, 1964; Miller, 1966). On the other hand, negative after images have largely been associated with the retina and are thus likely to be caused when the cone cells are overstimulated and become refractory (Shimojo et al., 2001). For example, when gazing at a reddish colour stimulus for several

seconds, the L cones of the retina are the most strongly activated. If the subject's gaze is then immediately diverted to a uniform spectrally neutral background, the same L cones generate reduced signals which arise as a consequence of the bleached photopigment. However, if the remaining cone classes (*i.e.* M and S cones) are otherwise unaffected by bleaching they will continue to generate normal signals. Given that the ensuing colour signal generated will contain proportionally less red L cone output, it will therefore appear to be more greenish (corresponding mainly to M cones) in hue. This explanation forms the basis for a working model which has been proposed to explain pupillary responses to the after image caused by a coloured stimulus in 'blind sight' subjects (Barbur et al., 1999).

Psychophysical methods used in the assessment of after image strength can also be adapted to study pathological examples of extended afterimage strength and duration. In examining the origin of after image effects, one should consider the role of spatial and temporal adaptation (Barbur et al., 1999), especially to natural images, as the stage of neural adaptation is indistinguishable from visual after-effects (Webster, 2015; Cohen,1965). One notable point is that the recovery time of adapting neurons plays an as yet undefined role in determining the strength of an after image (Virsu, 1978; Lorenceau, 1987; Mei et al., 2015), and so any dysfunction in the process of adaptation or neuronal recovery might serve to explain the perceptual phenomena we refer to as visual snow. VS patients, despite being visually handicapped to some degree, do not actually experience the classical experimental conditions employed in the study of long-term adaptation within their daily lives. There is, however, one potential explanation, as recent studies have revealed that, in addition to classical long-term visual spatial and temporal adaptation, similar recovery mechanisms operate within the process of contrast adaptation (Yang et al., 2010). The fact that neural adaptation is believed to occur at a cortical level (Shimojo et al., 2001; Pavan et al., 2012), has led researchers to investigate other electrophysiological aspects of visual after-effects in order to substantiate this viewpoint. The findings of Zaidi et al. (2012) indicate that, although after image signals are primarily generated within the retina, they may subsequently be modified (as for other retinal signals) by upstream cortical processes which have been implicated in the generation of colour after images. On the other hand, Poiroux

et al. (2001) had previously reported electrical activity arising within the posterior cortex during an after image of high frequency luminance gratings in the form of visual evoked potentials (VEPs).

The accruing evidence thus suggests that reported VS phenomena may have to be viewed as a cortical dysfunction rather than as a consequence arising from early stage visual processing deficits. Although several studies have reported pupillary responses during stimulus offset in addition to its onset, these secondary responses are referred to as pupil afterimage responses. Barbur (1999) employed double-isoluminant stimuli with opponent colours (reddish and greenish), reporting that the pupillary colour responses were normal within the sighted hemifields of two hemianopia subjects whereas, in their blind hemifields, there was only an onset pupillary response to the reddish stimulus and an offset response to the greenish stimulus. Such pupillary after image responses have also been observed in many other pupil studies (Kohn and Clynes, 1969; Kimura and Young, 1995; Tsujimura et al., 2001). Despite the number of attendant studies, the underlying mechanisms involved in generating such effects remain poorly understood.

6.3 After image assessment. The QAA test.

Patients with palinopsia tend to experience a longer persistence of visual images as compared to normal subjects (Bender et al., 1968; Meadows and Munro, 1977). Palinopsia often appears in association with other visual disturbances such as VS and has been attributed to a number of conditions affecting the brain including tumours, visual pathway lesions, and medications. However, many patients presenting with palinopsia and/or VS syndrome appear to have essentially normal vision, according to standard measures of visual performance, and otherwise show no clinical abnormalities. This effectively means that extant clinical tests fail to detect abnormal visual function in these patients. It is therefore of considerable scientific interest to ascertain the extent to which the perceived after image contributes to visual perception and how such anomalies may affect image quality in the subject.

With respect to the strength and duration of perceived chromatic after images, a new computer-based vision test known as the Quantitative Afterimage Assessment (QAA), was specially developed for such studies. The test employs an efficient

psychophysical technique which has been designed to obtain results in a relatively short time. Figure 6.2 illustrates an example of the displayed 'real' stimuli and the corresponding perceived images as experienced by a normal trichromat. The top row illustrates the temporal sequence of the stimuli (*i.e.* reference stimulus, blank screen and the test stimulus) which are displayed on the screen, while the bottom row shows the corresponding images as perceived by a normal trichromat. The normal subject first perceives the reference stimulus (*top left picture*), but when the reference stimulus is removed, the subject perceives the negative afterimage of the reference stimulus (*middle pictures in the bottom row*).

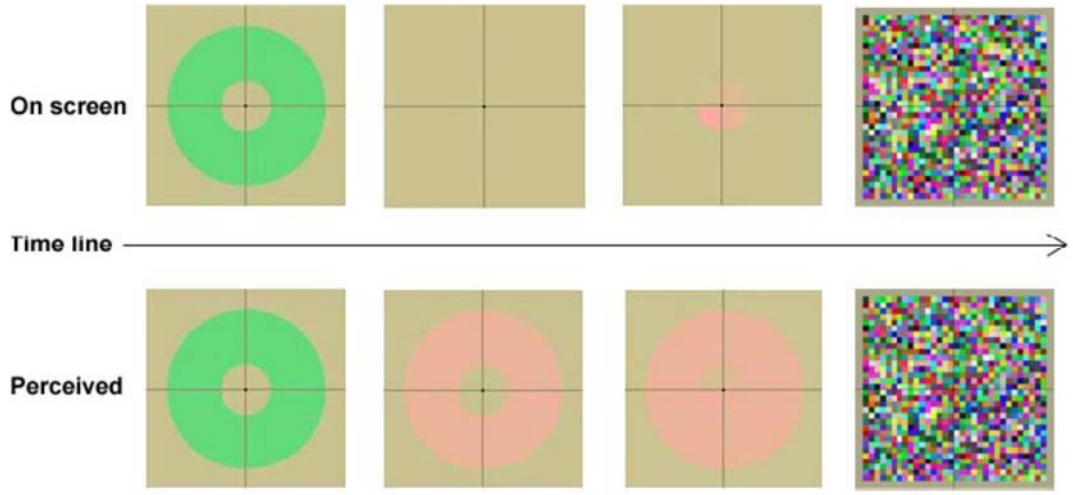

Figure 6.2. The four-alternative forced choice QAA test. The upper row shows the stimulus presentation sequence on the screen. In a typical QAA test, the reference (adaptation) stimulus is presented for 5s, followed by a blank screen for certain durations according to the gap time. Then the test stimulus is presented. Finally, a square patch with random luminance and coloured noise is presented. The bottom row shows an example of perceived images from a normal trichromatic observer. The trichromat sees the reference stimulus when it is presented on the screen. However, when the reference stimulus is turned off and when the blank screen is seen, the subject perceives a coloured afterimage of the reference stimulus, which has an opposite colour to the reference stimulus. At the time when the test stimulus is displayed, the subject perceives the coloured afterimage as well as the test stimulus and the subject's task is to choose which quadrant of the test stimulus matches most closely with the coloured afterimage. Finally, the random noise is used to minimize or eliminate any perceived afterimages before the next trial.

As soon as the test stimulus (top right picture) is displayed, the subject presses one of the four buttons that corresponds to the quadrant that most closely matches the strength of the after image. A typical QAA experiment involves two tests: a four-alternative forced-choice test and a staircase test. Figure 6.2 depicts a schematic diagram for the four-alternative forced-choice after images, in which an approximate threshold is obtained, usually within 1 minute. The subject is then instructed to look

at the fixation point located in the centre of the background at all times. When the subject hears the first beep, the reference stimulus is displayed (*top left*). After a specified period of around 5 seconds, the reference stimulus disappears and the subject perceives the afterimage of the stimulus. Next, the test stimulus is displayed followed by a second beep. When the test stimulus is displayed, the smaller test stimulus and the bigger afterimage together form an entire disc. Because the strength of the colour signal used in each of the four quadrants in the test stimulus is always different, subjects are asked to select the quadrant that matches most closely the appearance of the surrounding afterimage. The algorithm allocates the Chromatic Displacement (CD) for each of the four quadrants that differ significantly from one another, which may be as great as ten times the normal colour detection threshold.

The four quadrants change their CD values according to subjects' response until the subject selects the same answers twice in succession, at which point the test terminates. In the typical staircase algorithm, when the approximate threshold is unknown, a large number of reversals are needed (usually > 11). In the QAA staircase test, the starting increment value is based upon an approximate threshold which is derived from the rapid four alternative forced choice test. This procedure effectively decreases the number of reversals needed in the main staircase. Seven reversals were used, and the threshold was estimated by averaging the final four reversals. The standard error associated with the last four reversals rarely exceeded 11% of the mean. The QAA program was developed to investigate the strength of after images in subjects with congenital red/green deficiency and also for the use in another related study that involved patients with VS and palinopsia syndrome (Bi, 2012).

6.4 Pupillometry. The P-Scan system

Of particular interest is the observation that pupil size in humans is dependent upon many factors, ranging from 2 to 8mm. Pupil responses are affected by age, the ambient light level, accommodation state, fatigue, circadian rhythms, drugs and various psychological factors, including attention, alertness, mental workload and emotional state. In addition to the main lateral geniculostriate projection, the pupillary

pathway is also controlled by retinal signals that ascend to extrastriate regions of the cortex (including V2, V3, V4 and V5), either through small direct projections which bypass V1 (Stoerig and Cowey, 1997), or else through indirect projections from midbrain nuclei, such as the superior colliculus (Gross, 1991), which receive either direct retinal inputs or inputs from the LGN. In addition to the retinal input, the Olivary Pretectal Nuclei (OPN) may also receive direct inputs from the cortex, possibly V1 (Barbur, 2003). The Edinger-Westphal (EW) nucleus receives inputs from the OPN and also from extrastriate areas of the visual cortex. The latter may be responsible for the generation of stimulus-specific, transient pupillary constrictions, such as those which are measured in response to colour, gratings or movement, even when such stimuli cause a net reduction in retinal illumination (Barbur, 2004b). A single dilated pupil may thus be indicative of the presence of a brain injury, stroke or tumour (Bi, 2012).

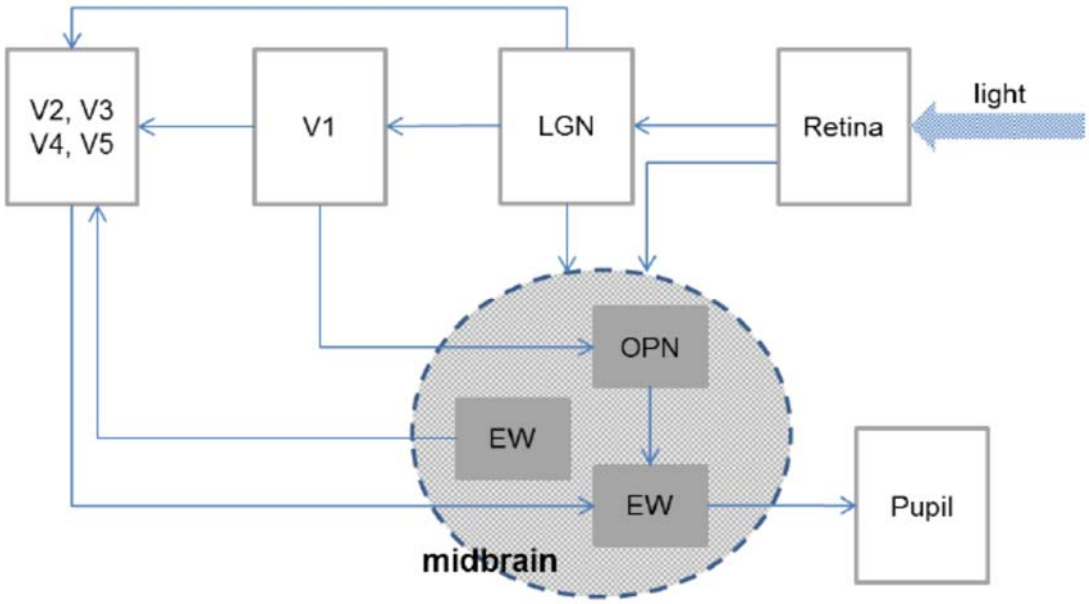

Figure 6.3. A typical schematic diagram of known pupillary pathways *(from Barbur, 2004b).*

Pupil measurements were performed using the P-SCAN system, which enables the simultaneous, binocular measurement of pupil size and the corresponding 2D movements of the eyes. The statistical methods employed in extracting the parameters of interest are equivalent to fitting the best circle to the pupil. From these data, the diameter of the pupil at any given point in time is then determined by

calculating the diameter of the best-fit circle. The resultant data thus yields a resolution for the measurement of pupil diameter and eye movements which are better than 0.01 mm and 4 min arc, respectively (Alexandridis, 1991; Barbur et al., 1992; Barbur et al., 1987). The P-SCAN system employs bespoke hardware for the processing of the video image and the determination of pupil size (Barbur, 1987).

The pulsed, infra-red illumination lasts for ~ 3 ms and is synchronized to correspond to the centre of each video frame. The iris is illuminated from below to produce a high contrast, dark image of the pupil onto an infrared sensitive CCD camera which has a temporal resolution at 50Hz. The algorithm which is employed to determine the pupil diameter is based on calculating the spatial coordinates of the pupillary centre from intersection points between the circumference of the pupil and a specified pattern of lines. Various types of visual stimuli can be generated using the P_SCAN system, including stimuli with different spatial structures, such as sinusoidal/square gratings; achromatic stimuli with different luminance contrasts; and isoluminant chromatic stimuli with different chromatic displacement and angles (see Figure 6.4).

Figure 6.4. Two double isoluminant stimuli. Two double isoluminant stimuli which are employed in various studies are shown on the left and in the middle which also used in our study. Both are photopically and scotopically isoluminant when presented against the display background. An achromatic sinusoidal grating is shown on the right.

All the stimuli can be modulated with sine/square envelopes with different durations. A spatial and temporal luminance contrast modulation can also be added to any stimulus. Figure 6.5 shows a typical pupil response trace to a 480ms light flash stimulus. The duration of the tests depends on the stimuli employed and the number of trials required to gain an accurate measurement.

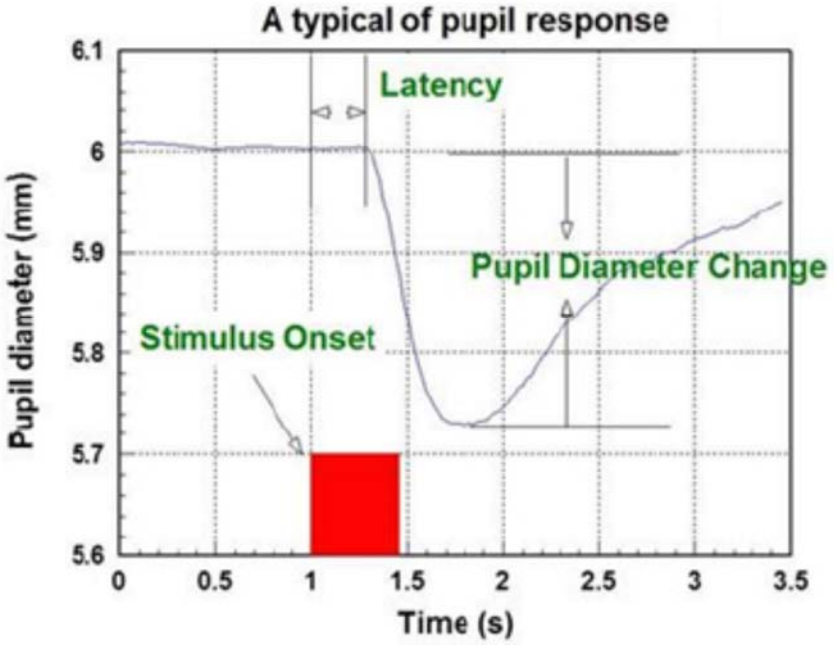

Figure 6.5. Typical pupil response trace to a 480ms light flux increment (from Barbur, 1987).

6.5 Aim of the study

As discussed above, although patients complain of persisting “visual noise”, often referred to as “visual snow” (VS), they otherwise exhibit no obvious clinical abnormalities in standard ophthalmic tests. The purpose of this study was to investigate the extent to which the processing of different stimulus attributes remains normal in VS patients. Advanced vision tests were used to assess visual acuity (VA), colour sensitivity, chromatic afterimage strength and duration as well as pupil response amplitudes to chromatic stimuli.

6.6 Materials and methods

6.6.1 Study population

Seven VS patients were recruited from the National Hospital for Neurology and Neurosurgery of the University College London Hospital. Nine subjects with a healthy ocular status were recruited from the City, University of London student and staff population to serve as controls. The exclusion criteria for the normal subjects were any binocular abnormalities that might compromise binocular function, such as strabismus or amblyopia, and/or the existence of other ocular diseases. Subjects

were also required to have a minimum best corrected visual acuity of 6/6 (which corresponds to an acuity of 1 min arc, or 0 on the LogMAR scale). which was measured using a refracted and high contrast Bailey-Lovie logMAR back-illuminated chart.

The age range for the VS group was 28 to 51 years, with the average age being 38 (±8) years, while for the normative group, the age range was 24 to 51 years, with the average age being 32 (±9) years. These patients sought clinical help with their condition, but the examinations carried out at the hospital failed to identify any factors that may have contributed to their symptoms.

Subjects participating in this study were derived from a range of different ethnic backgrounds including Caucasian, British Asian, and East Asian African and Middle Eastern. All experimental procedures were conducted in accordance with the guidelines set out by the Research and Ethics Committee of City, University of London. All procedures were thoroughly explained to subjects prior to obtaining informed consent .

Prior to each measurement, all VS subjects were asked to complete a detailed questionnaire to assess possible associations between VS perception and various other predictive factors including migraine, aura, alcohol and drug (recreational or medical) usage, as well as to identify any other perceptual or developmental disorders.

6.6.2 Experimental procedure

Gap acuity and chromatic sensitivity were assessed using CAA and CAD tests, respectively, as previously described. For CAA tests, two stimulus presentation times of 60ms and 1200ms were employed under monocular (for each eye) and binocular viewing conditions. To determine after image strength and duration the QAA test was used (as described in section 6.3). The background employed had a fixed luminance of 26cd/m^2 and a fixed chromaticity of 0.305, 0.323. The luminance and the chromaticity of the background were chosen to be identical to those of the CAD test. Therefore, the measured strength of the chromatic after images can be readily compared and contrasted to those of colour sensitivity. The background

chromaticity selected corresponds to the white point used by MacAdam (1942), which forms the centre of the MacAdam ellipse (MacAdam, 1942). Colour sensitivity was measured in relation to this background chromaticity at 26cd/m^2, allowing the program to generate an optimum number of coloured stimuli for any chromatic directions in the CIE 1931 (x, y) colour space. The strength of an after image was measured as a function of the gap time between the offset of the reference and the onset of test stimulus.

As for the pupil measurements, a uniform background (30° x 24°) with CIE coordinates (0.298, 0.335) and a luminance of 12cd/m^2 was used throughout the pupil afterimage studies. The variant chromaticity of the background employed maximised the extent of the chromatic displacement that could be achieved using d-isoluminant stimuli. The latter are 'doubly-isoluminant' with no luminance contrast for both rods and cones. The stimulus was a disc 9.5° in diameter, which was presented at the centre of the background for a duration of 2.4 seconds. The subjects were instructed to view the screen binocularly, and the pupil traces that were obtained represent the average of 32 measurements for each stimulus. The selected chromatic angle required for this test was 118°. This greenish stimulus had the same photopic luminance as the background and had absent rod contrast.

6.7 Results

6.7.1 Visual snow linkage with various factors

All VS subjects reported both VS and after image problems with equal probability, although some had greater difficulty with after images whilst others found VS more debilitating. With 83% and 100% of our VS patients tested (7), did not suffer from migraine or visual aura, respectively. However, no safe conclusion can be drawn about the heredity of such symptoms, given that around 43% of the patients reported a family history of migraine and visual aura. On the other hand, 57% of the patients reported experiencing tinnitus, with over half describing their symptoms as being either mild or occurring with low frequency. All the VS subjects tested were non-smokers and 83% reported drinking small amounts of alcohol on a weekly basis. All subjects reported experiencing unpleasant emotions, with 57% reporting anxiety while 17% and 43% reported panic and low mood, respectively. Medical drugs (in

the treatment of depression) were used by 28% of the patients, while no subject had ever used recreational drugs (according to their reports). Moreover, all subjects reported normal immune system function, with no evidence of infectious disease, hyperactivity, autism or any other developmental problem. Four subjects reported an onset of their VS symptoms at a mean age of 22 years, except for two of the subjects who first experienced the problem at 9 years of age. Although one subject associated the onset of his symptoms with a head trauma, all other subjects reported an association with general fatigue and/or stressful situations. Half of the patients (57%) reported experiencing visual discomfort under bright ambient light, while 28% experienced visual problems in the dark, even with closed eyes.

6.7.2 Effect of visual snow and after images on visual acuity

Figures 6.6 depict the comparison in gap acuity between those subjects with normative vision and those presenting with VS and/or after images. All measurements were conducted under monocular viewing conditions for each eye and also under binocular viewing conditions. Two stimulus presentation times of 60ms and 1200ms were employed. For both stimulus presentation times, binocular viewing was found to be enhanced and VA was also improved for the longer stimulus presentation time. Comparing the two groups, no statistically significant differences in gap acuity arose ($p>0.05$ in all cases) suggesting that VA does not significantly impair VA. Specifically, for the 60ms stimulus duration, the average threshold gap acuity measurements in the normative group were 1.07±0.29, 1.02±0.17 and 0.9±0.14 arcmins, respectively, for the right eye, left eye, and under binocular viewing conditions. The corresponding values for the VS group were 1.05±0.27, 1.02±0.22 and 0.75±0.09 arcmin, respectively. For the 1200ms stimulus, the duration time average gap acuity measurements were 0.71±0.08, 0.79±0.07, 0.61±0.07 for the normative group, and 0.75±0.11, 0.71±0.11, 0.65±0.07 for the VS group, respectively.

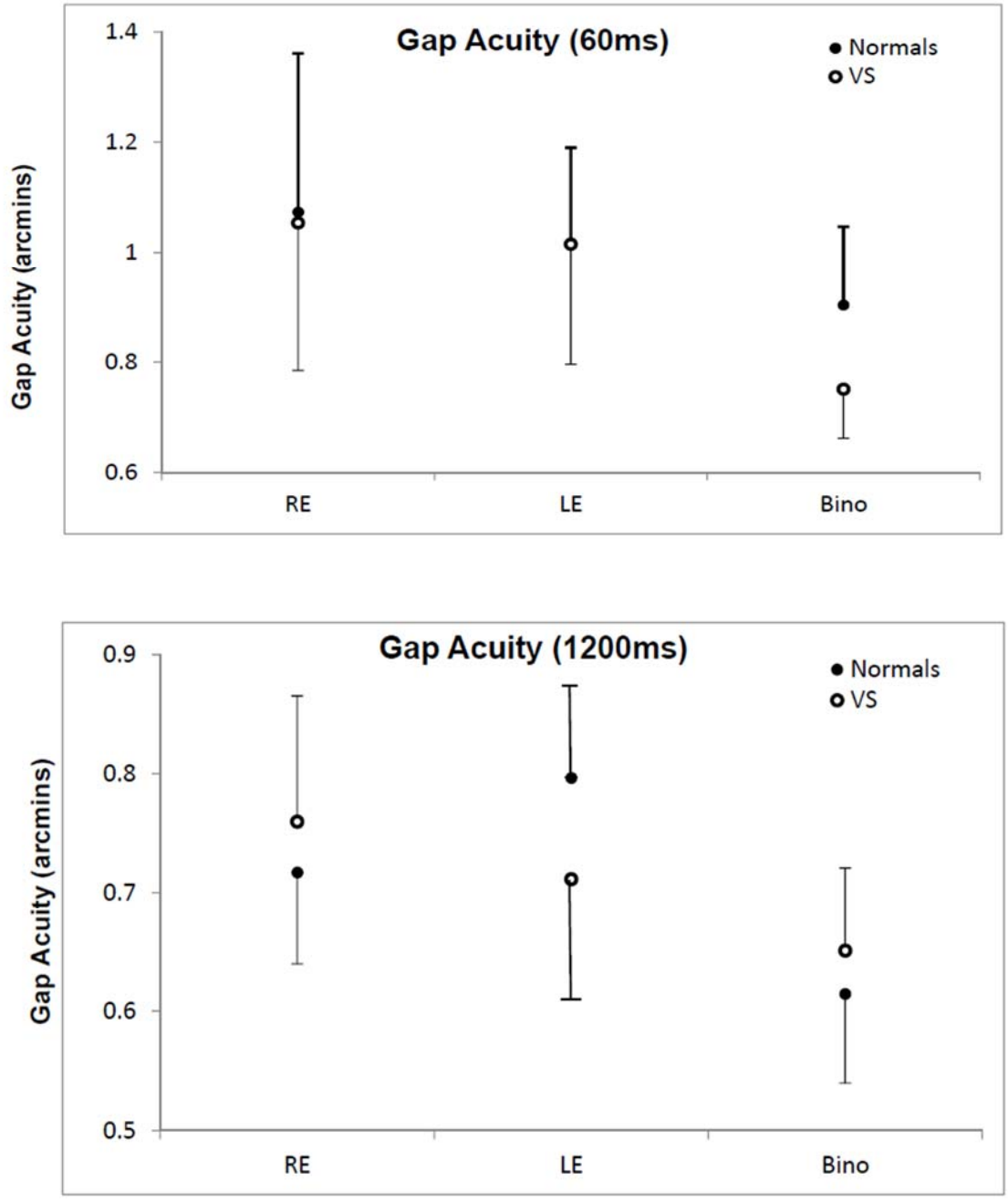

Figure 6.6. Monocular and binocular gap acuity comparison between normative subjects and those presenting with VS for the 60ms and 1200ms stimulus presentation times. Error bars represent (±) standard error of the mean.

6.7.3 Effect of visual snow and after images on colour sensitivity

Colour sensitivity was also assessed in both normative and VS subjects. Figure 6.7 presents colour sensitivity (in CAD units) for both RG and YB colour channels within both the normative and VS subject groups. Both groups showed a slightly better

colour sensitivity for the YB channel than for the RG channel. Although the normative subjects demonstrated a better chromatic sensitivity, on average, for both channels, these findings were not found to be statistically significant (p=0.09) owing to the relatively small control group (3 observers). More specifically, the average colour thresholds for the normative group were 1.11±0.28 and 0.82±0.11 for the RG and YB colour channels, respectively, while in the VS group the corresponding values were 1.14±0.21 and 1.01±0.14. The within subject variability in normal trichromats and in subjects with congenital colour deficiency rarely exceeds 20% of the mean. The latter is based on two standard deviations computed from repeated measurements.

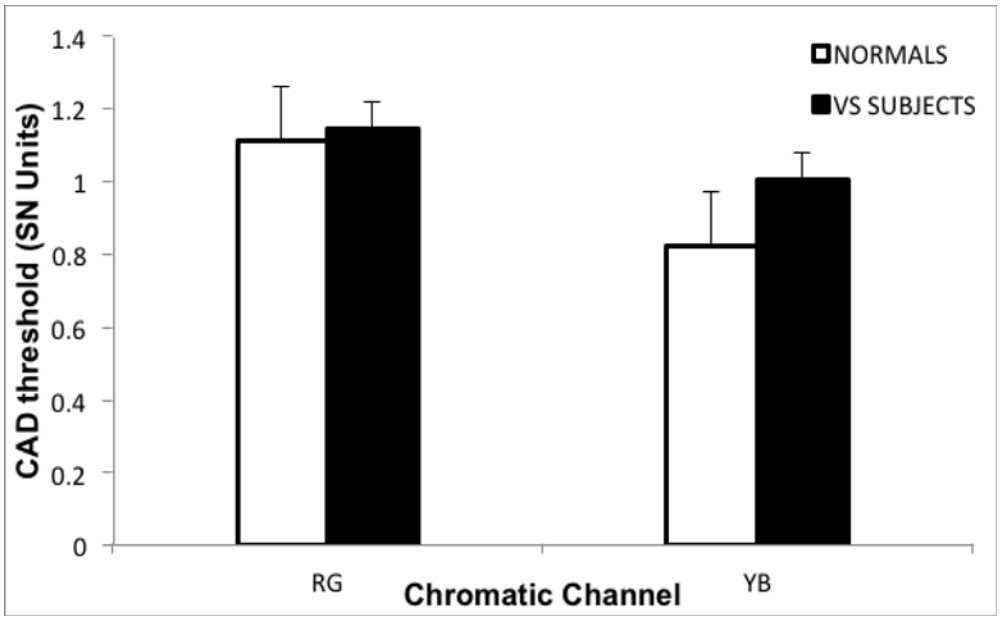

Figure 6.7. Comparison of RG and YB chromatic channel threshold between the control and VS groups. Error bars represent (**±**) standard error of the mean.

The similarity in chromatic sensitivity between one normative and one VS subject may be found depicted in Figure 6.8. These findings strongly suggest that chromatic sensitivity remains essentially unaffected by the VS syndrome.

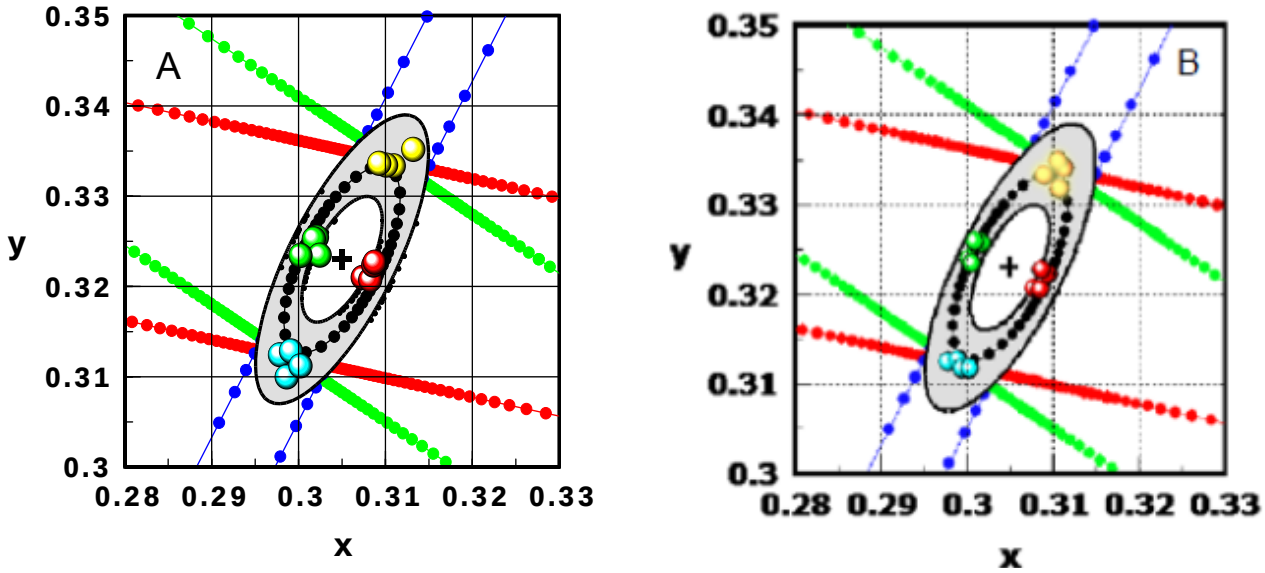

Figure 6.8. Typical CAD template graph obtained from a normal (left) and a VS (right) subject.

6.7.4 Chromatic after image strength evaluation

A comparison of after image strength between normative and VS groups is presented in Figures 6.9 and 6.10, in which characteristic plots of the chromatic displacement as a function of gap time are given for two subjects with normal vision and VS. Figure 6.11 plots average after-image strength for the two groups. Gap time is the time interval between the reference and the test stimulus (see paragraph 6.3). No statistically significant difference was found between the two groups ($p>0.05$) at all gap times.

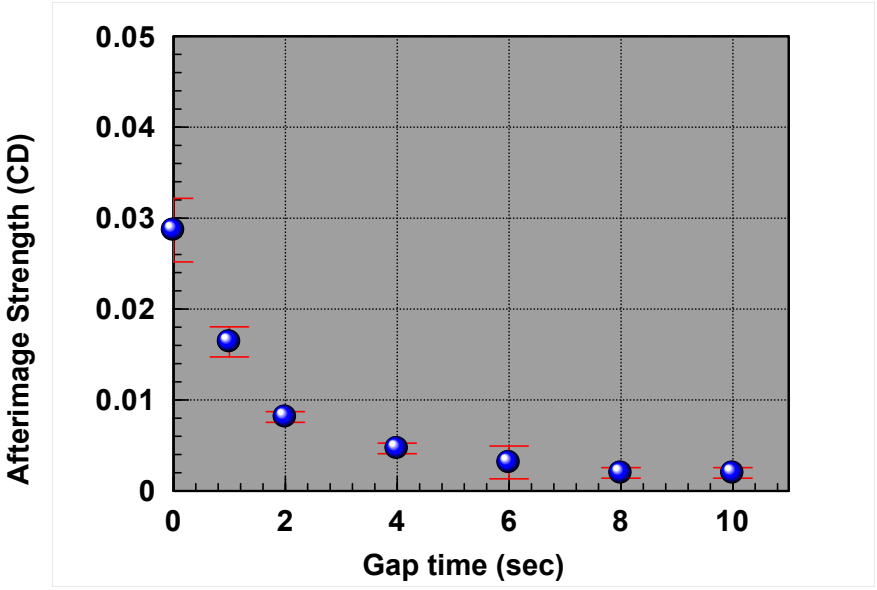

Figure 6.9. Typical after image strength for one normal subject. Error bars represent (±) standard error of the mean.

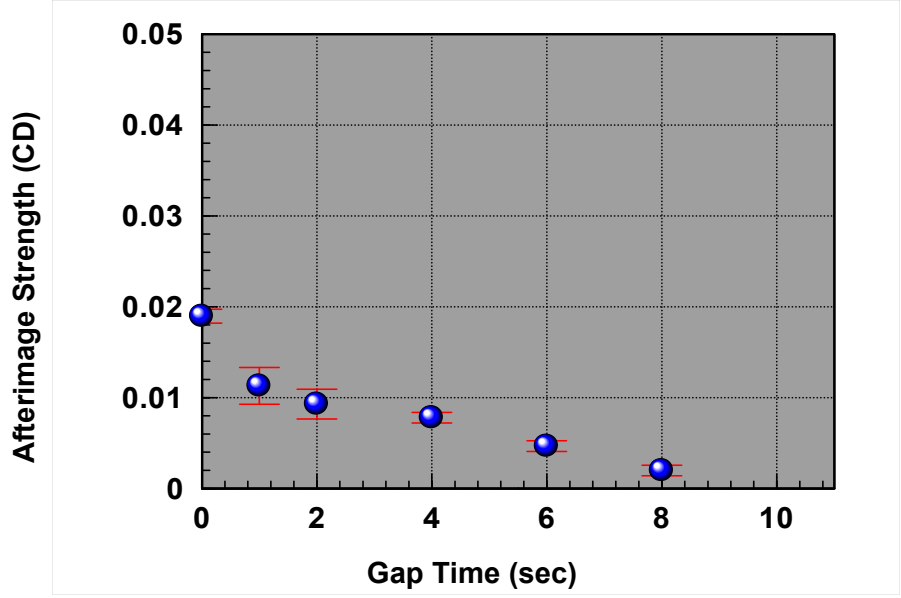

Figure 6.10. Typical after image strength for one visual snow subject. Error bars represent (±) standard error of the mean.

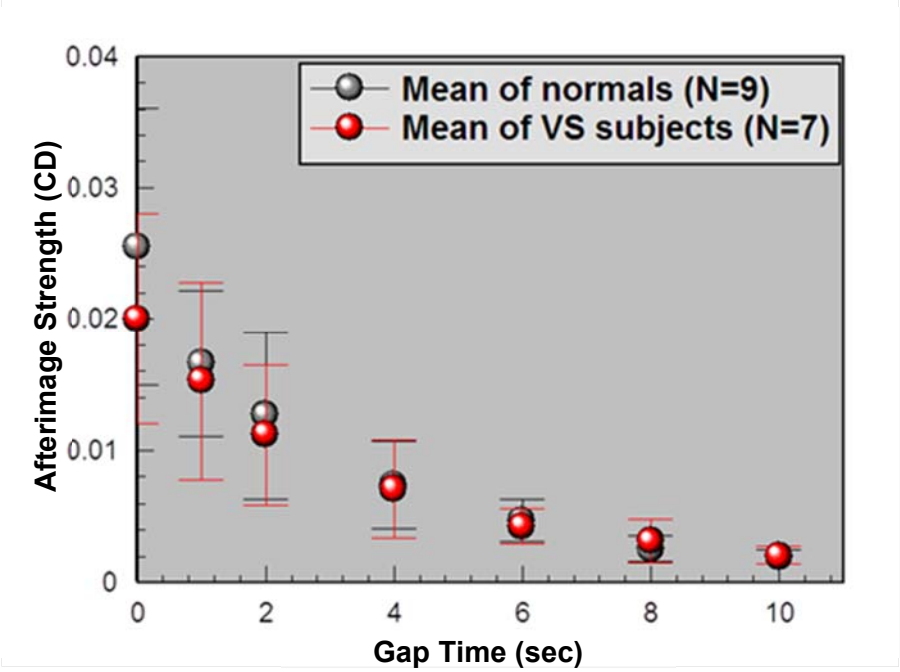

Figure 6.11. After image strength comparison between normal and visual snow groups. Data points represent mean values of each group while error bars represent standard error (±) of the means.

6.7.5 Pupil response evaluation

In order to evaluate possible differences in pupillary response between those with normal vision (n=6) and VS (n=6), we measured their pupillary responses to coloured stimuli. Figure 6.12 shows individual pupillary responses from each of the subjects tested, together with the stimulus trace. White lines represent the responses obtained from normal subjects, while the black lines were derived from VS subjects. It is evident that three of the six VS subjects tested demonstrated normal pupil responses at the onset and offset of the stimulus, while three other VS subjects exhibited a slowed recovery phase.

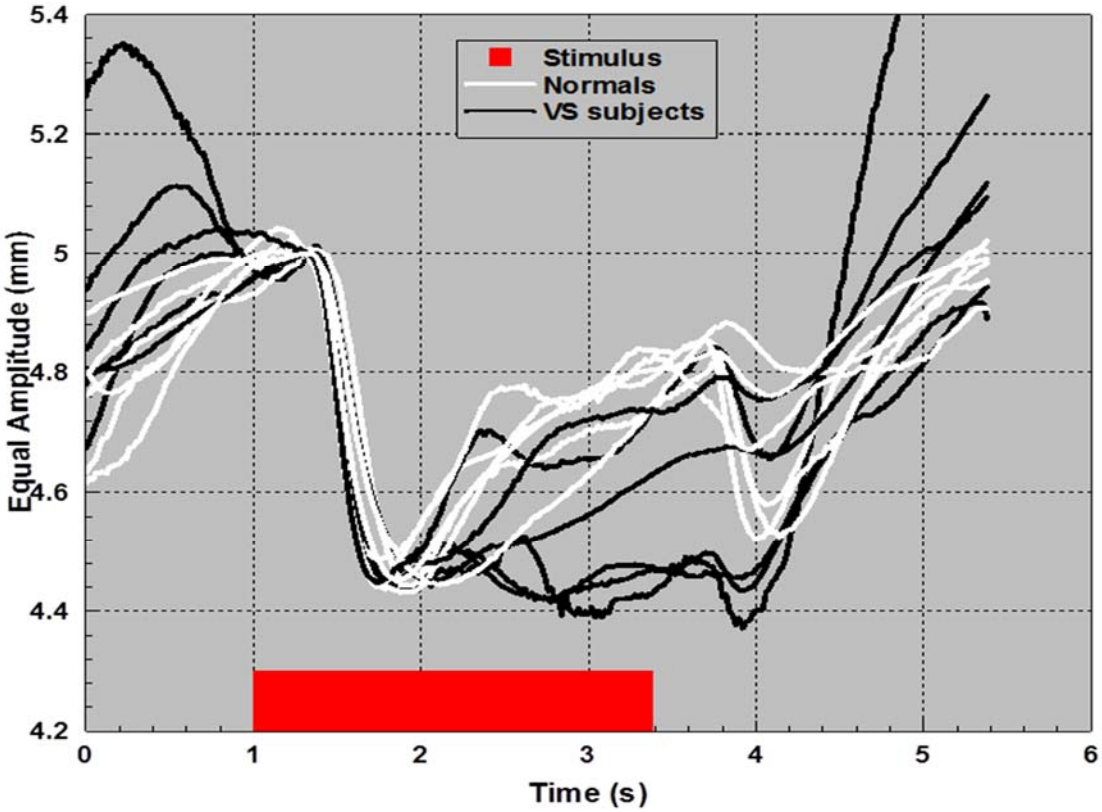

Figure 6.12. Twelve individual pupil responses from normal and VS subjects on stimulus onset and offset. The red bar at the bottom of the graph represents the duration of the stimulus.

To more clearly represent the differences in the responses observed between the VS subjects and those with normal vision, Figure 6.13 presents individual traces obtained from each of the three sub-groups identified (left: normal vision; middle: VS group A; and right: VS group B). The graphs from the normative group correspond to the modal pupillary responses from three typical subjects; while the graphs from VS Group A correspond to those three VS subjects who exhibited similar pupillary responses to those of the normative group. All normal subjects and the VS Group A subjects initially exhibited pupillary constrictions at the onset of the coloured stimulus, which was followed by a recovery phase during the onset of the stimulus plus a further constriction at the offset of the stimulus, a response normally attributed to perception of chromatic after images. The VS Group B pupil responses correspond to the three VS subjects who showed normal pupil constriction on stimulus onset but failed to exhibit the rapid recovery phase of the control group.

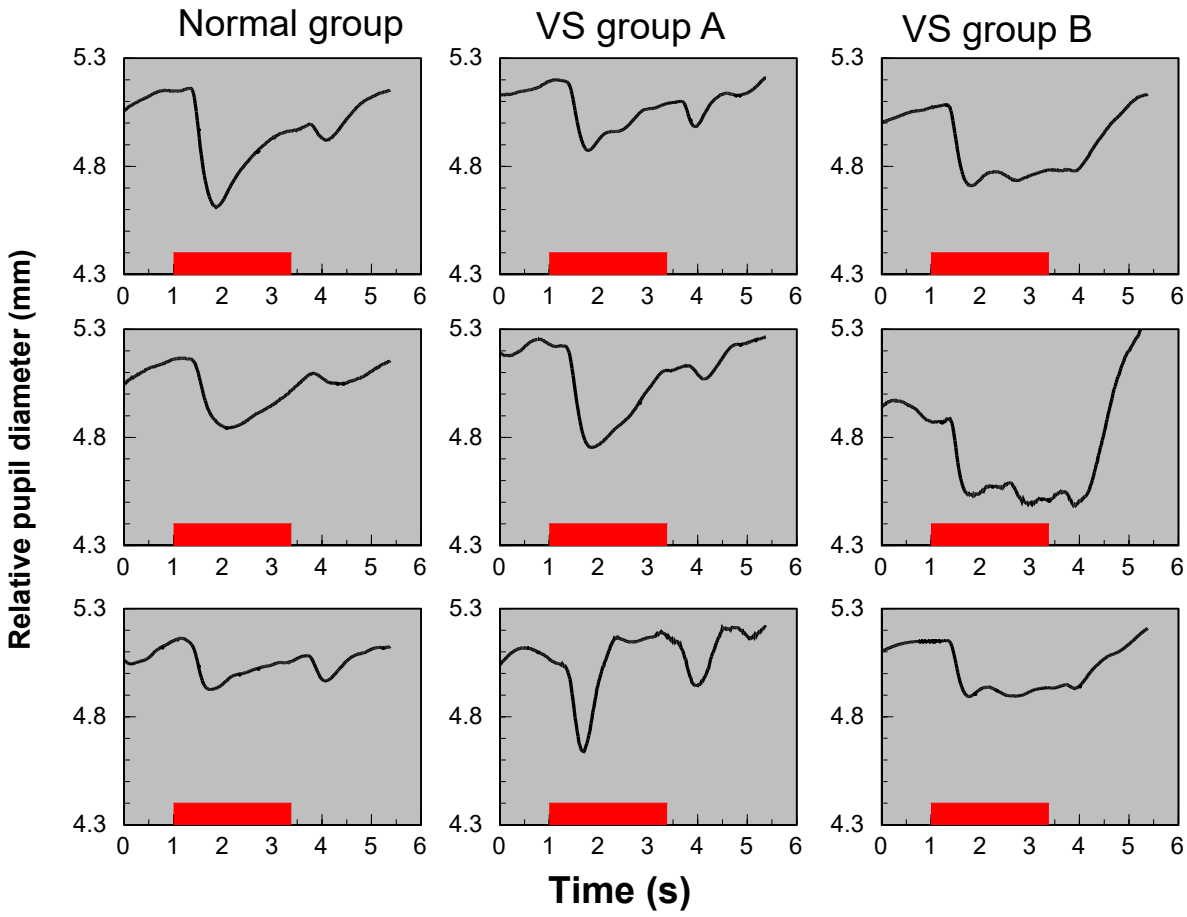

Figure 6.13. Pupillary responses of normal *(left)* **and two VS groups** *(middle and right).* VS group A exhibited normal pupillary responses at the onset and offset of the visual stimulus; while the VS group B showed a failure of the rapid pupillary recovery phase following stimulus onset.

6.8. Discussion

The principal aim of this study was to identify specific deficits in the processing of different stimulus attributes in those affected by VS. Owing to its relative infrequency within the general population, and the difficulties in its detection by standard methods of measuring VA, VS remains poorly understood and as yet largely uncharacterised. This has led to considerable confusion as to the potentially predictive linkage between VS with other neurological phenomena which are more readily detected, such as migraine and associated visual aura. One of the primary conclusions from this study and, more specifically, from the responses in the completed questionnaires, is that VS and after image formation appear to be a conjoined

phenomenon, as all VS subjects reported suffering from both deficits in visual processing. On the other hand, it seems that there is no reliable association between migraine attacks (with or without visual aura) and VS. Thus, our study would suggest that VS is not a specific symptom of a wider malaise, although there may be a link to the sufferer's extant emotional state, as VS symptoms seem to be heightened by stressful situations and general mental fatigue.

In this study, we tested for VA, colour sensitivity, chromatic afterimage strength and duration, and pupil response amplitudes and latencies to chromatic stimuli. While VA and chromatic sensitivity were not measurably affected in VS sufferers, there were however underlying trends that merit further investigation in a larger study. Although normal subjects exhibited a slightly enhanced chromatic sensitivity in both RG and YB channels, this difference may have become statistically significant given a larger population of VS sufferers, especially for the YB colour channel.

In addition to the assessment of VA and colour sensitivity, the measurement of after image strength, one of the primary symptoms of VS, was also evaluated at various intervals between the onset of the reference and test stimuli. Both groups showed a similar chromatic displacement at all gap times tested, and thus we may conclude that there is no measurable difference arising in terms of after image chromatic perception that can be attributable to VS. Although VS patients report the extended perception of visual scenes, this experience is not related to classic chromatic afterimages and appears more like a visual overlay that cannot be attributed to the same processing mechanisms that are responsible for chromatic afterimages in normal subjects.

One major deficit was, however, identified from a comparison of the pupillary responses to the onset and offset of a greenish light stimulus. Although both the control subjects and three of the six VS subjects tested exhibited normal pupillary constrictions in response to the onset of the coloured stimulus, which was followed by a recovery phase during the maintenance of the stimulus and further constriction at the offset of the stimulus, this was demonstrably not the case for three of the VS subjects who failed to exhibit a rapid pupillary recovery during the maintenance

phase of the stimulus. Moreover, these three subjects exhibited a sustained recovery phase following the initial constriction in response to the onset of the stimulus.

The absence of a normative pupil recovery phase is consistent with a longer, more sustained light stimulus, which would tend to suggest that there might be either a sustained input signal arising from the retina or else other prolonged feedback signals arising from within the cortex, which are also known to drive pupil responses. The data imply that these three VS subjects continue to process the coloured stimulus throughout the period of its presentation and, as a result, exhibit more sustained retinal afferent signals which drive the pupillary response. This may in turn be linked to the observed differences in the retinal and/or cortical processing of visual signals which cause the perception of VS.

In conclusion, although the onset of VS has hitherto been attributed to or associated with a number of different factors, its precise aetiology and neurological basis remain unclear. Given that no existing visual test can detect or evaluate the deficits in visual performance arising from VS, there may be an opportunity to develop new technology which specifically addresses and measures noise within the visual signal, for instance by progressively reducing the duration of a presented stimulus until its identity is no longer discernible. This ‘critical stimulus presentation threshold’ might be expected to be significantly shorter for those suffering from VS, leading to a higher error rate in identifying specific symbols, letters or numbers. However, the difference in the pupillary responses observed in half of our VS subjects may yet serve to provide fresh insights into the neurological deficits underlying VS syndrome. It remains to be demonstrated that these sustained pupillary responses are in fact related to the perceptual experience known as VS.

Chapter 7. Summary and future work

This doctoral study investigated related aspects of visual performance in both normal subjects and in patients with selective damage to visual pathways. An important aim was to elucidate further the extent to which binocular advantage is conferred across a range of metrics of visual performance and also addressed the principal visual deficits which are associated with two specific pathologies of vision, namely AMD and VS. The thesis further employed a number of visual experiments which were designed to assess the consequences of aging and AMD upon spatial vision and acuity. Since many experiments have been performed using several experimental techniques, this summary is intended to capture the major findings and seek to highlight the principal outcomes.

The initial aim, as presented in **Chapter 3**, was placed upon the role of binocular summation and the measurement of differences between the two eyes given that the rate of impairment is often asymmetrical. The advantage of binocular over monocular sensitivity across a range of tasks measuring visual performance has been discussed with special emphasis upon the effects of aging on binocular summation.

The absence of a specific binocular advantage in the accommodation response in presbyopes aged over 40 had not previously been reported as most studies had focused upon younger subjects with higher level of residual accommodation. Although presbyopes exhibited a higher degree of lag (~1.00D at 2.67D vergence), which results in considerable retinal blurring, it is unlikely that the level of defocus, experienced under these experimental conditions, would be sufficient to drive an accurate convergence response and to cause enhanced accommodation under binocular viewing conditions.

The difference in the average accommodation response between the two age groups tested was both anticipated and observed, but a significant binocular advantage was only found for the near distance within the non-presbyopic group. Further, this binocular advantage was notably higher for younger adults, an advantage that decreased progressively with increasing age until there was no significant advantage by the early thirties. Further, the binocular advantage conferred within early

presbyopes might serve to delay the onset of the symptoms of presbyopia and that monocular individuals or severely binocularly impaired individuals may thus experience an earlier onset of presbyopia.

Chapter 4 went on to address the effects of visual crowding on VA across a range of retinal eccentricities using a Landolt C optotype with and without surrounding distractors, investigating whether the extent of the crowding effect is actually more pronounced under binocular than monocular viewing conditions. It was noted that the binocular advantage conferred was, on average, higher at the central location in relation to the periphery, while the presence of distractors significantly reduced visual resolution at every eccentricity tested, with the effect being more pronounced in the periphery. In general, changes in VA arising at the fovea due to crowding are relatively small for high contrast stimuli, although such effects are inevitably accentuated within the periphery of the visual field which is allocated less cortical processing 'power' per unit of visual angle.

Moreover, no statistically significant difference in the magnitude of the visual crowding effect was observed between binocular and monocular viewing conditions at any eccentricity tested. The lack of such a difference strongly suggests that visual crowding may involve only monocularly driven neurons at the early stages of visual processing within the primary visual cortex. For the purposes of future work, evaluating the magnitude of the crowding effect under both binocular and monocular viewing conditions across a range of stimulus contrast levels may yield further insights into the neural mechanisms underlying the crowding effect and reveal any further advantage conferred by binocular summation.

Chapter 5 employed new refinements in the measurement of chromatic sensitivity, such as changes in the stimulus presentation time, to evaluate colour processing, in both the YB and RG channels. In addition, the effect of stimulus presentation time on VA and achromatic contrast sensitivity were also investigated. These techniques were employed to enhance the assessment of both spatial and chromatic visual performance in elderly subjects and to differentiate between the role of normative aging and ocular disease in compromising both optical and retinal components in the determination of perceived image quality.

In the first part, visual resolution (i.e. gap acuity) was evaluated in both normal subjects and in patients presenting with AMD across a range of stimulus presentation times which were designed to make it more difficult to achieve adequate resolution. In other words, visual resolution was assessed using both a single location for short duration tests and across a wider range of locations spanning the macular region for longer durations. To achieve this, the recently designed, Contrast Acuity Assessment test was employed, which enables a variation in background luminance level under both monocular and binocular viewing conditions. It was noted that the presentation time in such gap acuity tasks constitutes an important parameter which can be used to reveal the diminished spatial visual performance in early clinical stages of AMD that are normally not detected using the standard ETDRS (logMAR) acuity test. Although acuity was generally improved for all presentation times tested, the advantage increased with presentation time, with significant improvements in AMD patients. Thus, although no significant difference was found between the Landolt C gap acuity test and the standard logMAR test in AMD patients for the 3s presentation time (which enables multiple fixations), this is evidently not the case for shorter stimulus presentation times. Longer stimulus presentations times enable multiple fixations and more complete temporal processing. Both of these effects may help conceal the extent of visual loss within the early stages of the disease process in AMD.

Of great interest was also the discovery that the effect of binocular viewing conditions, which was found to improve significantly gap acuity, was independent of stimulus duration in control subjects with normal vision. However, the binocular advantage in gap acuity for AMD subjects was somewhat less evident, which might be attributable to the reduced stereoacuity observed in these patients as a consequence of the differential progression of the disease process within each of the two eyes. Gap acuity was also found to be influenced by background luminance, but only at low levels of luminance (e.g., ~ 2 cd/m^2 or less). Finally, in general agreement with the literature, negative contrast (i.e. presentation of a “black” letter on a “white” background) confers a greater sensitivity than positive contrast (a “white” letter on a “darker” background).

Any loss in chromatic sensitivity across the RG and YB channels was assessed in AMD patients using the CAD test which was designed to isolate the use of colour signals and to eliminate other cues. The CAD test results quantify the severity of both RG and YB deficits in colour vision and enable accurate classification of the subject's class of colour vision. The data revealed that, at photopic light levels, the loss of chromatic sensitivity in the YB pathway is slightly greater than for the RG pathway (when the tests are carried out in the least affected eye). As no data were collected in elderly observers with normative vision, the results were compared to standard published data. The changes may be attributed in part as a result of normal again since the measured thresholds are well above the upper normal limits. Respectively, suggesting that the retinal mechanisms involved in chromatic processing are severely impaired in AMD.

Chapter 6 investigated the visual performance of seven individuals who complained of 'visual noise', variously described as 'visual snow' (VS). These individuals otherwise presented no indication of any clinical abnormalities as measured by standard ophthalmic tests. More advanced visual tests were administered to these individuals to assess their VA, colour sensitivity, chromatic afterimage strength/duration, and pupillary responses to fixed chromatic stimuli and the corresponding colour afterimages. Owing to its rarity and the aforementioned difficulties in its diagnosis, the nature of VS remains poorly understood, a confusion which has been further compounded by anecdotal associations with other non-visual pathologies such as migraine. In support of the battery of visual tests performed, a detailed questionnaire was also completed by the VS subjects which unexpectedly highlighted the fact that all subjects also reported suffering from after images. Contrary to previous reports, there was no significant correlation between the incidence of migraine attacks (with or without visual aura) and VS, although the severity of VS symptoms appeared to be heightened by stress and general mental fatigue.

As far as the remaining tests are concerned, VS sufferers revealed no measurable impairment in gap acuity and their chromatic sensitivity was not demonstrably affected, although this could be attributed to the relatively small sample size. The

strength and duration of chromatic afterimages were also measured in normal and in VS sufferers and the results compared to normal subjects. VS sufferers exhibited similar chromatic after image strength to control subjects at all gap times tested. These findings suggest that the neural mechanisms involved in the generation of chromatic after images remain unaffected in VS subjects. In spite of these normal findings, three of the VS patients tested, however, failed to exhibit the normal, rapid pupil recovery response during the continued presentation of a coloured stimulus. The absence of such a normative pupil recovery response is consistent with a more sustained signal which may serve to explain the perception of VS. Further research is needed to demonstrate that such sustained pupillary responses are indeed the causative explanation for the perceptual experience known as VS. It could be argued that a specific test might be developed to screen for such visual noise within the general population under mesopic, photopic and scotopic conditions.

In conclusion, the programme of research described in this thesis employed a number of advanced vision and optometric tests to reveal new information in relation to changes in vision that arise due to both normal and degenerative aging processes and to establish the extent to which the binocular advantage is maintained. As far as the AMD study is concerned, an important limitation is the small number of subjects examined. Future studies should employ a larger number of subjects which may make it possible to correlate the severity of colour vision loss severity with VA and structural changes in the retina.

Bibliography

ALGUIRE, P.1990. Clinical methods: the history, physical, and laboratory examinations, London, Butterworths.

ALLEN, P.M., O'LEARLY, D.J. 2006. Accommodation functions: Co-dependency and relationship to refractive error. Vision Research**,** 46(4); pp. 491–505.

ANDERSON, H. 2010. Age-Related Changes in Accommodative Dynamics from Preschool to Adulthood. Invest Ophthalmol Vis Sci.**,** 51(1): 614–622.

ARTAL, P. 2000. Understanding aberrations by using double-pass techniques. Journal of Refraction Surgery**,** 60. pp. S560-S562.

BAILY,G. 2014. Available: http://www.allaboutvision.com/conditions/cataracts.htm [Accessed December 18].

BARTEN, P. 1999. Contrast Sensitivity of the Human Eye and Its Effects on Image Quality, Eindhoven, HV Press.

BERWER, A.A., BARTON, B. 2012. Effects of healthy aging on human primary visual cortex. Health**,** 4(9A): 695-702.

BLAKE, R.& FOX, R. 1973. The psychophysical inquiry into binocular summation. Perception & Psychophysics**,** 14(1) pp 161–185.

BONILHA,V.L. 2008. Age and disease-related structural changes in the retinal pigment epithelium. Clin Ophthalmol.**,** Jun; 2(2): 413–424.

BOUR, L. 1981. The influence of the spatial distribution of a target on the dynamic response and fluctuations of the accommodation of the human eye. Vision Res**,** 21(8) pp. 1287-96.

BOU GHANNAM, A. & PELAK, V.S. 2017. Visual Snow: a Potential Cortical Hyperexcitability Syndrome. Current treatment options in Neurology**,** 19 (3): 9.

BRODAL,P. 2010. The central nervous system : structure and function. (4th Ed.), New York, Oxford University Press.

CAGENELLO, R., ARDITI, A. & HALPERN, D. 1993. Binocular enhancement of visual acuity. J Opt Soc Am A Opt Image Sci Vis**,** 10(8): pp. 1841-8.

CALKINS, D. 2013. Age-related changes in the visual pathways: Blame it on the axon. Invest. Ophthalmol. Vis. Sci.**,** 54(14)

CASAGRANDE,V.A. 1994. A third parallel visual pathway to primate area V1. Trends Neurosci**,** 17:305–310.

CHARMAN, G. 2008. The eye in focus: accommodation and presbyopia, Oxford, Wiley.

CHARMAN, G. 2010. Optics of the eye. Handbook of Optics: Vision and Vision Optics. London: McGraw-Hill.

CHARMAN, W.N. 1991. Optics of the human eye. In: Cronly-Dillon, J. Visual Optics and Instrumentation. CRC Press, Boca Raton.1-22.

COLENBRANDER, A .2001.ski. organization [Online]. Available: http://www.ski.org/Colenbrander/Images/Measuring_Vis_Duane01.pdf.

CUNHA-VAZ, J. 2011. Diabetic Retinopathy, New Jersey, World Scientific.

CURCIO, C. A., SLOAN, K. R.,KALINA,R.A.&HEND,A.E.1990. Human photoreceptor topography. The Journal of Comparative Neurology.**,** 292 (4): 497–523.

CURTIS, D.W & RULE, S.J. 1978. Binocular processing of brightness information: a vector-sum model. J Exp Psychol Hum Percept Perform**,** 4(1): pp. 132-43.

DAVIES, L.N., MALLEN, E.A., WOLFFSOHN, J.S.& GILMARTIN, B. 2003. Clinical evaluation of the Shin-Nippon NVision-K 5001/Grand Seiko WR-5100K autorefractor. Optom Vis Sci,**,** 80(4) pp. 320-4.

DELAMERE, N. 2005. Ciliary Body and Ciliary Epithelium. Adv Organ Biol**,** 1(10): 127–148.

DESCARTES, R.1677. Traité de l'Homme 1677, Boston, Harvard University Press.

DE VALOIS, R.L., COTTARIS, N.P., MAHON, L.E., EIFAR, S.D.&WILSON, J.A. 2000. Spatail and temporal receptive fields of geniculate and cortical cells and directional selectivity. Vis Res, 40, 3685-702.

DOWLING, J. E. 1987. The Retina: An Approachable Part of the Brain, Boston, Harvard University Press.

DREXLER, W.,BAUMGARTNER.A.,FIND,O.,HITZENBERGER,C.K.&FERCHER,A.F. 1997. Biometric investigation of changes in the anterior eye segment during accommodation. Vision Res**,** 37(19): p. 2789-800.

DUANE, A.1912. Normal values of the accommodation at all ages. J Am Med Assoc**,** 59: 1010-3.

ELLIOTT, S.L., CHOI, S.S., DOBLE, N., HARDY, J.L., EVANS, J.W. & WERNER, J.S. 2009. Role of high-order aberrations in senescent changes in spatial vision. Journal of Vision, 9**,** 27;9(2):24.1-16.

FARNSWORTH, D. 1947. The Farnsworth dichotomous test for color blindness -panel D-15. Psychological Corporation, New York.

FINCHAM, E.F.& WALTON, J. 1957. The reciprocal actions of accommodation and convergence. J Physiol**,** 137(3): p. 488-508.

FLAMANT, F. 1955. Étude de la répartition de lumière dans l'image rétinienne d'une fente. Rev Opt**,** 34: pp 433-459.

FUENSANTA A, V.D.& NATHAN, D. 2012. The Human Eye and Adaptive Optics. Boston. DOI: 10.5772/31073.

GARNER, L. F.1997. Changes in ocular dimensions and refraction with accommodation. Ophthalmic and Physiological Optics, 17**,** 12-17.

GOEL, M., PICCIANI, R.G., LEE, R.K. & BHATTACHARYA, S.K. 2010. Aqueous Humor Dynamics: A Review. Open Ophthalmol J**,** 52–59.

GONZALEZ, E.G. 2012. Eye position stability in amblyopia and in normal binocular vision. Invest Ophthalmol Vis Sci, 53(9): pp. 5386-94.

GORDON, S. 2000. The Aging Eye, New York, Simon & Schuster.

GRAY, L.S. 1993. Accommodative microfluctuations and pupil diameter. Vision Res, 33(15):2083-90.

GROSVENOR, T. 1987. A Review and a Suggested Classification System for Myopia on the Basis of Age-Related Prevalence and Age of Onset. Optometry & Vision Science, 64(7); pp. 545-554.

GROSVENOR, T. 1988. High axial length/corneal radius ratio as a risk factor in the development of myopia. American Journal of Optometry and Physiological Optics, 65: 689.

GREENE,H.A.& MADDEN,D.J. 1987. Adult Age Differences in Visual Acuity, Stereopsis, and Contrast Sensitivity. Optometry & Vision Science, 64(10); pp. 749-753.

GUNKEL, R.D & GOURAS, P. 1963. Changes in scotopic visibility thresholds with age. Arch Ophthalmol, 69; pp. 38–43.

GLASSER, A., CAMPBELL, M,C. 1999. Biometric, optical and physical changes in the isolated human crystalline lens with age in relation to presbyopia. Vision Res, 39(11): p. 1991-2015.

HEATH, G.G. 1956. Components of accommodation. Am J Optom Arch Am Acad Optom, 33(11): p. 569-79.

HEITING, G. 2014. All About Vision [Online]. Available: http://www.allaboutvision.com/eye-exam/contrast-sensitivity [Accessed May].

HELMHOLTZ, H. V. & SOUTHALL,J.1924. Helmholtz's Treatise on Physiological Optics. Optical Society of America, 3: p. 143-172.

HERAVIAN, J.S., JENKINS,T.C. & DOUTHWAITE,W.A. 1990. Binocular summation in visually evoked responses and visual acuity. Ophthalmic Physiol Opt, 10(3): pp. 257-61.

HERON, G. 2004. Accommodation as a function of age and the linearity of the response dynamics. Vision Res, 44(27): p. 3119-30.

HOME, R. 1978. Binocular summation: a study of contrast sensitivity, visual acuity and recognition. Vision Res, 18(5): pp. 579-85.

HOWARD,I.P.& ROGERS, B.J. 1995. Binocular Vision and Stereopsis. Oxford University Press.

IBI, K .1997. Characteristics of dynamic accommodation responses: comparison between the dominant and non-dominant eyes. Ophthalmic Physiol Opt, 17(1): p. 44-54.

TIMOTHY,J. & JACKSON, T. 2008. Moorfields Manual of Ophthalmology, London, Elsevier.

JAKOBIEC, F.& IWAMOTO, T.1982. Ocular adnexae: introduction to lids, conjunctiva and orbit. In: Ocular Anatomy, Embryology and Teratology. Philadelphia: Harper & Row, pp. 677–731.

JOHNSON, C. 1976. Effects of Luminance and Stimulus Distance On Accommodation and Visual Resolution. Journal of the Optical Society of America**,** 66(2): p. 138-142.

KAAS, J., HUERTA, MF, WEBER, JT& HARTING, JK. 1978. Patterns of retinal terminations and laminar organization of the lateral geniculate nucleus of primates. Journal of Comparative Neurology**,** 182(3), pp 517–553.

KAARNIRANTA, K .2011. How to study autophagy in RPE cells? Acta Ophthalmologica.

KAUFMAN, P.L., LEVIN, L.A., ADLER, F.H.& ALM, A.1950. Adler's Physiology of the Eye, London, Elsevier.

KINNUNEN, K., PETROVSKI, G., MOE, M., BERTA, A. & KAARNIRANTA, K. 2012. Molecular mechanisms of retinal pigment epithelium damage and development of age-related macular degeneration. Acta Ophthalmologica**,** 90(4) pp. 299–309.

KENNEDY,C.J., RAKOCZY,P.E., CONSTABLE,I.J. 1995. Lipofucin of the retinal pigment epithelium: A review. Eye**,** 9; pp. 763-771.

KORETZ, J.F., COOK, C. A., KAUFMAN, P.L. 2002. Aging of the human lens: changes in lens shape upon accommodation and with accommodative loss. J Opt Soc Am A Opt Image Sci Vis.**,** 19(1): pp. 144-51.

LANE,L.K. 2005. Developing Ocular Motor and Visual Perceptual Skills: An activity workbook. Slack Incorporated.

LAFRAMBOISE, S., DE GUISE, D.& FAUBERT,J. 2006. Effect of Aging on Stereoscopic Interocular Correlation. Optom. Vis. Sci.**,** 83 (8), 589-593.

LANKHEET, M.J.,LENNIE, P. 1996. Spatio-temporal Requirements for Binocular Correlation in Stereopsis. Vision Res.**,** 36(4), pp. 527-538.

LEIBOWITZ, H.W. & OWENS,D.A. 1978. New evidence for the intermediate position of relaxed accommodation. Doc Ophthalmol**,** 46(1): p. 133-47.

LIM, J.S. 2012. Age-Related Macular Degeneration, 3rd Ed., Boca Raton, CRC Press.

MATHER, G. 2006. Foundations of Perception, New York, Psychology Press.

MATIN, J. 1962. Binocular Summation at the Absolute Threshold of Peripheral Vision. Journal of the Optical Society of America**,** 52(11) pp. 1276-1286.

MCKEE, S.P.& TAYLOR, D.G. 2010. The precision of binocular and monocular depth judgments in natural settings. Journal of Vision**,** 10(5); doi. doi:10.1167/10.10.5.

MCKEE, S.T.&TAYLOR, D.G. 2010. The precision of binocular and monocular depth judgments in natural settings. Journal of Vision**,** 10(5); doi. doi:10.1167/10.10.5.

MCKENDRICK, A.M, SAMPSON, G.P, WALLAND, M.J. & BADCOCK, D.R. 2007. Contrast sensitivity changes due to glaucoma and normal aging: low-spatial-frequency losses in both magnocellular and parvocellular pathways. Invest Ophthalmol Vis Sci.**,** 48(5):2115-22.

MITCHELL, P. 2011. A systematic review of the efficacy and safety outcomes of anti-VEGF agents used for treating neovascular age-related macular degeneration: comparison of ranibizumab and bevacizumab. Current Medical Research and Opinion, 27(7); pp. 1465-1475.

MYROWITZ, E.H.2012. Juvenile myopia progression, risk factors and interventions. Saudi Journal of Ophthalmology, 26(3); pp. 293-7.

NELSON-QUIGG, J.M., CELLO, K. & JOHNSON, C.A. 2000. Predicting Binocular Visual Field Sensitivity from Monocular Visual Field Results. Investigative Ophthalmology & Visual Science, 41, 2212-2221.

ORGANISCIAK, D.T., VAUGHAN, D. K. 2011. Retinal Light Damage: Mechanisms and Protection. Prog Retin Eye Res., 29(2): 113–134.

OTAKE, Y. 1993. An experimental study on the objective measurement of accommodative amplitude under binocular and natural viewing conditions. Tohoku J Exp Med., 170(2):93-102.

OWSLEY, C. 2011. Aging and vision. Vision Research, 51(13), pp. 1610–1622.

PANDA-JONAS, S.,JONAS, J.B. & JAKOBCZYK-ZMIJA, M. 1995. Retinal photoreceptor density decreases with age. Ophthalmology, 102(12):1853-9.

PENNINGTON, K. L.& DEANGELIS, M. M. 2016. Epidemiology of age-related macular degeneration (AMD): associations with cardiovascular disease phenotypes and lipid factors. Eye Vis., 3(34).

PESUDOYS ,K.& ELLIOTT,D.B. 2003. Refractive error changes in cortical, nuclear, and posterior subcapsular cataracts. British Journal of Ophthalmology 87: 964-967.

PLAINIS, S., GINIS,H.S.& PALLIKARIS,A.2005. The effect of ocular aberrations on steady-state errors of accommodative response. J Vis, 5(5): p. 466-77.

RAGHAVAN, M., REMLER, B., ROZMAN, S. & PELLI, D. 2010. Patients with visual 'snow' have normal equivalent input noise levels. Investigative Ophthalmology & Visual Science, 51 ARVO E-Abstract 1808/D660.

ROSENRTHAL, J., WERNER, D. L.1969.Tonometry and Glaucoma Detection. Glaucoma. Professional Press.

REMINGTON, L..A. .2011. Clinical Anatomy of the Visual System, E-Book. Elsevier Health Sciences.

REUTER, T. 2011. Fifty years of dark adaptation 1961–2011. Vision Research, 51(21-22), pp.2243-2262.

ROHEN, J. 1979. Scanning electron microscopic studies of the zonular apparatus in human and monkey eyes. Invest Ophthalmol Vis Sci, 18(2): p. 133-44.

ROSALES, P. ,DUBBELMAN,M.,MARCOS,S.& HEIJDE,R. 2006. Crystalline lens radii of curvature from Purkinje and Scheimpflug imaging. J Vis, 6(10): p. 1057-67.

ROSENFIELD,M.& CIUFFREDA, K.J.1991. Effect of surround propinquity on the open-loop accommodative response. Invest Ophthalmol Vis Sci, 32(1) pp. 142-7.

SACKS,O. 2012. An Anthropologist on Mars, New York, Pan Macmillan.

SCHANKIN, C., MANIYAR, F., HOFFMANN, J., CHOU, D. & GOADSBY, P. Clinical characterization of "visual snow" (Positive Persistent Visual Disturbance). The Journal of Headache and Pain, 2013. Springer, 14(Suppl 1):P132.

SEKULER, R.,HUTMAN,L.P.& OWSLEY,C.J.1980. Human aging and spatial vision. Science, 209(4462):1255-6.

SHARPE, L. T., STOCKMAN, A., FACH, C.C. & MARKSTAHLER, U. 1993. Temporal and spatial summation in the human rod visual system. J Physiol., Apr;463:325-48.

SHEEDY, J.E.BAILLEY,I.L.,BURI,M.&BASS,E. 1986. Binocular vs. monocular task performance. Am J Optom Physiol Opt, 63(10): p. 839-46.

SHER, N.A. 1997. Surgery for Hyperopia and Presbyopia., Williams & Wilkins.

SHINOMORI, K. 2005. Ageing effects on colour vision - Changed and unchanged perceptions. AIC Colour 05 - 10th Congress of the International Colour Association, pp. 7 - 12.

SHINOMORI, K. & WERNER, J. S. 2003. Senescence of the temporal impulse response to a luminous pulse. Vision Research, 43, 617-627.

SLOAN, L.L. 1959. New test Charts for the Measurement of Visual Acuity at far and Near Distances. American Journal of Ophthalmology, 48 (6) pp 807-813.

SlOAN, M.E., OWSLEY, C. & ALVAREZ, S.L. 1988. Aging, senile miosis and spatial contrast sensitivity at low luminance. Vision Research, *28*(11), pp.1235-1246.

SPADEA, L., MARAONE, G., VERBOSCHI, F., VINGOLO, E. M. & TOGNETTO, D. 2016. Effect of corneal light scatter on vision: a review of the literature. International Journal of Ophthalmology, 9, 459-464.

STEVEN, D.M. 1946. Relation between dark adaptation and age. Nature, 157; pp. 376–377.

STIDWILL,D., FLETCHER, R. 2011. Normal Binocular Vision: Theory, Investigation and Practical Aspects, Wiley-Blackwell.

TAYLOR, R., BATEY, D. 2012. Handbook of Retinal Screening in Diabetes: Diagnosis and Management, Oxford, Wiley-Blackwell.

TOVÉE, M.J .1996. An Introduction to the Visual System., Cambridge, Cambridge University Press.

TOWNSEND, J.T. 1968. Binocular information summation and the serial processing model. Perception & Psychophysics 4(2); pp. 125-128.

TROPE, G. 2011. Glaucoma: A Patient's Guide to the Disease, Fourth Edition, Toronto, University of Toronto Press.

VARADHARAJAN,L.S.2012.Available:http://link.springer.com/referenceworkentry/10.1007%2F978-3-540-79567-4_8.

VENTURE, A.S., WÄ LLT, R., BÖHNKE, M. 2001. Corneal thickness and endothelial density before and after cataract surgery. . British Journal of Ophthalmology, (85) pp. 18-20.

VEMALA, R., SIVAPRASAD, S. & BARBUR, J.L. 2017. Detection of Early Loss of Color Vision in Age-Related Macular Degeneration–With Emphasis on Drusen and Reticular Pseudodrusen. Investigative ophthalmology & visual science, 58(6), pp. BIO247-BIO254.

WALSH,G.& CHARMAN, W.N.1988. Visual sensitivity to temporal change in focus and its relevance to the accommodation response. Vision Res**,** 28(11):1207-21.

WERNER, J. S. 2016. The Verriest Lecture: Short-wave-sensitive cone pathways across the life span. J Opt Soc Am A Opt Image Sci Vis, 33**,** A104-22.

WOLFFSOHN, J.S., EPERJESI, F. 2004. The effect of relative distance enlargement on visual acuity in the visually impaired. Clinical and Experimental Optometry**,** 88(2) pp 97-102.

WOLF,E.& SCHRAFFA, A.M.1964. Relationship Between Critical Flicker Frequency and Age in Flicker Perimetry. Arch Ophthalmol.**,** 72(6):832-843.

WILLOUGHBY, C.E.,PONZIN, D., FERRARI, S., LOBO,A., LANDAU,K. & OMIDI,Y. 2010. Clinical and Experimental Ophthalmology 38: 2–11 doi: 10.1111/j.1442-9071.2010.02363.

YOONESSI, A. & YOONESSI, A. 2011. Functional assessment of magno, parvo and konio-cellular pathways; current state and future clinical applications. J Ophthalmic Vis Res, 6**,** 119-26.

YOUNG, T.1801. On the mechanism of the eye. Phil Trans Roy Soc**,** 91: p. 39-72.

ZEKI, S.1993. A Vision of the Brain., Oxford, Blackwell.

ZEKI, S. M. 1974. Functional organization of a visual area in the posterior bank of the superior temporal sulcus of the rhesus monkey. J Physiol, 236**,** 549-73.

Appendix A: Information sheet

CITY UNIVERSITY LONDON

Tait Building,
Northampton Square,
London EC1V 0HB.

Telephone: +44 20 70405060
Fax: +44 20 70408355
www.city.ac.uk/avrc

Applied Vision Research Centre
The Henry Wellcome Laboratories for Vision Sciences City University

John L Barbur
Director & Head of Colour Vision Laboratory

Chris Hull
Head of Department

David Crabb Head of Applied Vision Group
Ron Douglas Head of Visual Neuroscience

INFORMATION SHEET

Title of project:
Assessing the binocular advantage: Are two eyes better than one in providing better accommodation response?

Good vision is facilitated by combining signals from the two eyes at higher levels of visual processing in the brain. Information contained in the retinal image is processed separately in each eye but these signals are brought together in at some stage of visual processing to enhance what we see and to also process depth information. The purpose of the study is to quantify the binocular advantage on the process of accommodation. As for most aspects of the visual system, an advantage is predicted when fusion of the two retinal images is achieved, although whether the proposed advantage is significant and its dependence on age remains to be confirmed.

As part of this investigation, an ophthalmic assessment will be offered to you. In addition, you will be asked to view high-contrast letters placed at three different distances (near, intermediate and far) whilst your accommodation is measured.

The assessment of your vision will last approximately forty-five minutes. It will take place at City University, Northampton Square, London, which is approximately 7 minutes walk from Moorfields Eye Hospital.

Thank you for taking the time to read these notes. If you have further questions or queries, please do not hesitate to contact me, details given below.

Please contact:

Ms Ruba Alissa
[redacted]

Appendix B: Consent form

CITY UNIVERSITY LONDON

Tait Building,
Northampton Square,
London EC1V 0HB.

Telephone: +44 20 70405060
Fax: +44 20 70408355
www.city.ac.uk/avrc

Applied Vision Research Centre
The Henry Wellcome Laboratories for Vision Sciences
City University

John L Barbur
Director & Head of Colour Vision Laboratory

Chris Hull
Head of Department

David Crabb Head of Applied Vision Group
Ron Douglas Head of Visual Neuroscience

CONSENT FORM

Title of project: Assessing the binocular advantage: Are two eyes better than one in providing better accommodation response?

1. I confirm that I have read and understand the information sheet dated _____ for the above study. I had the opportunity to consider the information provided, ask questions and had these answered satisfactorily.

2. I understand that my participation is voluntary and that I am free to withdraw at any time without giving a reason. _____

3. I understand that personal data collected during the study will be treated as strictly confidential and stored securely. No information that could lead to the identification of any individual will be disclosed in any project reports. _____

4. I agree for the data collected in this study to be shared with other researchers (if required) or to be used in other research studies. The data shared with other researchers will not, however, have any personal details so that no data can be traced back to individual participants. _____

5. I understand that this is a research investigation and that the results of the tests carried out cannot be used for any kind of diagnosis. _____

6. I **agree** / **do not agree** (delete as appropriate) to be contacted and invited in the future to participate in similar research studies. I understand that I can decline any such invitation without to provide any reasons for doing so.

7. I agree to take part in the above study. _____

_____	_____	_____
Name of participant	Date	Signature
_____	_____	_____
Name of person taking consent	Date	Signature

1 copy for participant; 1 copy for researcher site file